

# Magnetic Thin Films for Heads and Media

Jack Judy

The Center for Magnetics and Information Technologies

University of Minnesota

## OUTLINE

- I. MAGNETIC PHENOMENA RELEVANT TO MAGNETIC RECORDING
- II. MAGNETIC MEASUREMENT TECHNIQUES
- III. THIN FILM DEPOSITION AND CHARACTERIZATION TECHNIQUES
- IV. MATERIALS FOR THIN FILM HEADS
- V. MATERIALS FOR THIN FILM MEDIA
- VI. PERFORMANCE AND FUTURE OF RECORDING SYSTEMS
- VII. REFERENCES

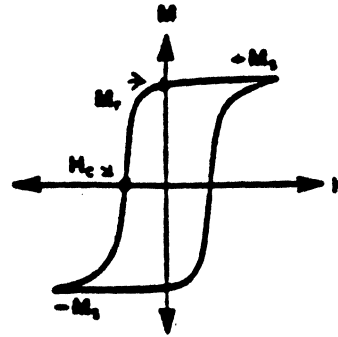
# MAGNETIC PROPERTIES

## Extrinsic

remnant magnetization  $M_r$

coercivity  $H_c$

permeability  $\mu = \frac{B}{H}$



## Intrinsic

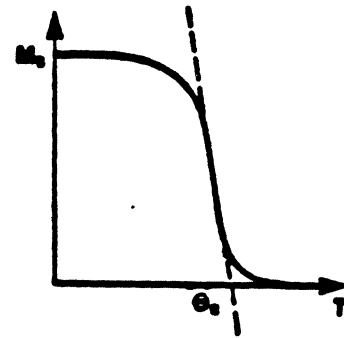
saturation magnetization,  $M_s$

Curie temperature,  $\theta_c$

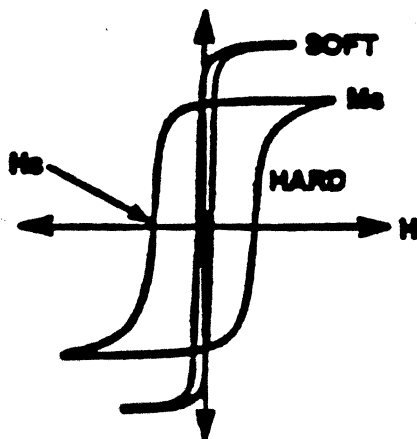
magneto-crystalline anisotropy,  $K_1, K_2$

magnetostriction  $\lambda$

$B = H + 4\pi M_s$



# HARD AND SOFT MAGNETIC MATERIALS



## Soft:

pure Fe

80 Ni: 20 Fe

Mn Zn ferrite

Fe N  
Co Zr Nb  
Al Fe Si  
(SEDDUST)

## Hard:

Particles  $\gamma\text{-Fe}_2\text{O}_3$

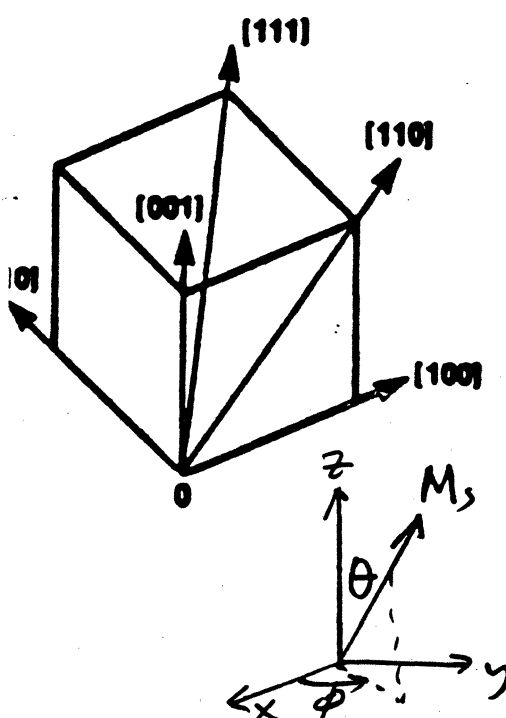
$\text{BaO} \cdot 6\text{Fe}_2\text{O}_3$

$\text{SmCo}_5$

(Co Ni P-  
Co Cr/Cr  
Co Cr Ta/C  
THIN FILMS)

(Bate)

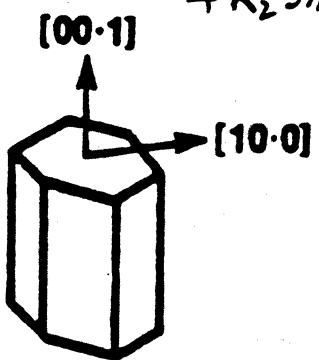
# MAGNETO-CRYSTALLINE ANISOTROPY



MAGNETO-CRYSTALLINE ENERGY DENSITY

UNIAXIAL:  $E_K = K_1 \sin^2 \theta + K_2 \sin^4 \theta$

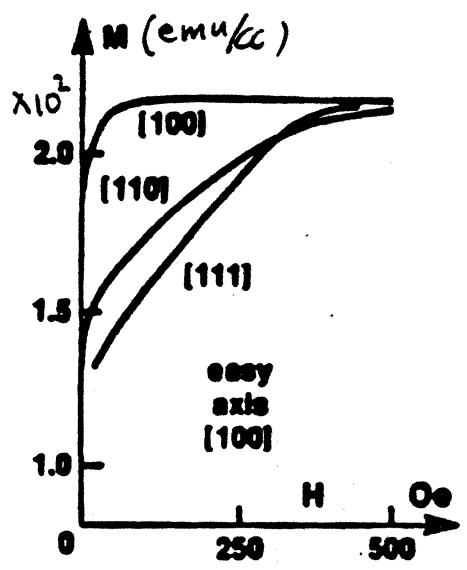
CUBIC:  $E_K = K_0 + K_1 [\alpha_1^2 \alpha_2^2 + \alpha_2^2 \alpha_3^2 + \alpha_3^2 \alpha_1^2] + K_2 \alpha_1^2 \alpha_2^2 \alpha_3^2$



$K_1 = +3.98 \times 10^6 \text{ erg/cc}$   
 $K_2 = +1.98 \times 10^6 \text{ erg/cc}$

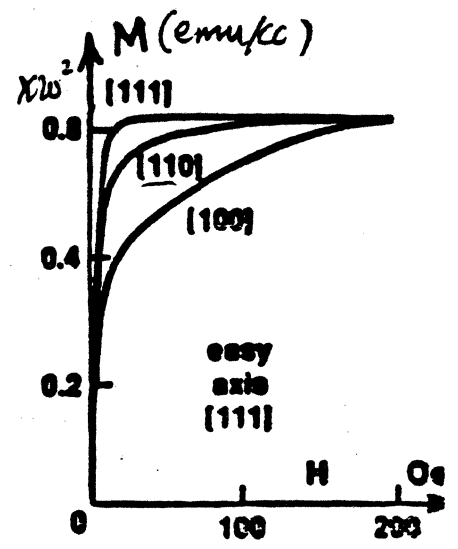
(Bate)

## Iron



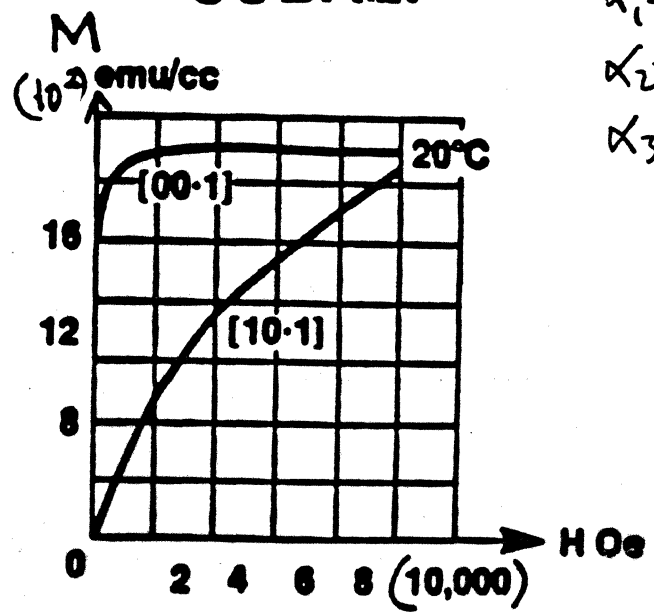
$K_1 = 4.8 \times 10^5 \text{ erg/cc}$   
 $K_2 = 5 \times 10^4$

## Nickel



$K_1 = 4.5 \times 10^4$   
 $K_2 = 2.34 \times 10^4$

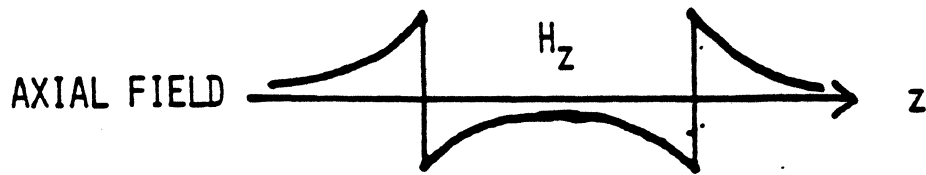
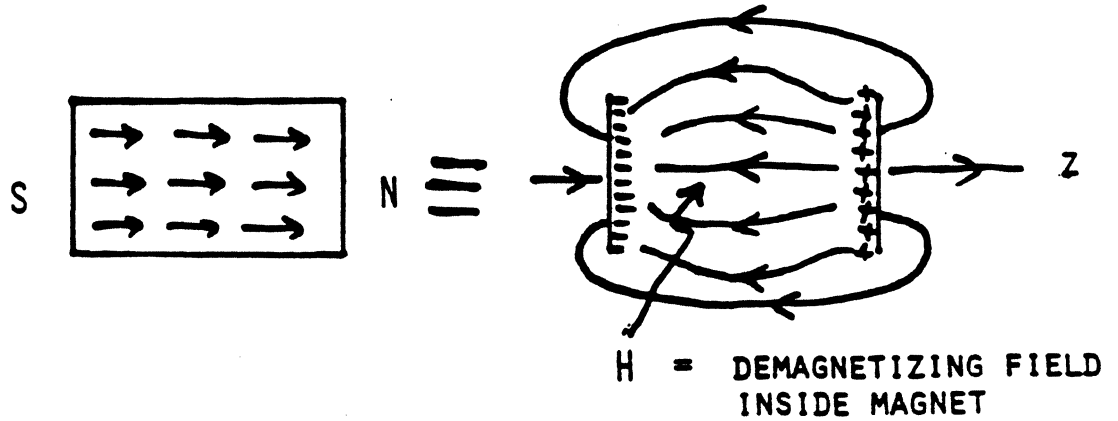
## COBALT



$\alpha_1 = \sin \theta \cos \phi$   
 $\alpha_2 = \sin \theta \sin \phi$   
 $\alpha_3 = \cos \theta$

# DEMAGNETIZING FIELDS

UNIFORMLY MAGNETIZED BAR MAGNET OR RECORDED BIT



$$\text{AVERAGE DEMAGNETIZING FIELD} = \vec{H}_{\text{DEMAC}} = - N_D \vec{M}$$

$$\text{AVERAGE DEMAGNETIZATION FACTOR} = N_D$$

$$\text{SUM OF DEMAGNETIZATION FACTORS} = N_x + N_y + N_z = 4\pi$$

$$\vec{B}_{\text{INT}} = \vec{H}_{\text{INT}} + 4\pi \vec{M}_{\text{INT}}$$

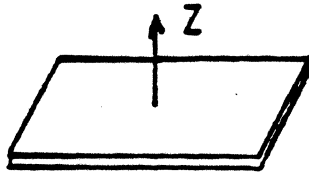
$$\vec{H}_{\text{INT}} = \vec{H}_{\text{APP}} + \vec{H}_{\text{DEMAC}}$$

CGS:  $B$ [gauss],  $H$ [oersteds],  $M$  [ $\frac{\text{emu}}{\text{cm}^3}$ ]

# SHAPE ANISOTROPY

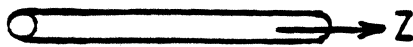
## DEMAGNETIZATION FACTORS OF DIFFERENT SHAPES

SHEET



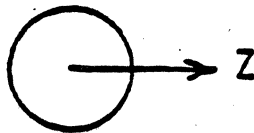
$$N_x = N_y = 0, N_z = 4\pi$$

CYLINDER



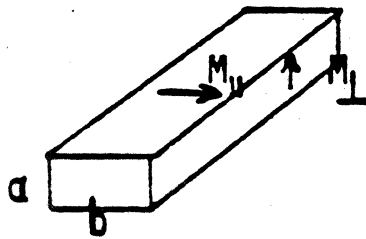
$$N_x = N_y = 2\pi, N_z = 0$$

SPHERE



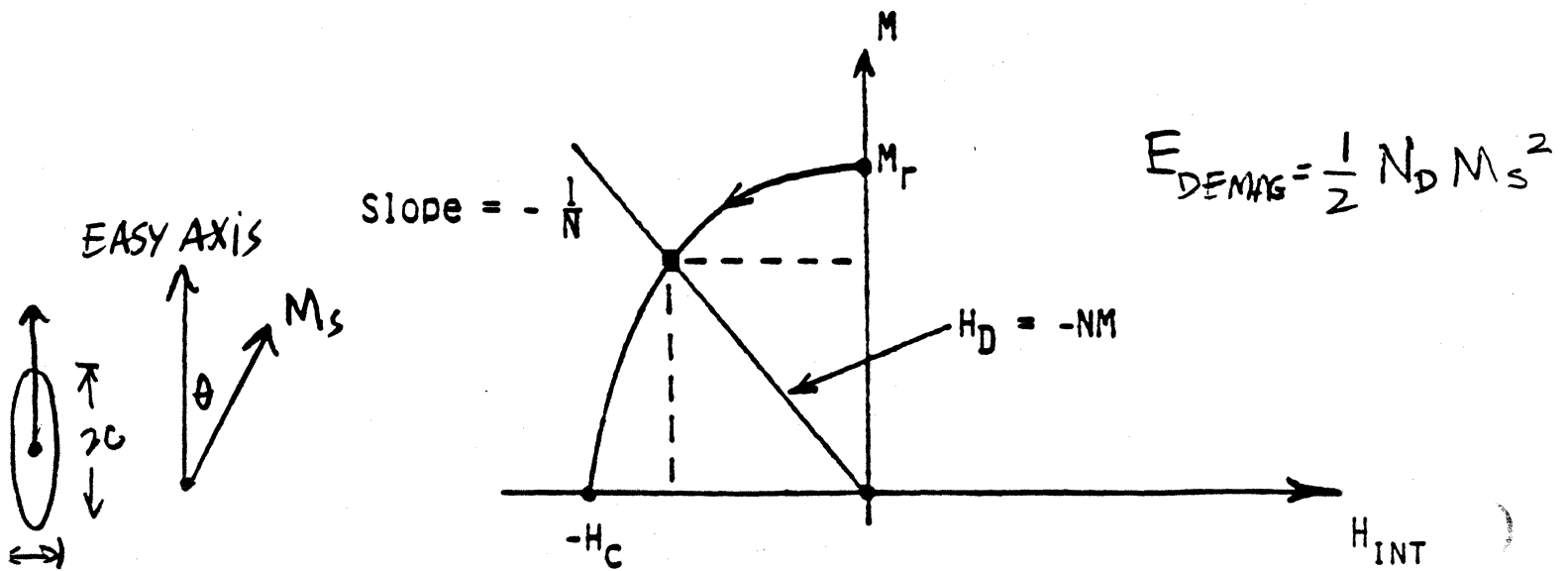
$$N_x = N_y = N_z = \frac{4\pi}{3}$$

RECTANGULAR BAR



$$N_{\parallel} = \frac{a}{a+b} 4\pi, N_{\perp} = \frac{b}{a+b} 4\pi$$

(approximately)



MAGNETOSTATIC DEMAGNETIZATION ENERGY DENSITY

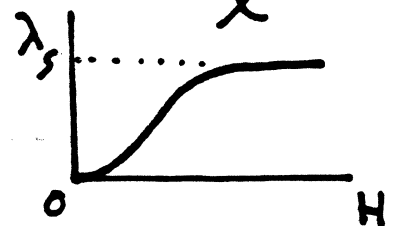
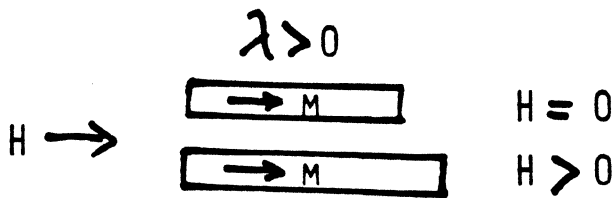
$$E_{\text{Demag}} = K_s \sin^2 \theta$$

$$K_s = \frac{1}{2} (N_a - N_c) M_s^2$$

# MAGNETOSTRICTION

DIMENSIONS OF MATERIAL CHANGE WHEN MAGNETIZED

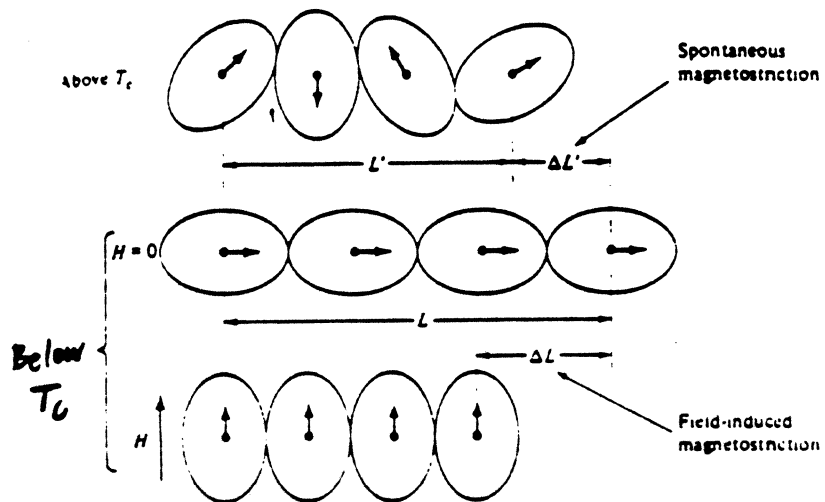
MAGNETOSTRICTION COEFFICIENT =  $\lambda = \frac{\Delta l}{l}$



(parts per 10<sup>6</sup>)

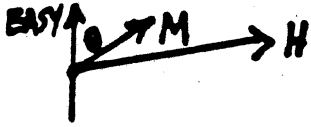
	$\lambda_{100}$	$\lambda_{111}$	$\lambda_{poly}$
Fe	+ 21	- 21	- 7
Ni	- 46	- 24	- 34
FeO · Fe <sub>2</sub> O <sub>3</sub>	- 20	+ 78	+ 40
Co <sub>0.9</sub> Fe <sub>0.1</sub> O · Fe <sub>2</sub> O <sub>3</sub>	- 590	+ 120	
CoO · Fe <sub>2</sub> O <sub>3</sub>			- 110

PHYSICAL ORIGIN IS SPIN-ORBIT COUPLING



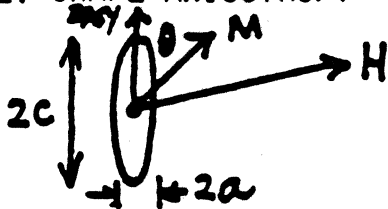
# MAGNETIC ANISOTROPY ENERGY DENSITY

## 1. CRYSTALLINE ANISOTROPY



$$E_K = K_U \sin^2 \theta$$

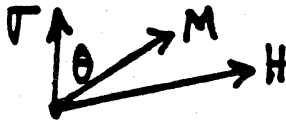
## 2. SHAPE ANISOTROPY



$$E_S = K_S \sin^2 \theta$$

$$K_S = \frac{1}{2} (N_A - N_C) M_S^2$$

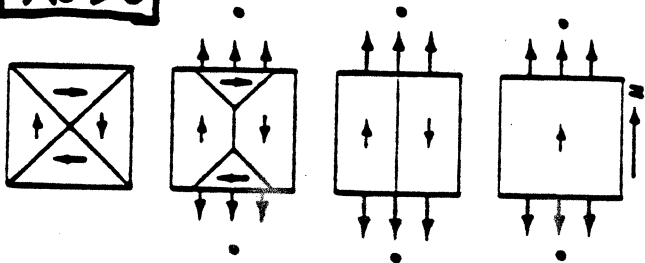
## 3. STRESS ANISOTROPY



$$E = K_\sigma \sin^2 \theta$$

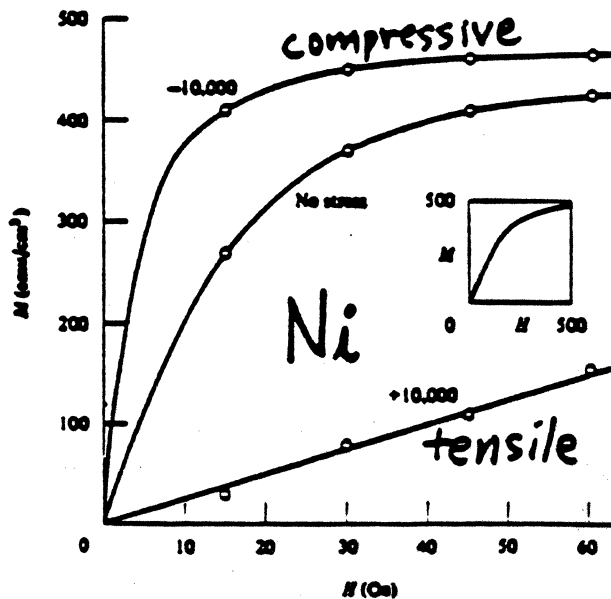
$$K_\sigma = \frac{3}{2} \lambda \sigma$$

$\lambda \sigma > 0$



TENSILE  $\sigma > 0$

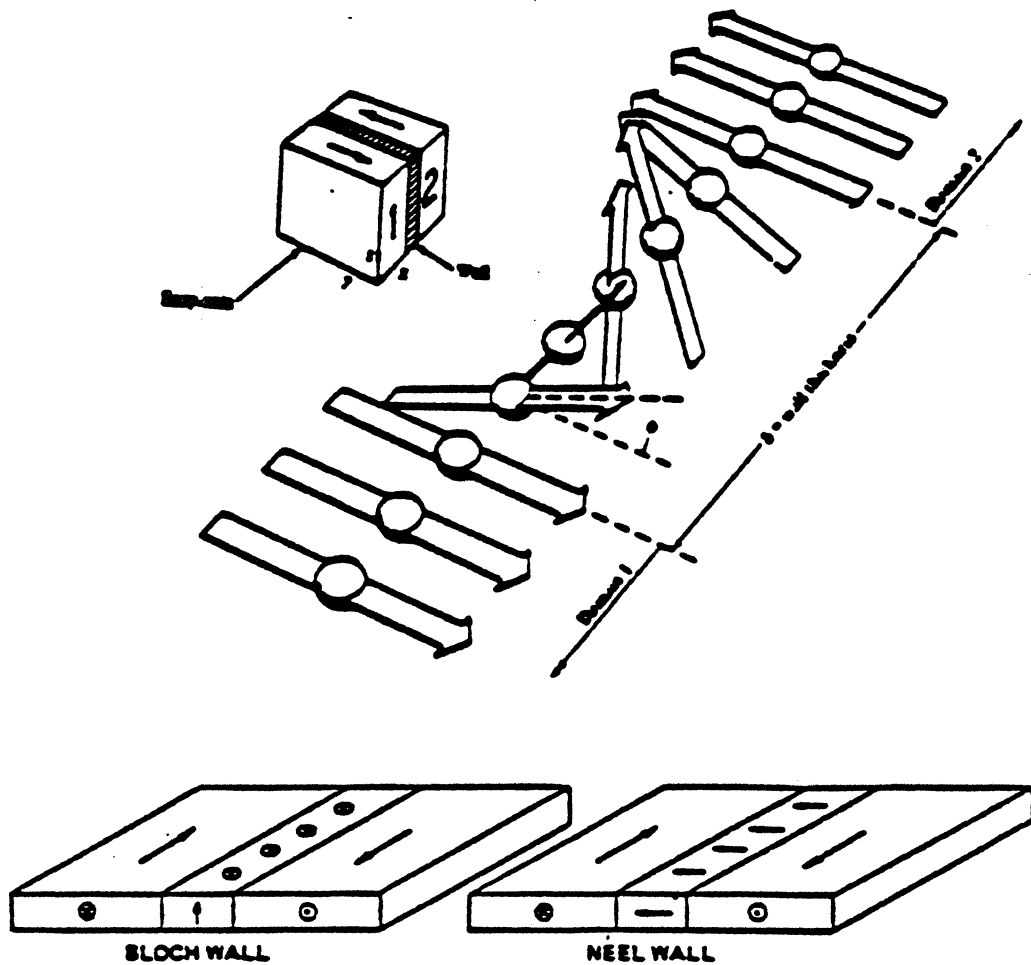
COMPRESSION  $\sigma < 0$



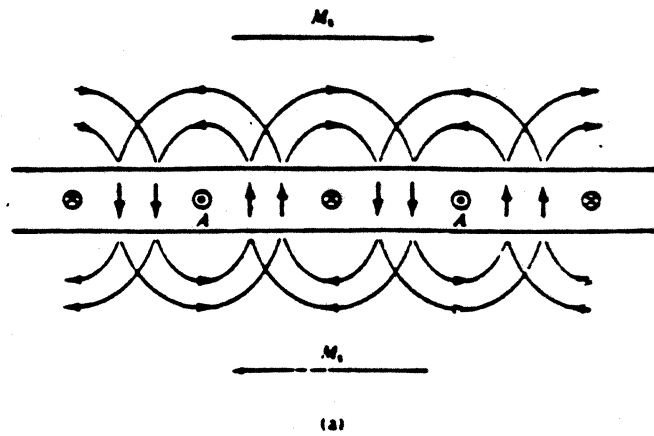


# MAGNETIC DOMAIN WALLS

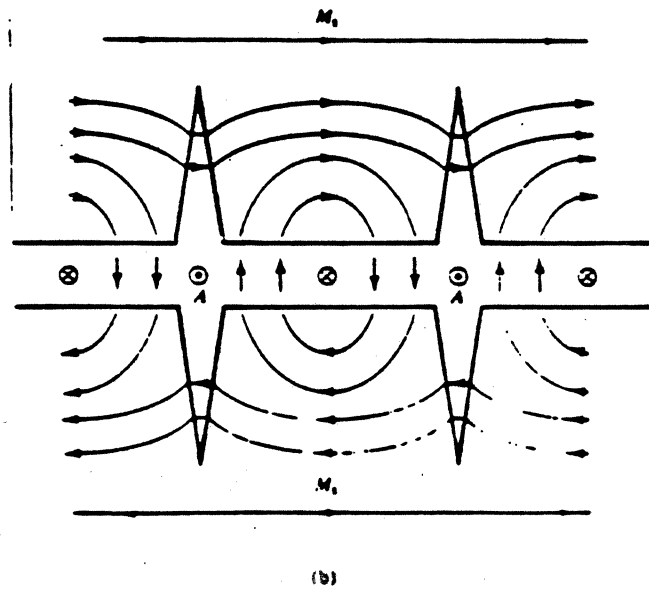
THE BOUNDARY BETWEEN OPPOSITELY MAGNETIZED DOMAINS IN BULK MATERIALS IS CALLED A 180° BLOCH WALL



# CROSS-TIE WALL FORMATION

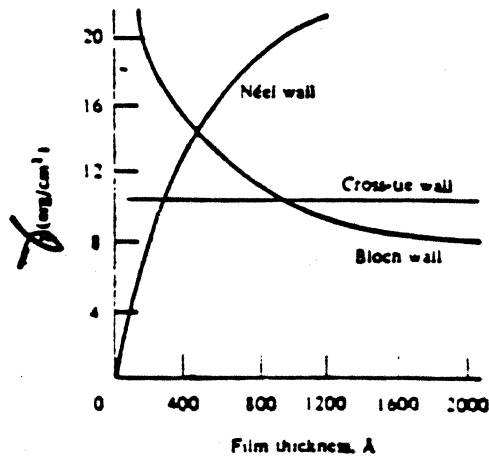


Alternating  
Néel Wall



Cross-Tie  
Walls

## THICKNESS DEPENDENCE OF WALL ENERGY DENSITIES



# MINIMUM DOMAIN WALL THICKNESS

ASSUME A SIMPLE CUBIC ARRAY OF SPIN DIPOLE MOMENTS

WITH A LATTICE PARAMETER  $a$  AND ASSUME THE WALL TO BE  $N$

ATOMS THICK SO THE WALL THICKNESS IS GIVEN BY  $\delta = Na$



THE NEAREST NEIGHBOR EXCHANGE ENERGY OF A PAIR OF

DIPOLE MOMENTS IS GIVEN BY  $W_{EX} = -2 J_{EX} S^2 \cos \phi$

AND THE ANGLE BETWEEN ADJACENT MOMENTS IS  $\phi = \pi/N$

THEN SINCE THE  $\cos(\phi) \approx 1 - \frac{1}{2}\phi^2$

THE EXCESS EXCHANGE ENERGY OF  $N$  PAIRS IS  $W_{EX} \approx \frac{J_{EX} S^2 \pi^2 a}{\delta}$

FINALLY, THE EXCHANGE ENERGY PER UNIT WALL AREA IS

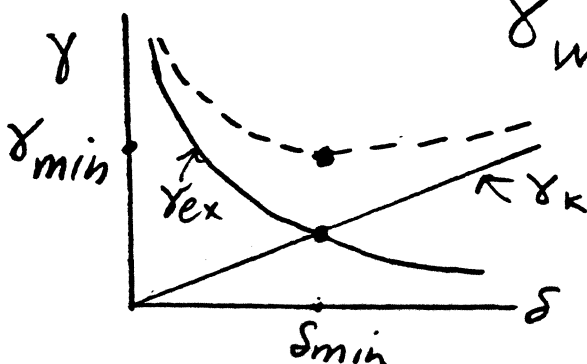
GIVEN BY  $\gamma_{EX} = \frac{J_{EX} S^2 \pi^2}{a} \frac{1}{\delta}$

THE MAGNETO-CRYSTALLINE ANISOTROPY ENERGY PER UNIT WALL

AREA IS GIVEN BY  $\gamma_K = K \delta$

THE TOTAL WALL ENERGY PER UNIT WALL AREA IS GIVEN BY

$$\gamma_{WALL} = \frac{A_{EX}}{\delta} + K \delta, \quad A_{EX} = \frac{J_{EX} S^2}{a}$$



THE MINIMUM WALL THICKNESS IS

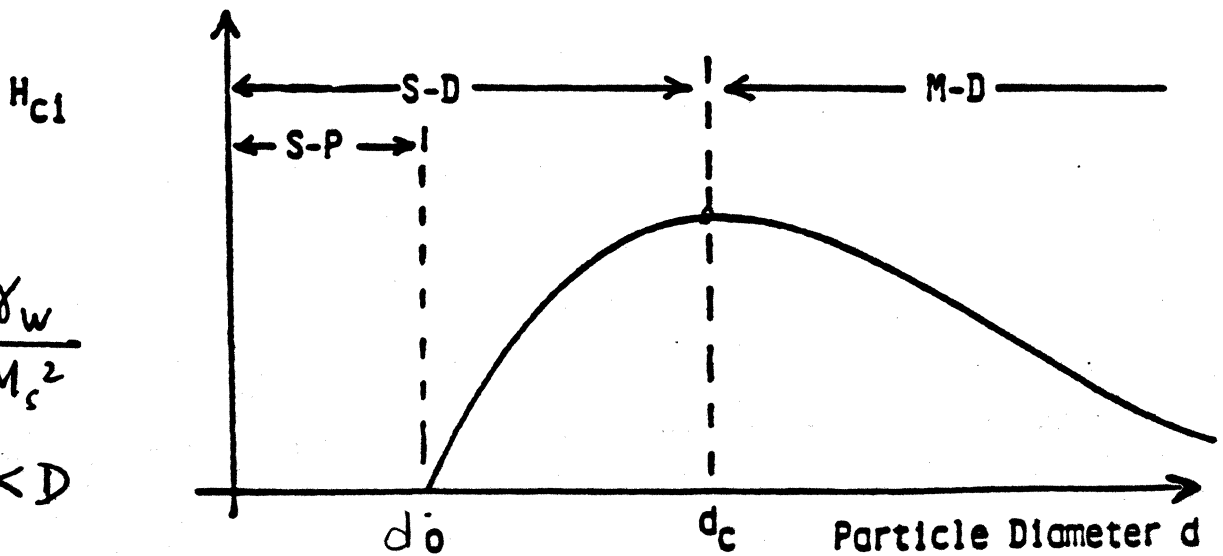
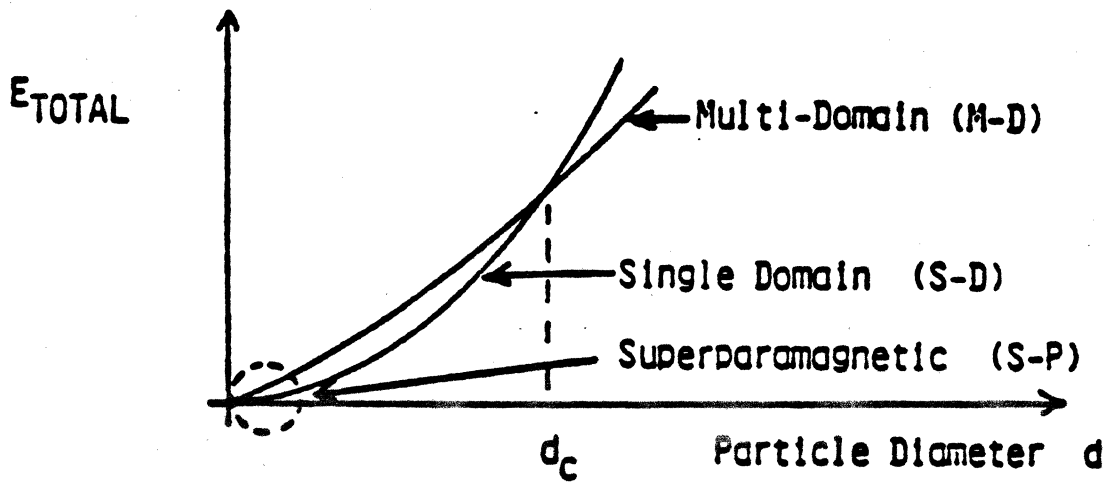
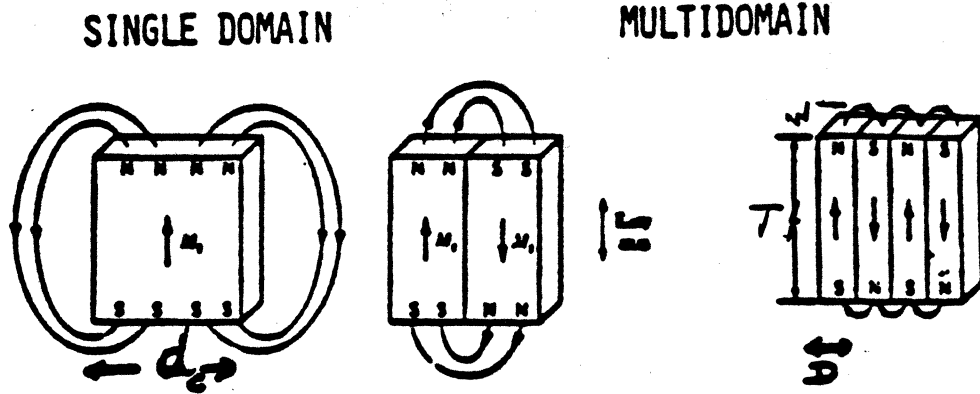
$$\delta_{min} = \sqrt{\frac{A_{EX}}{K}}$$

THE MINIMUM WALL ENERGY/WALL AREA IS

$$\gamma_{min} = 2 \sqrt{A_{EX} K}$$

$$\delta_{min} \approx \begin{matrix} Fe & Ni \\ 300 \text{ \AA} & 720 \text{ \AA} \end{matrix}$$

# SINGLE AND MULTIDOMAIN PARTICLES

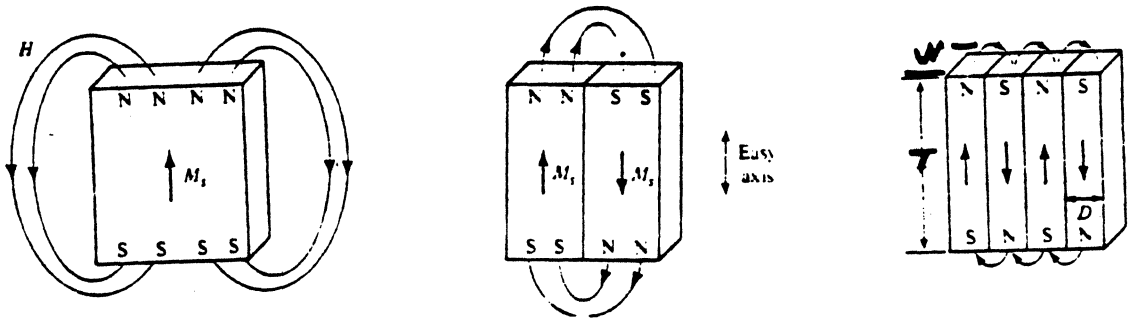


$$d_c = \frac{K \gamma_w}{\pi^2 M_s^2}$$

for  $\delta_w \ll D$

# MINIMUM MAGNETIC DOMAIN SIZE

ASSUME A UNIAXIAL SINGLE CRYSTAL WITH A PARALLEL-PLATE DOMAIN STRUCTURE WHICH IS EXPECTED TO EVOLVE IN MINIMIZING THE MAGNETOSTATIC DEMAGNETIZATION STRAY FIELD ENERGY.



THE TOTAL ENERGY PER UNIT AREA OF THE TOP OF THE CRYSTAL IS GIVEN BY

$$E_{\text{TOTAL}} = E_{\text{DEMAG}} + E_{\text{WALL}}$$

$$E_{\text{TOTAL}} = k M_S^2 D + \gamma_w \frac{T}{D}$$

WHERE  $k = 1.7$  FOR  $w =$  AND  $k = 1$  FOR  $w = D$  AND  $\gamma_w = 2\sqrt{A_{\text{ex}}}$

THE MINIMUM DOMAIN SIZE IS GIVEN BY

$$D_{\text{min}} = \sqrt{\frac{\gamma_w T}{k M_S^2}}$$

THE MINIMUM ENERGY PER UNIT SURFACE AREA IS GIVEN BY

$$E_{\text{min}} = 2\sqrt{k M_S^2 \gamma_w T}$$

Cobalt

$$M_S = 1422 \text{ emu/cm}^3$$

$$\gamma_w = 7.6 \text{ ergs/cm}^2$$

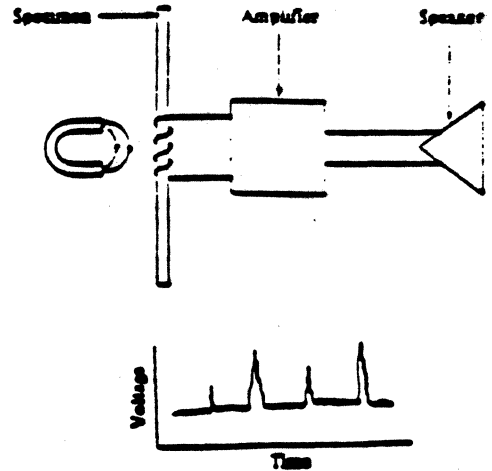
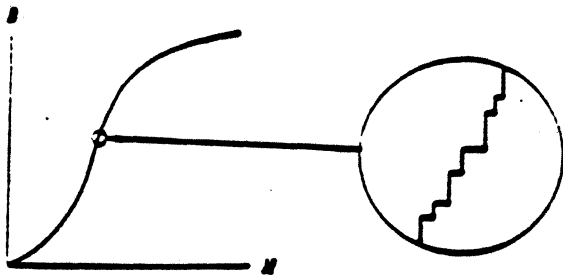
$$k = 1.7$$

$$T = 1 \mu\text{m}$$

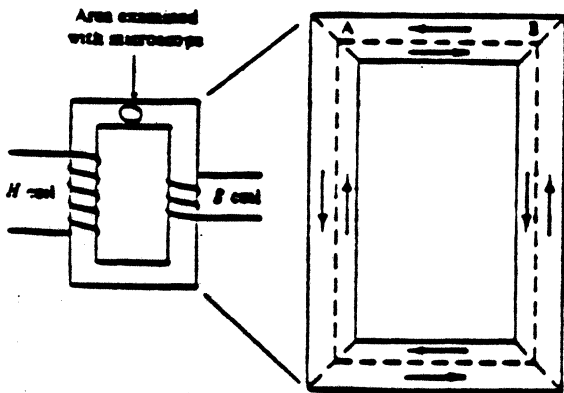
$$D_{\text{min}} \approx 1500 \text{ \AA}$$

# MAGNETIZATION BY WALL MOTION

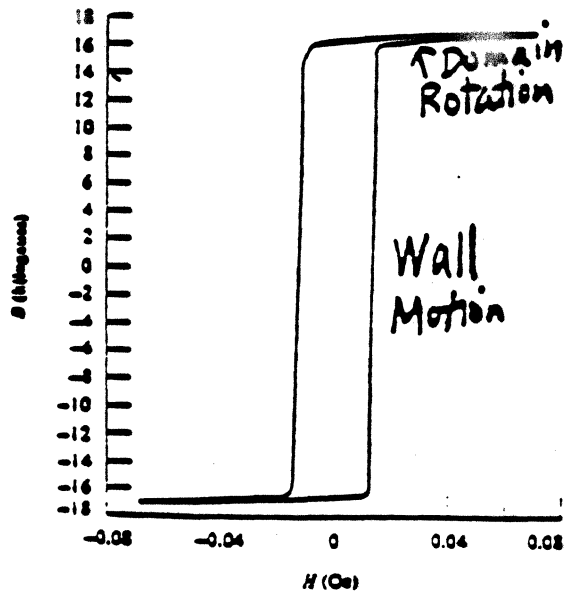
THE "BARKHAUSEN EFFECT" DEMONSTRATED IN 1919 THE EXISTENCE OF DOMAINS INDIRECTLY BY SHOWING DISCONTINUOUS WALL MOTION.



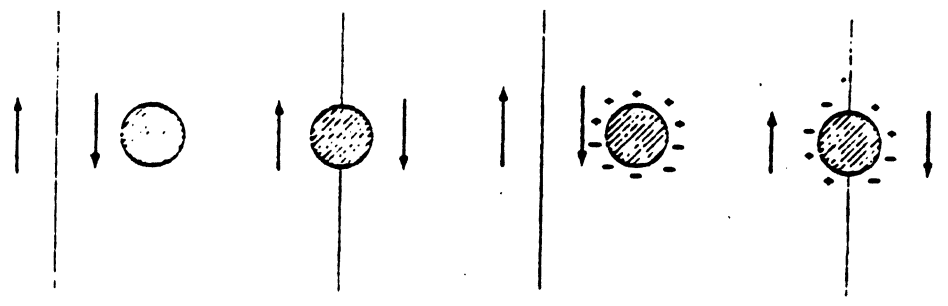
A DIRECT OBSERVATION OF MAGNETIC DOMAINS USING BITTER COLLOID WAS DISCLOSED BY WILLIAMS & SHOCKLEY & BOZORTH IN 1949. A BELL LABS MOVIE IS AVAILABLE FOR SHOWING THIS.



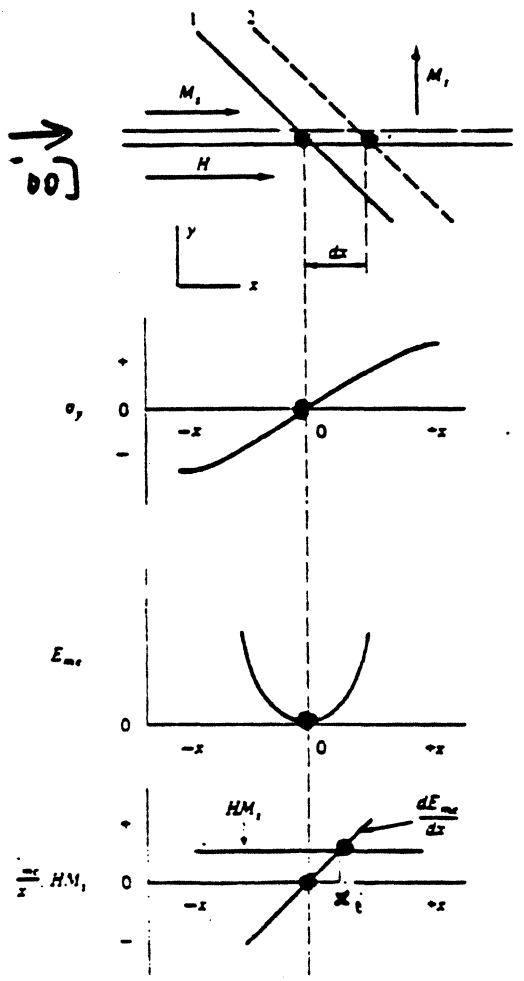
Magnetization results from 180° wall motion



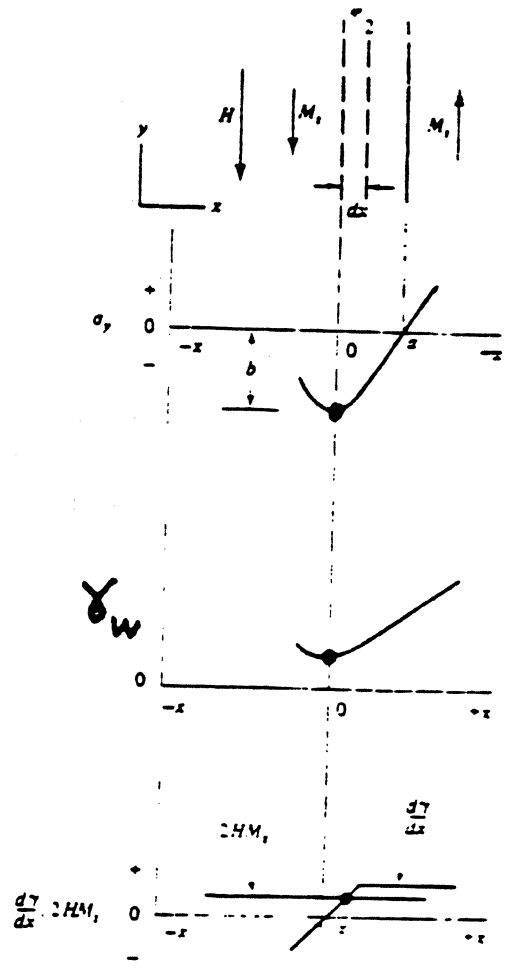
EFFECTS OF INCLUSIONS AND MICROSTRESSES ON WALL MOTION



90° WALL



180° WALL



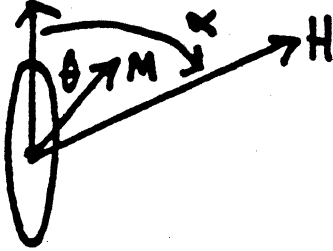
$\delta_w$  = wall thickness  
 $l$  = wavelength of microstresses

$$\frac{\lambda_R}{\lambda_{initial}} = 1 + \frac{2 M_s^2}{3 \lambda_{100} \frac{d\sigma_y}{dx} l}$$

$$\frac{\lambda_R}{\lambda_{initial}} = 1 + \frac{2 M_s^2}{3 \lambda_{100} \frac{d^2 \sigma_y}{dx^2} \delta_w l}$$

# MAGNETIZING BY DOMAIN ROTATION

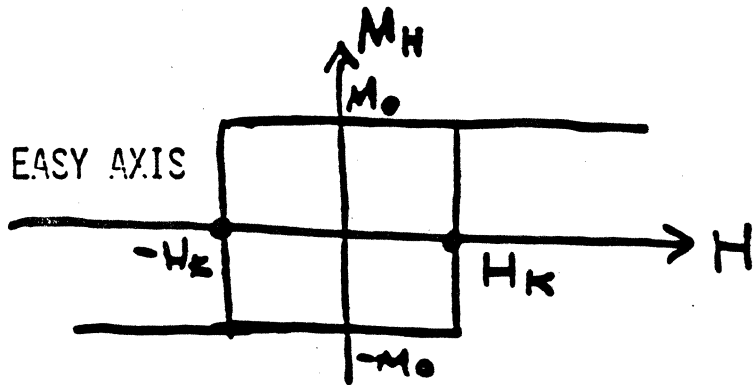
EASY AXIS



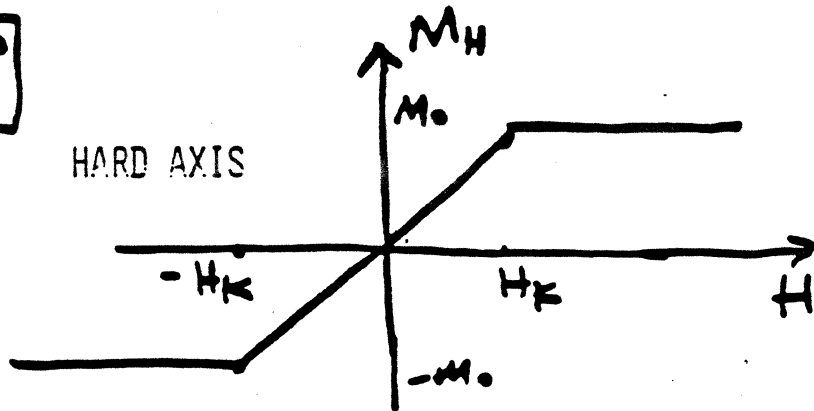
$$\text{ANISOTROPY ENERGY DENSITY} = K_u \sin^2 \theta$$

$$\text{ANISOTROPY FIELD} = 2 \frac{K_u}{M} = H_k$$

$$\alpha = 0$$



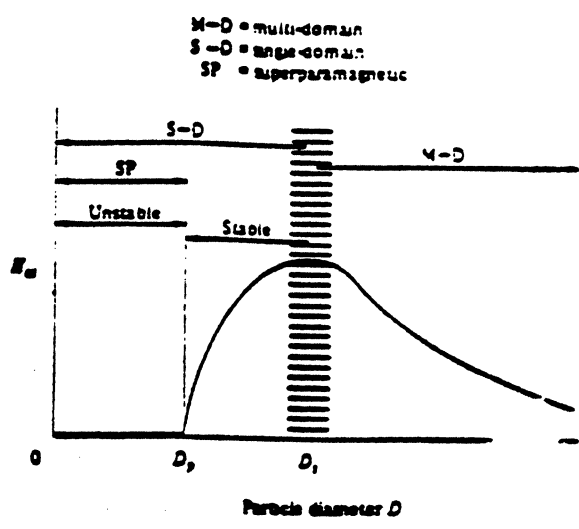
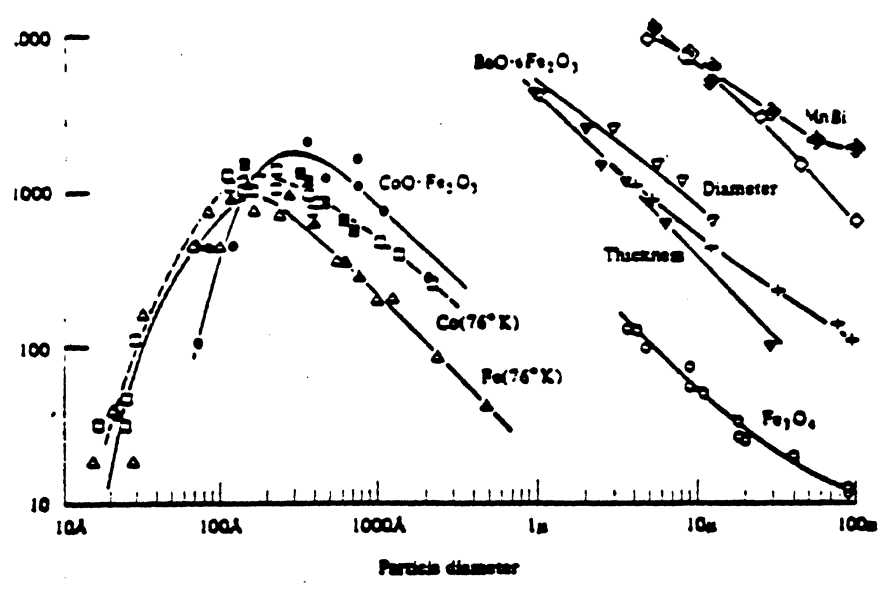
$$\alpha = 90^\circ$$



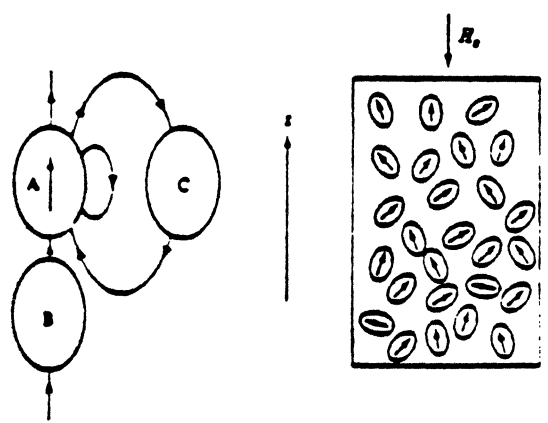


# FINE MAGNETIC PARTICLES

## A. COERCIVITY

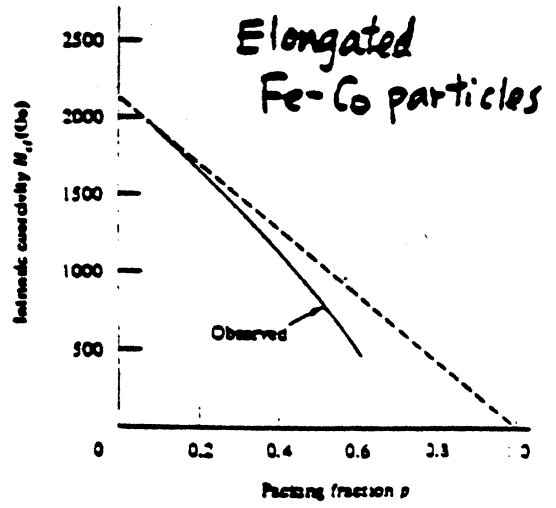


## B. PARTICLE INTERACTION



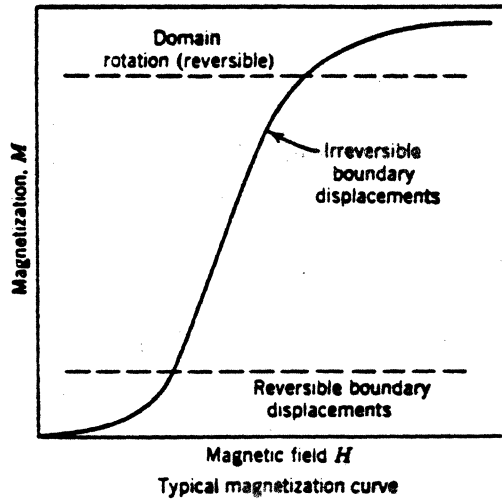
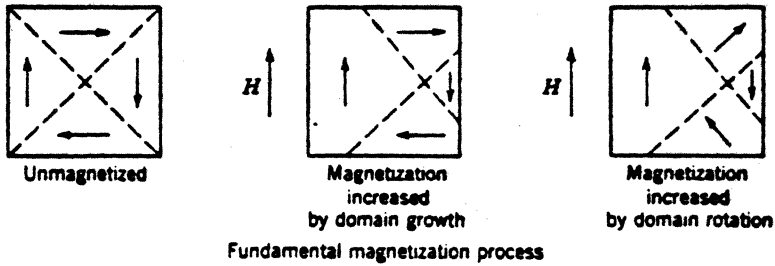
### ROTATION REVERSAL

1. COHERENT
2. INCOHERENT (FANNING, CURLING)

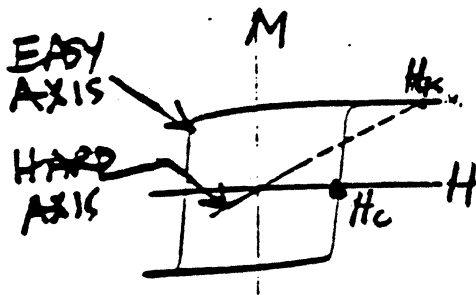


# MAGNETIZING PROCESSES

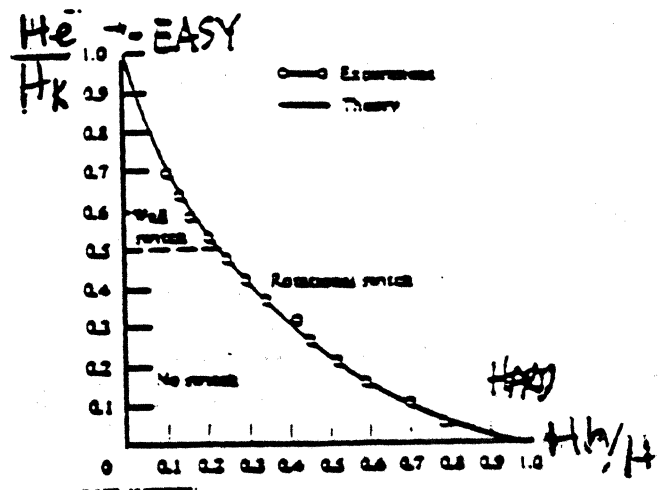
## DOMAIN WALL MOTION AND DOMAIN ROTATION



## THIN FILM HYSTERESIS LOOP AND SWITCHING



$$H_k = \frac{2K}{M_s}$$



FACTORS AFFECTING MAGNETIC PROPERTIES

1. COMPOSITION
2. TEMPERATURE
3. STRESS
4. SIZE, SHAPE, ORIENTATION  
OF GRAINS
5. CONCENTRATION AND DISTRIBUTION  
OF CRYSTAL IMPERFECTIONS
6. IMPURITIES

## MAGNETIC PROPERTIES

### A. INTRINSIC (STRUCTURE INSENSITIVE)

1. SATURATION MAGNETIZATION
2. CURIE TEMPERATURE

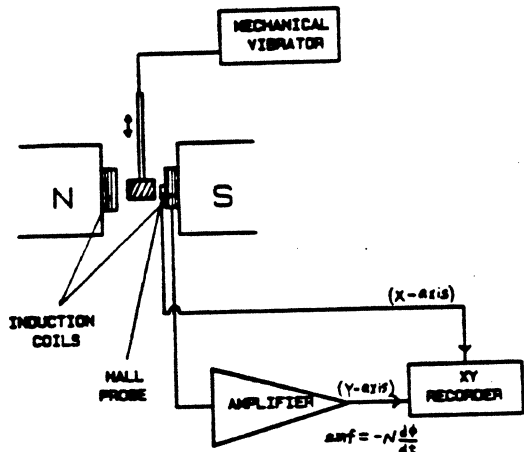
### B. EXTRINSIC (STRUCTURE SENSITIVE)

1. FLUX DENSITY (INDUCTION)
2. APPROACH TO SATURATION INDUCTION
3. PERMEABILITY
4. COERCIVE FORCE AND COERCIVITY
5. REMANENCE AND RETENTIVITY

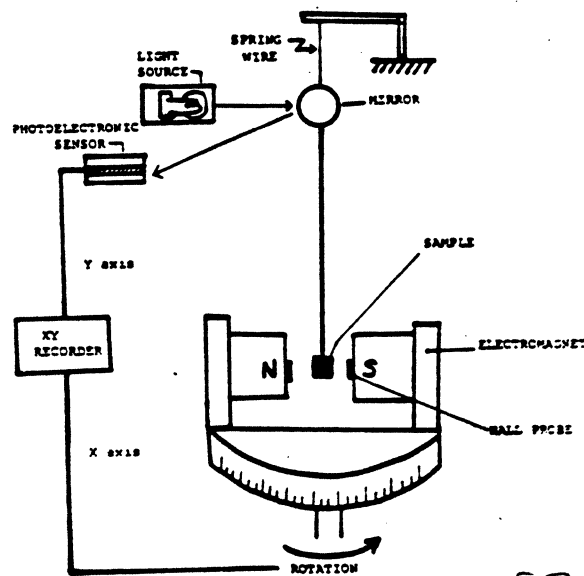
# MAGNETIZATION MEASUREMENT TECHNIQUES

## VIBRATING SAMPLE MAGNETOMETER

MEASURES  
MOMENT

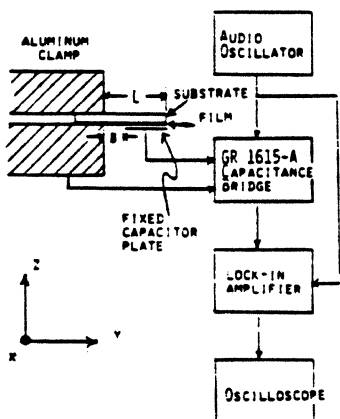


## TORQUE MAGNETOMETER

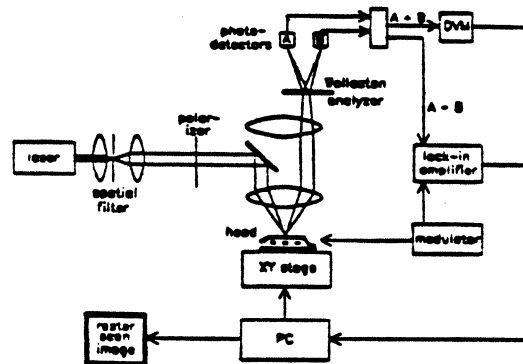


MEASURES  
"K"

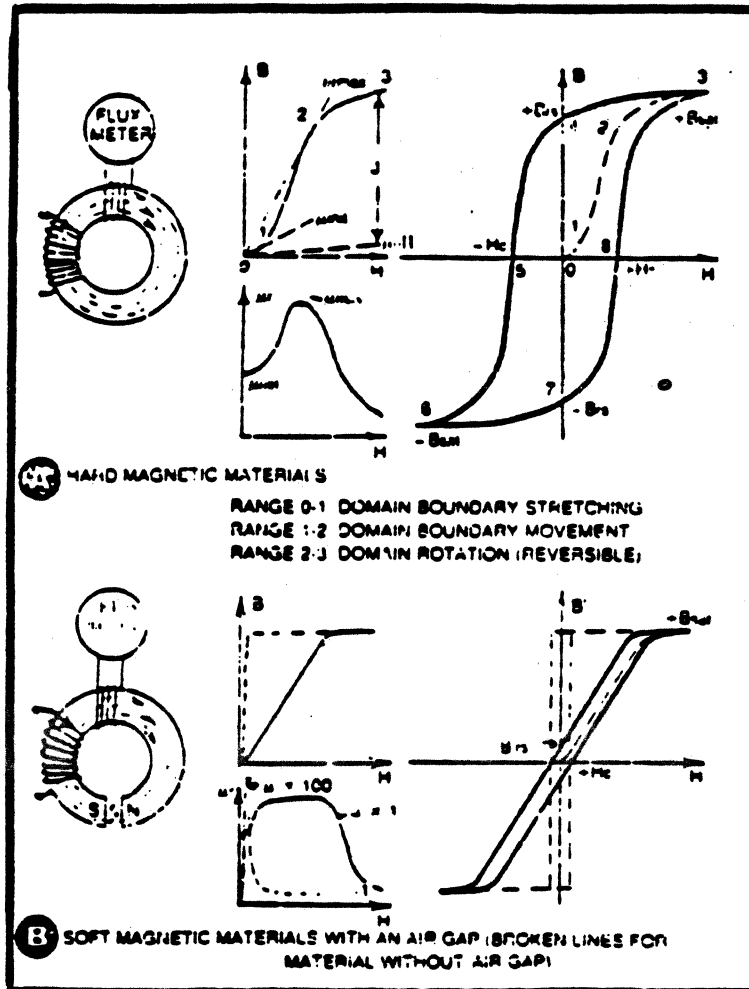
## MAGNETOSTRICTION MEASUREMENT



## Schematic of scanning Kerr microscope



# HYSTERESIS LOOPS OF HARD AND SOFT MATERIALS



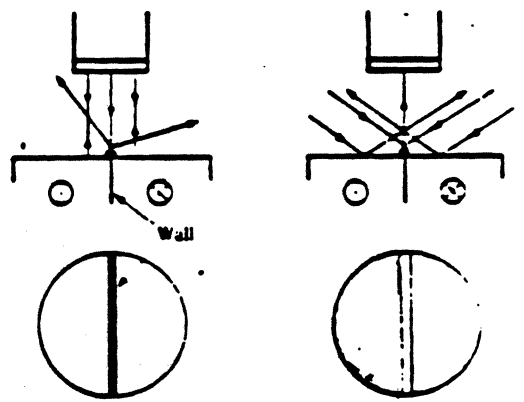
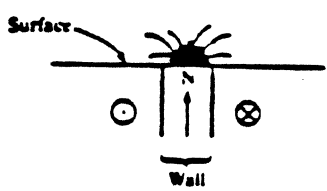
Magnetization curves and hysteresis loops.

# MAGNETIC DOMAIN AND WALL OBSERVATION TECHNIQUES

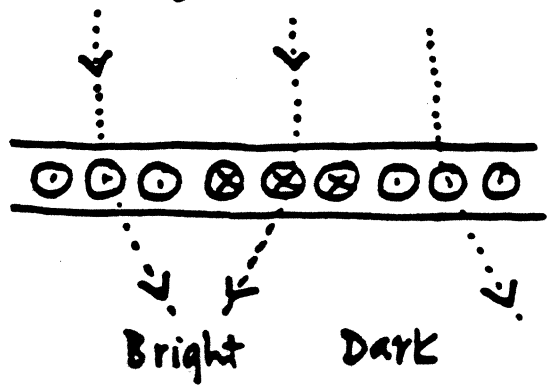
Method	Cause	Effect observed	Speed	Maximum magnification	Limitations
<b>TEM</b>	Bitter colloid	Walls (domains using extra applied fields)	Quasi-static	$\approx 1,000$ optically $\approx 10,000$ electron microscope	Possibility of interaction with sample. Static method
	Electron microscope (transmission)	Magnetization	Fast	$\approx 100 - \approx 20,000$ with diminishing sensitivity to magnetization with increasing magnification	Necessity of removing film from substrate
<b>ENM</b>	Electron microscope (reflection)	Walls	Fast	—	Complex to interpret
	Kerr effect	Magnetization	Fast	$\approx 250$	Low contrast
	Faraday effect	Magnetization	Fast	$\approx 400$	Useful only for extremely thin films

**SEM**  
**SEMPA**

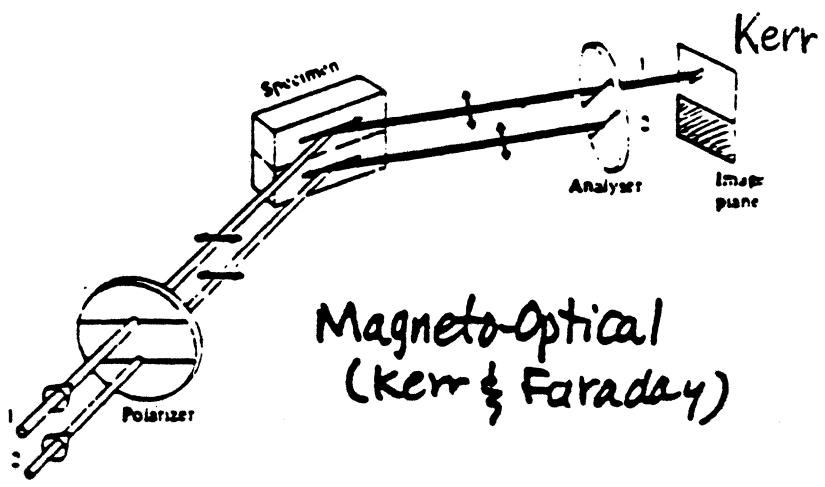
## Bitter Colloid



## Lorentz Electron Microscopy



(TEM, SEM, ENM)  
SEMPA



# THIN FILM DEPOSITION TECHNIQUES

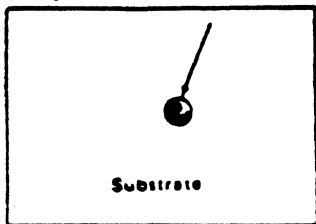
	<u>EVAPORATION</u>	<u>ION PLATING</u>	<u>SPUTTERING</u>
Mechanism of Production of Depositing Species	Thermal Energy	Thermal Energy	Momentum transfer
Deposition Rate	Can be very high (up to 750,000 Å/min.)	Can be very high (up to 250,000 Å/min.)	Low except for pure metals (e.g. Cu = 10,000 Å/min.)
Depositing Specie	Atoms and Ions	Atoms and Ions	Atoms and Ions
Throwing Power for:			
a. Complex Shaped Object	Poor line-of-sight coverage except by gas scattering.	Good, but nonuniform thickness distributions.	Good, but nonuniform thickness distribution.
b. Into Small Blind Holes	Poor	Poor	Poor
Metal Deposition	Yes	Yes	Yes
Alloy Deposition	Yes	Yes	Yes
Refractory Compound Deposition	Yes	Yes	Yes
Energy of Depositing Species	Low = 0.1 to 0.5 eV	Can be high (1-100 eV)	Can be high (1-100 eV)
Bombardment of Substrate/Deposit by Inert Gas Ions	Not normally	Yes	Yes or no depending on geometry.
Growth Interface Perturbation	Not normally	Yes	Yes
Substrate Heating (by external means)	Yes normally	Yes or No	Not generally

	<u>CHEMICAL VAPOR DEPOSITION</u>	<u>ELECTRODEPOSITION</u>	<u>THERMAL SPRAYING</u>
Mechanism of Production of Depositing Species	Chemical Reaction	Deposition from Solution	From Flames or Plasma
Deposition Rate	Moderate (200 - 3500 Å/min.)	Low to High	Very high
Depositing Specie	Atoms	Ions	Droplets
Throwing Power for:			
a. Complex Shaped Object	Good	Good	No
b. Into Small Blind Holes	Limited	Limited	Very Limited
Metal Deposition	Yes	Yes - Limited	Yes
Alloy Deposition	Yes	Quite Limited	Yes
Refractory Compound Deposition	Yes	Limited	Yes
Energy of Depositing Species	Can be high with Plasma-aided CVD	Can be high	Can be high
Bombardment of Substrate/Deposit by Inert Gas Ions	Possible	No	Yes
Growth Interface Perturbation	Yes (by rubbing)	No	No
Substrate Heating (by external means)	Yes	No	Not normally

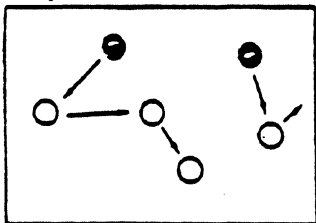


# FORMATION OF A THIN FILM

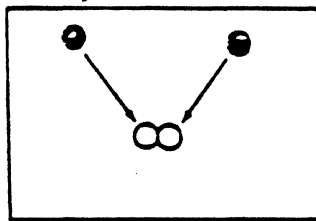
(a) Single Atom Arrives



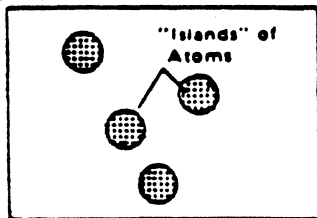
(b) Migration Re-evaporation



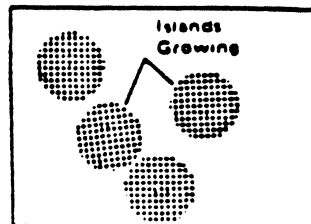
(c) Collision & Combination of Single Atoms



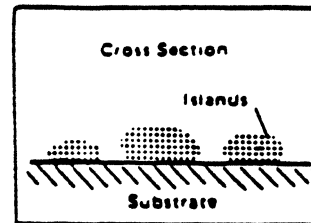
(d) Nucleation



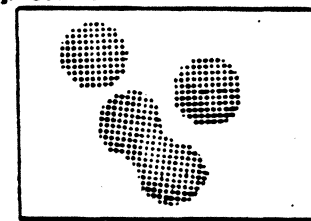
(e) Growth



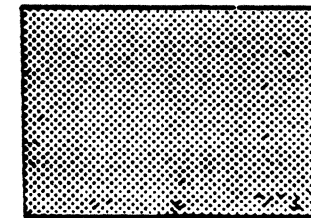
(f) Island Shape



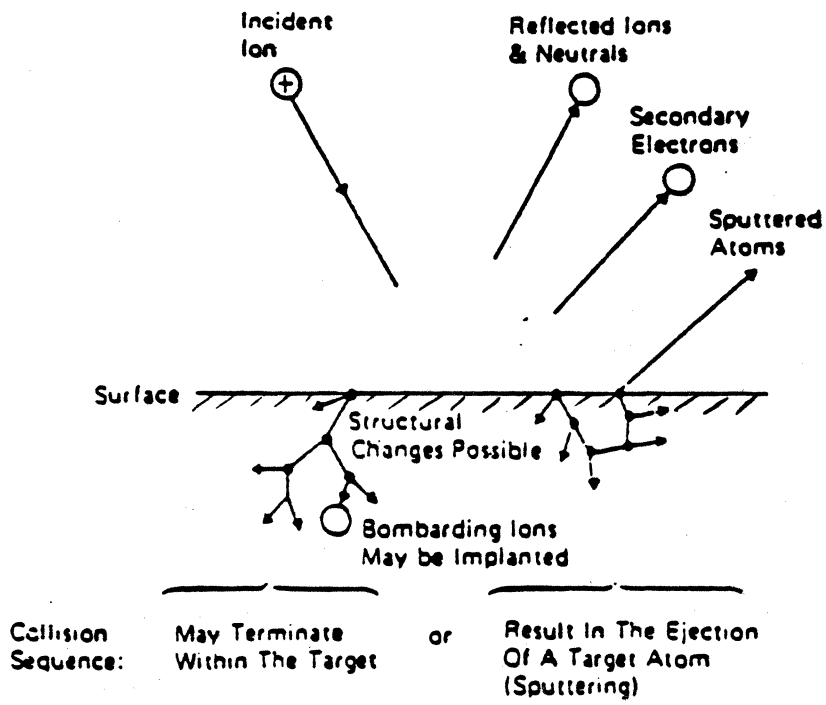
(g) Coalescence



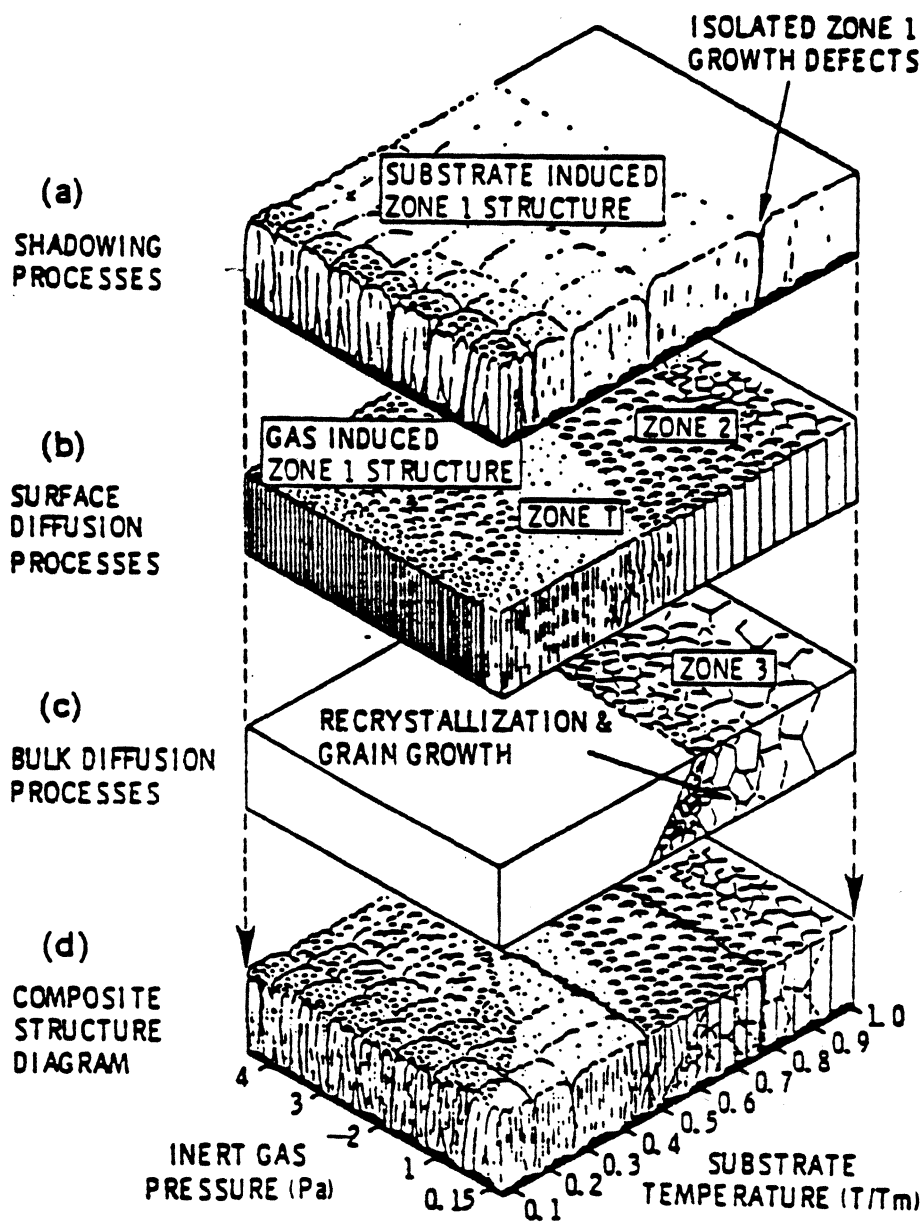
(h) Continuity



# SPUTTERING PROCESSES



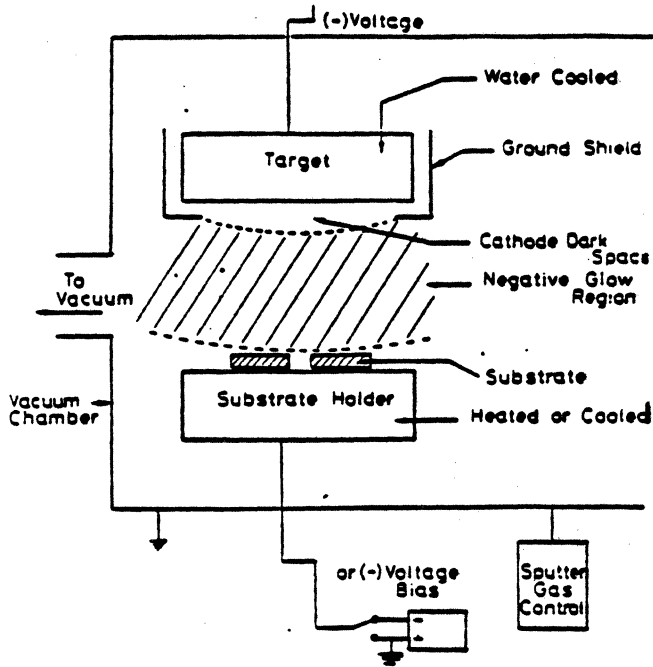
# PHYSICAL PROCESSES OF MICROSTRUCTURE ZONES



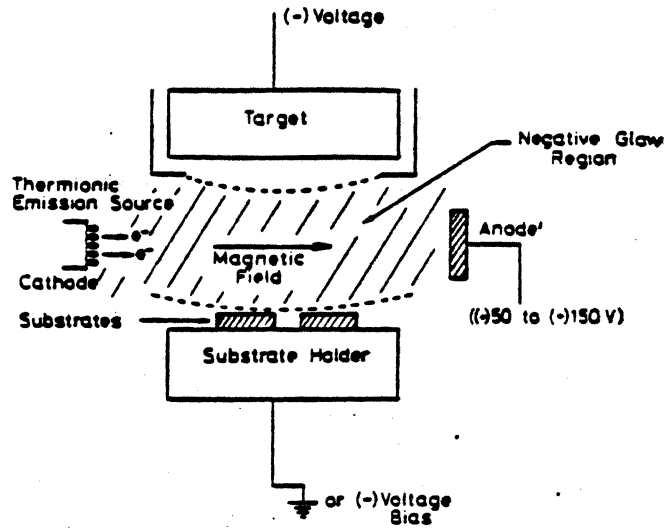
J. THORNTON

# THIN FILM SPUTTERING TECHNIQUES

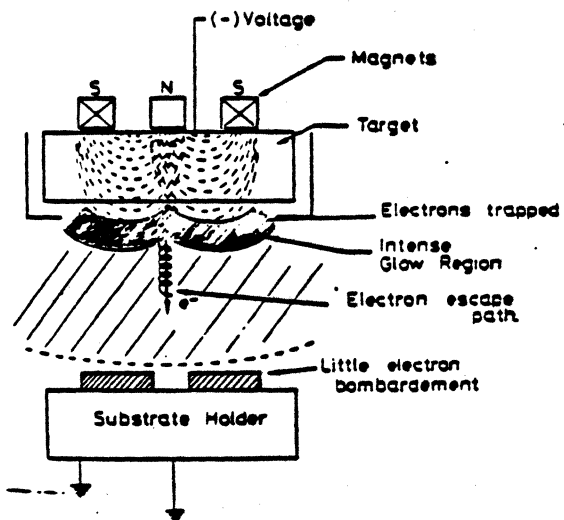
RF DIODE SPUTTERING WITH BIAS



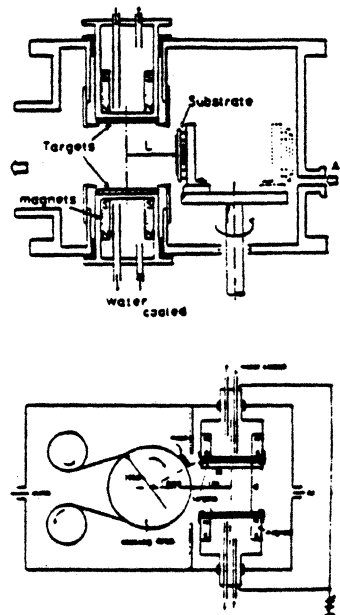
TRIODE SPUTTERING WITH BIAS



DC OR RF MAGNETRON SPUTTERING



FACING TARGET SPUTTERING



# THIN FILM MATERIALS CHARACTERIZATION TECHNIQUES

DETECTED EMISSION		OPTICAL	X-RAYS	ELECTRONS	IONS (+ AND -)
PRIMARY EXCITATION					
PHOTONS	OPTICAL	"AA": ATOMIC ABSORPTION "IR": INFRARED } SPEC. VISIBLE } TROS "UV": ULTRAVIOLET } COPY		"ESCA": ELECTRON SPECTR. F. CHEMICAL ANALYSIS	"UPS": VAC. UV PHOTOELECTRON SPECTROSCOPY - OUTER SHELL
	X-RAYS		X-RAY FLUORESCENCE SPECTROMETRY X-RAY DIFFRACTION		"XPS": X-RAY PHOTOELECTRON SPECTROSCOPY - INNER SHELL
ELECTRONS			"EPMA": ELECTRON-PROBE MICROANALYSIS	"AES": AUGER ELECTRON SPECTROSCOPY "SAM": SCANNING AUGER MICROANALYSIS	
IONS (+ AND -)		"SCANIR": Surf. Comp. by Anal. of Neutral and Ion Impact Radiation)	(Ion-Induced X-Rays)		"SIMS": SECONDARY ION MASS SPECTROMETRY "IPM": ION-PROBE MICROANALYSIS "ISS": ION SCATTERING SPECTROMETRY ("RBS": Rutherford Backscattering Spectrometry)
RADIATION		"ES": EMISSION SPECTROSCOPY			"SSMS": SPARK SOURCE MASS SPECTROGRAPHY

Characteristic	AES	XPS	ISS	SIMS	RBS	NRA	IX
<b>Elemental Analysis</b>							
Sens. Varia.	Good	Good	Good	Poor	Fair	Fair	Good
Resolution	Good	Good	Fair	Good	Fair	Good	Good
Detection Limits	0.1%	0.5%	0.1%	10 <sup>-4</sup> % or higher	10 <sup>-3</sup> or higher	10 <sup>-2</sup> or higher	10 <sup>-2</sup> or higher
Quantification	← with difficulty → req. standards			very difficult req. standards	← absolute → no standards		
Chemical State	Yes	Yes	No	Yes	No		
Depth Analysis	← Destructive → sputter			← Non-destructive →			very difficult
Depth Resolution	← Atomic layer to → % of sputter depth				10 nm	10 nm	None
Lateral Resolution	200nm	2nm	100µm	100-1µm	← 1µm →		
Sample Alteration	High for Alkali Halogen Organic Insulators	← Low →			← Very Low →		

# MATERIALS FOR THIN FILM HEADS

## METALS FOR HEADS

SOFT MAGNETIC MATERIALS FOR MAGNETIC HEADS						
	Compo- sition	Permeabilities		Coer- civity	Saturat. Induct.	Resist.
		$\mu_{ini}$	$\mu_{max}$	$H_c$ Oersted	$B_s$ Gauss	$\rho$ $\mu\Omega \cdot cm$
Permalloy	79 Ni 17 Fe 4 Mo	20,000	100,000	0.05	8,700	55
Mu-Metal	77 Ni 16 Fe 5 Cu 2 Cr	30,000	100,000	0.02	7,500	55
Hi-Mu 800B	80 Ni 16 Fe 4 Mo	70,000	250,000	0.008	8,000	68
Sandust	85 Fe 9 Si 6 Al	10,000		0.08	10,000	90

(F. Jorgensen)

name	Approximate composition (weight percent)			Initial permeability	Maximum perme- ability	Coercivity $H_c$ (Oe)	$B_s$ (gauss)	$T_c$ (°C)	Resistivity (microhm-cm)
	Ni	Fe	Other						
Low-Cost Alloys									
iron	-	100	-	150	5,000	1.0	21,500	770	10
silicon iron	-	96	4 Si	500	7,000	0.5	19,700	690	60
grain-oriented silicon iron	-	97	3 Si	1,500	40,000	0.1	20,000	740	47
High-Permeability Alloys									
Permalloy	78	22	-	8,000	100,000	0.05	10,900	580	16
permalok	90	90	-	4,000	70,000	0.05	16,000	500	49
79 Permalloy	79	17	4 Mo	20,000	100,000	0.05	8,700	460	55
mu-metal	77	16	5 Cu, 2 Cr	20,000	100,000	0.05	6,500		62
permalloy	79	16	5 Mo	100,000	1,000,000	0.002	7,900	400	60
High-Saturation Alloys									
permendur	-	50	50 Co	800	5,000	2.0	24,500	980	7
Permendur	-	49	49 Co, 2 V	800	4,000	2.0	24,500	980	27
pervac	-	64	35 Co, 0.5 Cr	650	10,000	1.0	24,200	970	28
permendur	-	49	49 Co, 2 V		60,000	0.2	24,000	980	27

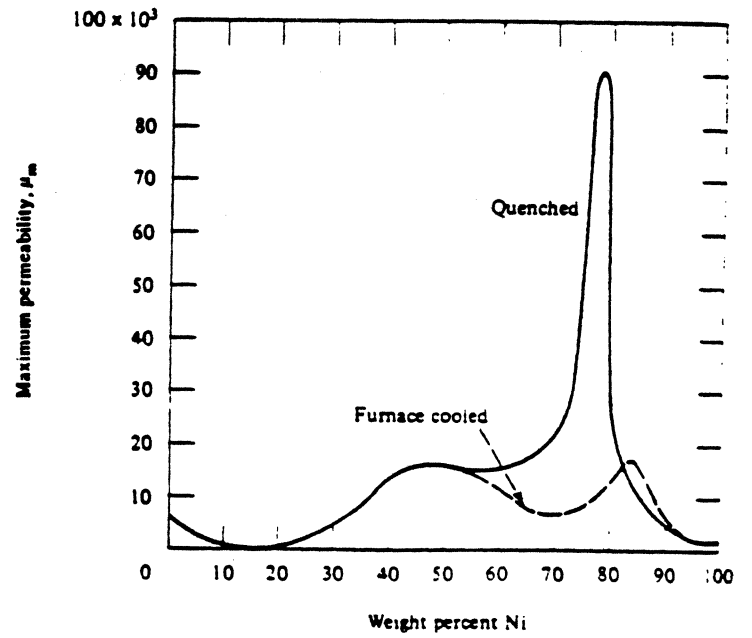
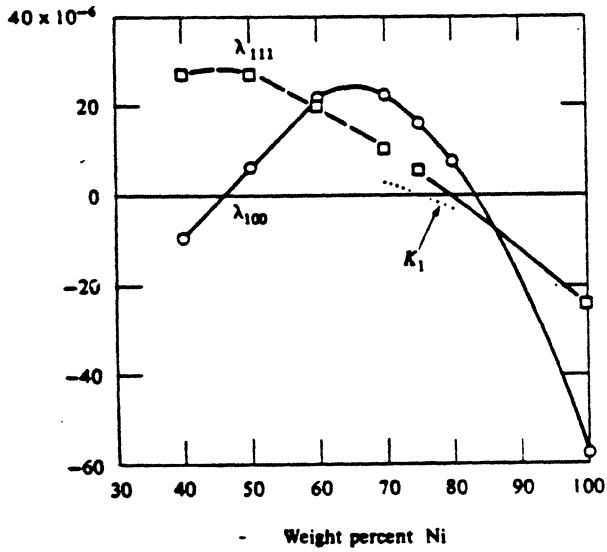
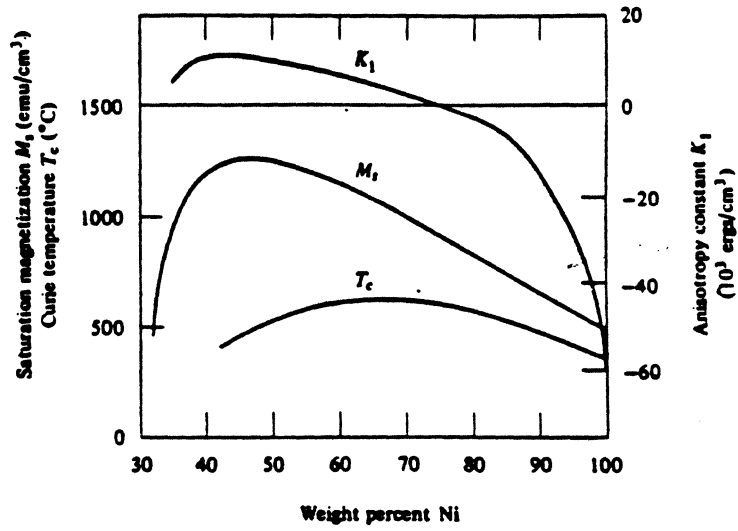
(Cullity)

$$\mu_{wall} \propto \frac{M_s^2}{K_{eff}}$$

$$\mu_{ROT} \propto \frac{M_s^2 d}{\sqrt{K_{eff}}}$$

$d = \text{grain diameter}$

# MAGNETIC PROPERTIES OF NI FE ALLOYS



(Curiosity)

3

## PROPERTIES OF AMORPHOUS MAGNETIC THIN FILMS FOR MAGNETIC RECORDING HEADS

Alloy film (at. %)	$4\pi M_s$ (kG)	$H_c$ (Oe)	$H_k$ (Oe)	$\lambda$ (10 <sup>3</sup> )	$\rho$ ( $\mu\Omega$ cm)
(1) Fe <sub>77</sub> B <sub>23</sub>	14	≤ 0.1	7	50	
(2) Fe <sub>80</sub> B <sub>20</sub>	-15	-0.04°	7		
(3) Fe <sub>70</sub> Si <sub>30</sub>	12	≤ 0.1	5	30	
(4) Fe <sub>77</sub> Si <sub>23</sub>	12	0.2	4	30	140
(5) Fe <sub>77</sub> C <sub>23</sub>	13	< 1.0°	< 100°	10-13	
(6) Fe <sub>80</sub> N <sub>20</sub>	9-12	< 100			
(7) Co <sub>83</sub> Ti <sub>17</sub>	9-10	≤ 0.45	14°	1.5	-130
(8) Co <sub>83</sub> Ta <sub>17</sub>	9-10	5-30			
(9) Co <sub>93</sub> Zr <sub>7</sub>	14-15	0.2°	2-5°	1-3	
(10) Co <sub>92.6</sub> Zr <sub>7.4</sub>	13	1.0			120-170
(11) Co <sub>93</sub> Hf <sub>7</sub>	14-15	0.3°	2-5°		
(12) Fe <sub>77</sub> B <sub>21</sub> Si <sub>6</sub>	12	-0.2	6	26	
(13) Fe <sub>80</sub> B <sub>15</sub> C <sub>5</sub>	14-16	≤ 1°	-10°		
(14) Fe <sub>77</sub> Si <sub>18</sub> C <sub>5</sub>	16-17	-0.2°	-7°		
(15) Co <sub>70</sub> Fe <sub>3</sub> B <sub>20</sub>	10-11	< 1	-0	< 1	
(16) Co <sub>70</sub> Fe <sub>3</sub> B <sub>15</sub>	11-13	0.05	-3°	-0.2	90
(17) Co <sub>70</sub> Fe <sub>3</sub> B <sub>15</sub> Mo	14-15	0.05	18	-0	
(18) Co <sub>83</sub> Ti <sub>12</sub> B <sub>5</sub>	8-9	0.03	10	-0	
(19) (CoFeB) <sub>90</sub> Cr <sub>10</sub>	10	-2	≤ 1000		115
(20) Co <sub>83</sub> Fe <sub>7</sub> Nb <sub>10</sub>	14	≤ 0.5			
(21) Co <sub>70</sub> Er <sub>10</sub> Nb <sub>20</sub>	14	0.25	2	0.1	

\* Annealed (field).

J.K. Howard  
J. Vac. Sci. Tech  
A4, 1-3 (1986)

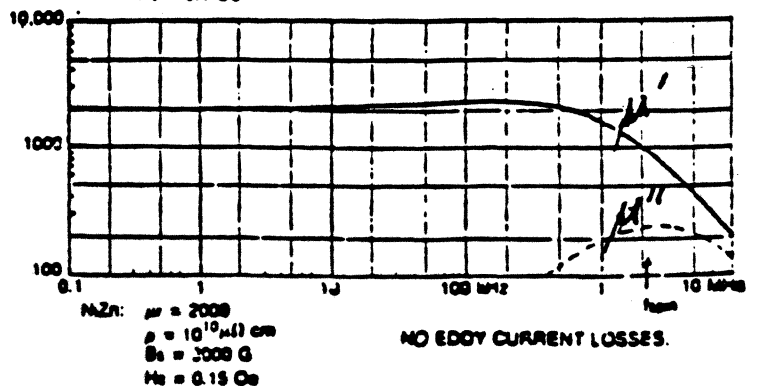
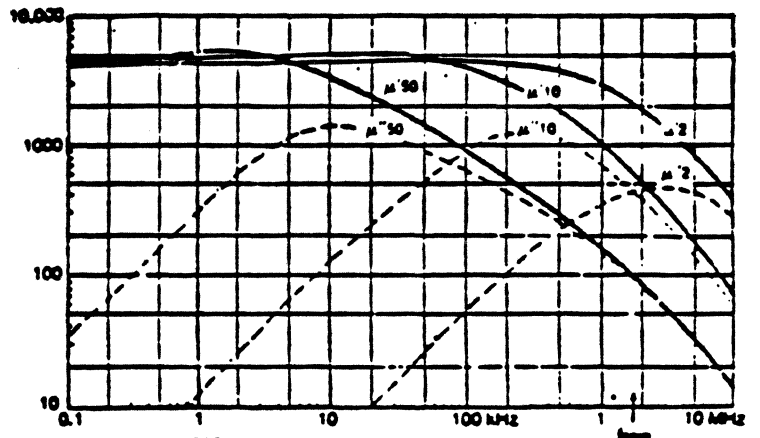


# FERRITES FOR HEADS

Properties	STANDARD FERRITE MATERIALS												LINEAR TEMPERATURE COEFFICIENT FERRITE MATERIALS			
	Symbol	Units	0-0	0-0	2-1	0-3	0	0-1	0-2	0-3	0-2	TC-7	TC-6	TC-3	TC-1	
Initial permeability	$\mu$	---	100 4700**	100 3000	100 2000	100 1500	1 850	1 125	1 40	1 16	1 430	100 1400	100 1300	100 1000	1 95	
Maximum permeability	$\mu_{max}$	---	6000	4000	3600	4000	4300	400	115	42	6000	1850	2600	2000	420	
Saturation flux density @ $H = 25$ oersteds	$B_s$	Gauss	4700	4700	4400	4500	3400	3300	2400	2600	3700	3500	4000	3600	3300	
Residual magnetism	$B_r$	Gauss	1400	1000	1000	1600	1470	1900	750	1470	2500 @ 0.C. $H_r = 1$ oersted	550	1600	700	2300	
Coercive force	$H_c$	Oersteds	0.10	0.12	0.18	0.15	0.18	2.1	4.7	21	36 @ 0.C.	0.25	0.42	0.25	3.2	
Temperature coefficient between +25°C to +80°C	T.C.	%/°C	---	---	---	0.32	0.05	.1 max.	.1 max.	.1 max.	---	0.8 to 2.2	...	0.8 to 3.5	3.5 to 6.5	
Curve point	T.	+°C	210	215	180	198	150	350	450	500	210	140	180	185	425	
Volume resistivity	$\rho$	Ω-Cm	LOW	LOW	LOW	LOW	MED.	HIGH	HIGH	HIGH	LOW	LOW	LOW	LOW	HIGH	
Loss factor x 10 <sup>-4</sup> 100 kc/s 1 MC/s 10 MC/s 50 MC/s 150 MC/s		1/μB	6	7	25	33	300	20 60	85 170	420	---	5	6.7 80	2.3	47	
Frequency range	Max.		400 mc	400 mc	400 mc	400 mc	1 mc	10 mc	50 mc	225 mc	---	500 mc	500 mc	1.5 mc	20 mc	
Configurations (special configurations on request)			Toroids Resistor Heads	Toroids, E. I. U. Cores, Cap. Resh. Powder	SAME	SAME	SAME	SAME	SAME	SAME	Toroids, E. I. U. Cores, Caps	Toroids, Cap Cores	SAME	SAME	SAME	

- \* Temperature Factor (TF) x 10<sup>4</sup> is Equal To  $\Delta\mu/\mu^\circ C$
- \*\* The Tolerance Of 0-6 Initial Permeability = ±1600
- \*\*\* Not to exceed = 7.5% from 0° C to + 80° C

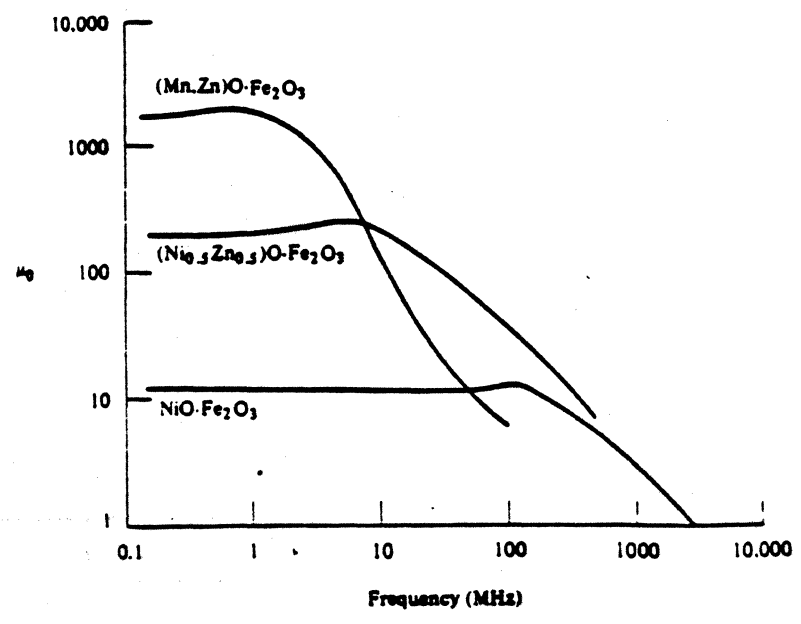
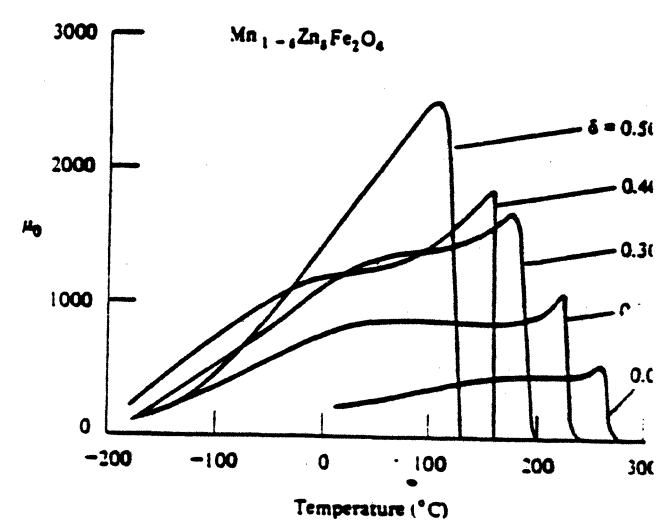
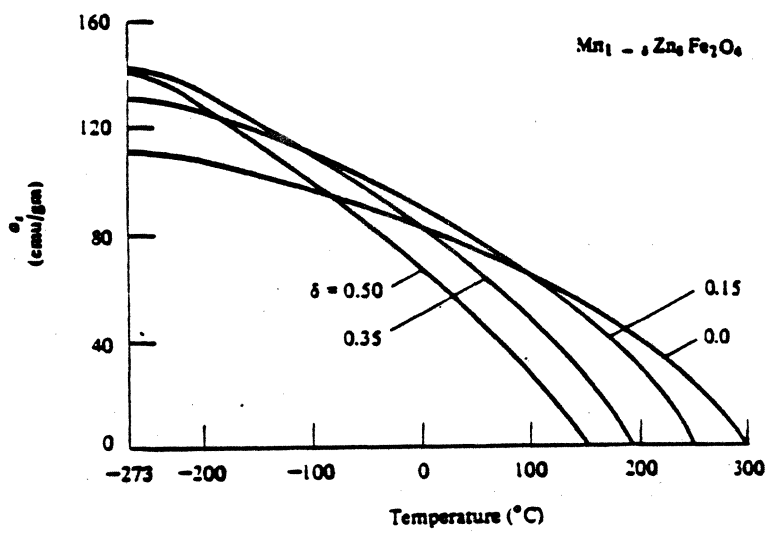
PERMEABILITY SPECTRA FOR MANGANESE-ZINC AND NICKEL-ZINC FERRITE



	$\mu_{max}$	$H_c$ (Oe)	$B_s$ (G)	$\rho$ ( $\mu\Omega\text{-cm}$ )	
Mn-Zn	2-5,000	5-10,000	0.05	4-8,000	$> 10^8$
Ni-Zn	2,000	2,000	0.15	3,000	$> 10^{10}$
Mn-Zn	3-10,000	7-20,000	0.02	4-8,000	$> 10^8$
			-0.15		

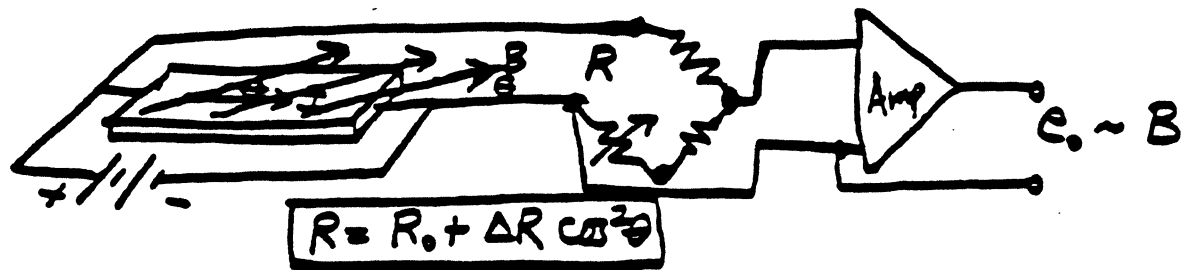
# MAGNETIC PROPERTIES OF FERRITES

Composition (mole %)		Sat. ind. (gauss)	Cure temp. (°C)	Initial perm. (gm Oe <sup>-1</sup> )	Density (gm cm <sup>-3</sup> )	Coercive force (Oe)	Resistivity (ohm cm)
<b>MnFe<sub>2</sub>O<sub>4</sub> ZnFe<sub>2</sub>O<sub>4</sub></b>							
48	52	3300	100	1400	4.9	0.2	20
58	42	4500	150	900	4.9	0.3	50
62	38	4700	150	1100	4.9	0.4	80
79	21	5100	210	700	4.8	0.5	80
<b>NiFe<sub>2</sub>O<sub>4</sub> ZnFe<sub>2</sub>O<sub>4</sub></b>							
36	64	3600	125	650	4.9	0.4	10 <sup>5</sup>
50	50	4200	250	230	4.5	0.7	10 <sup>5</sup>
64	36	4100	350	90	4.2	2.1	10 <sup>5</sup>
80	20	3600	400	45	4.1	4.2	10 <sup>5</sup>
100	—	2300	500	17	4.0	11.0	10 <sup>5</sup>



(Cullity)

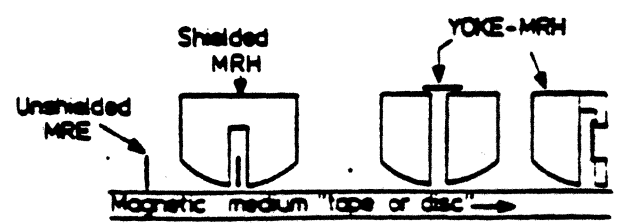
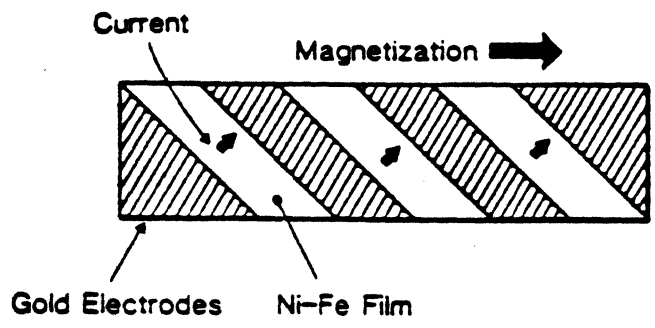
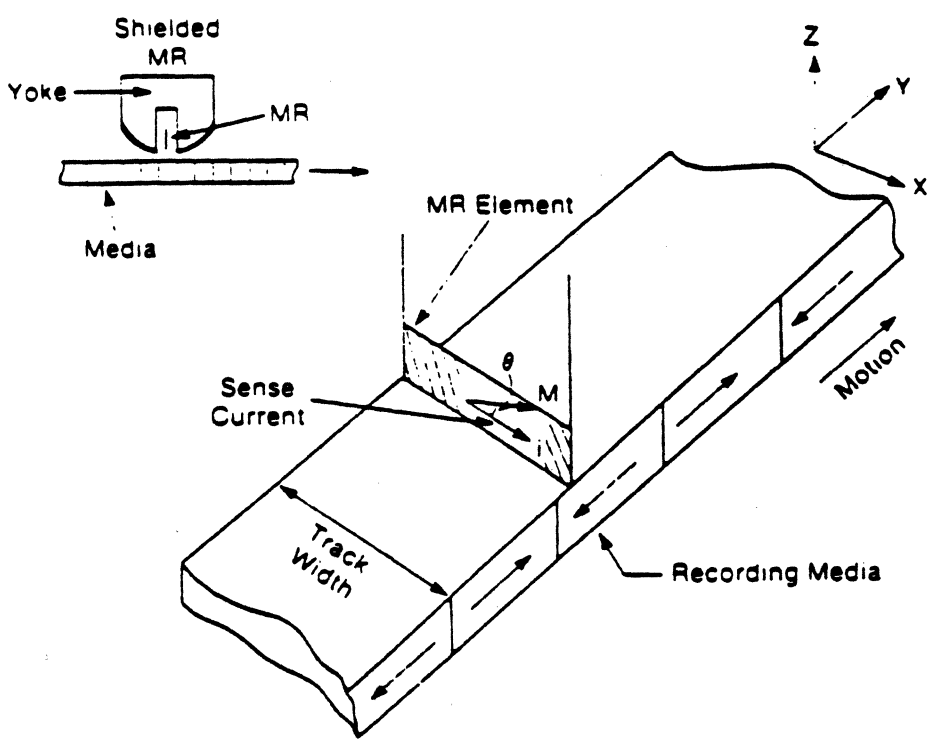
# MAGNETORESISTIVE EFFECT FOR THIN FILM READ HEADS



$$R = R_0 + \Delta R \cos^2 \theta$$



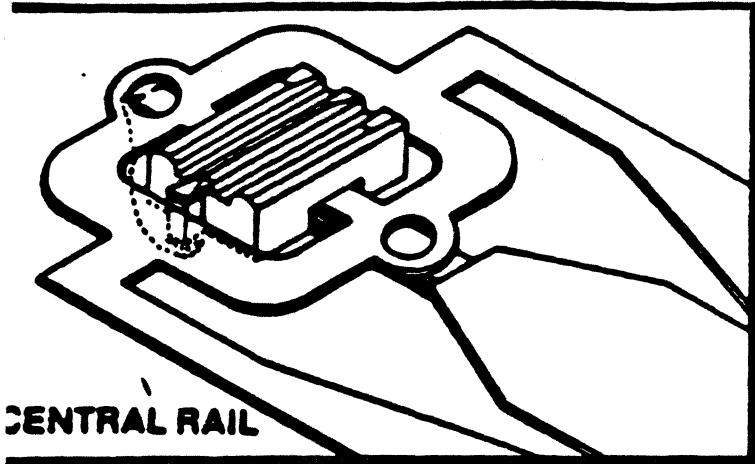
$\frac{\Delta R}{R_0} = 0.02$  for Permalloy ( $\text{Ni}_{0.8}\text{Fe}_{0.2}$ )



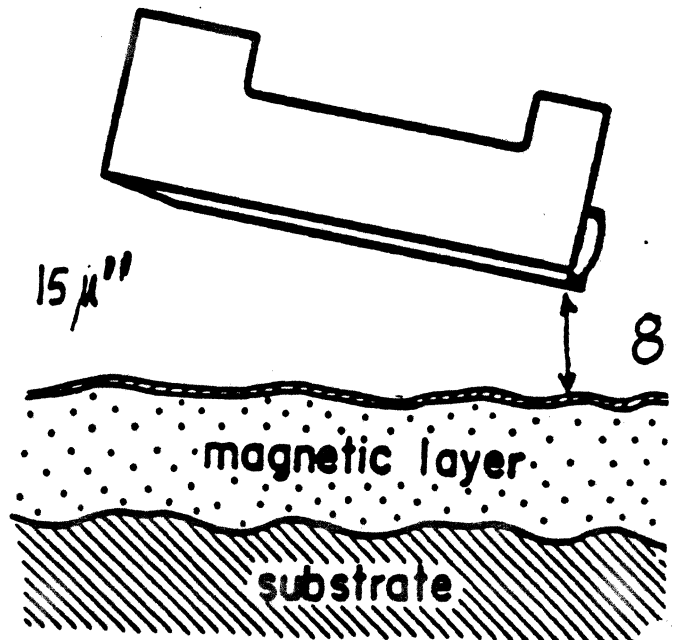
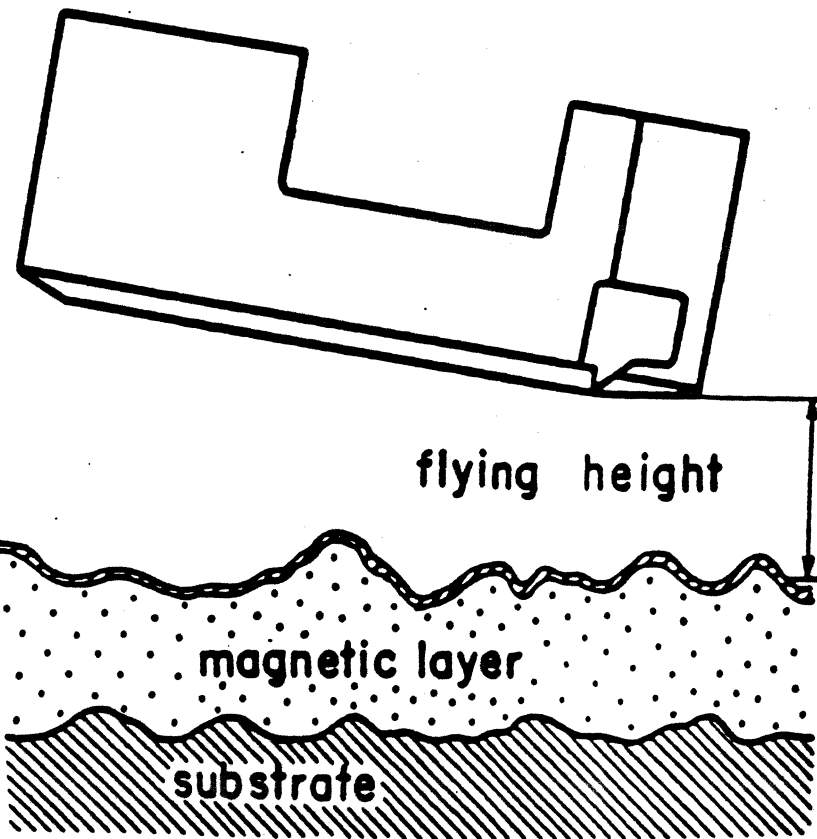
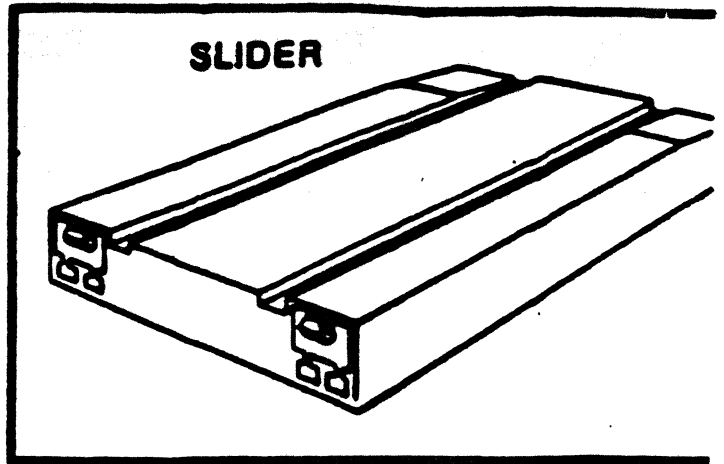
"Barber-pole" magnetoresistive element.

# THIN FILM HEAD VS FERRITE

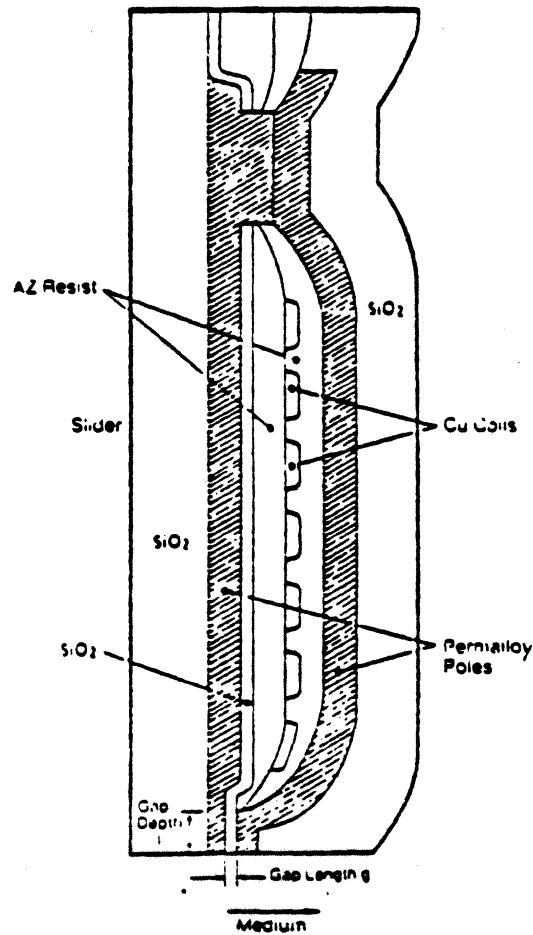
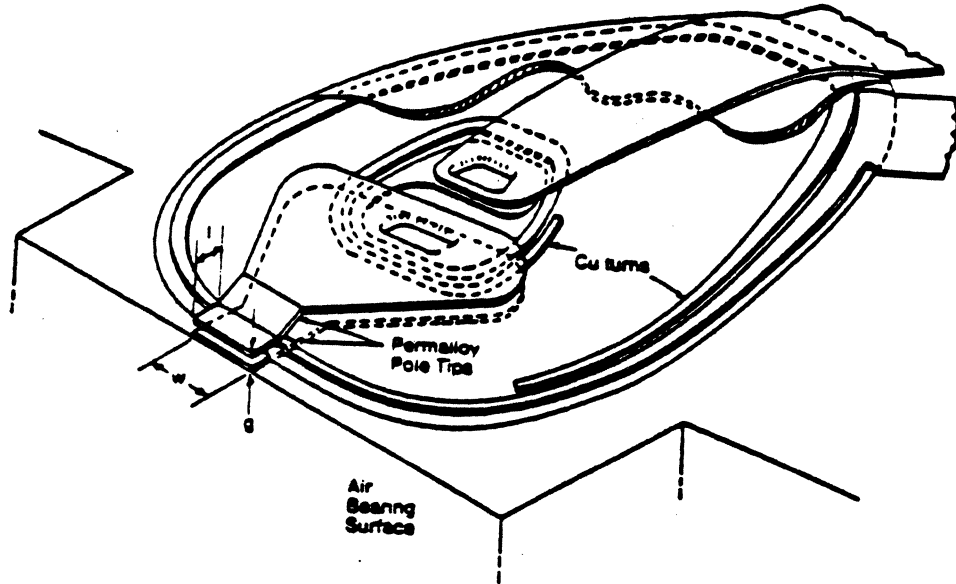
## CONVENTIONAL WINCHESTER FERRITE HEAD



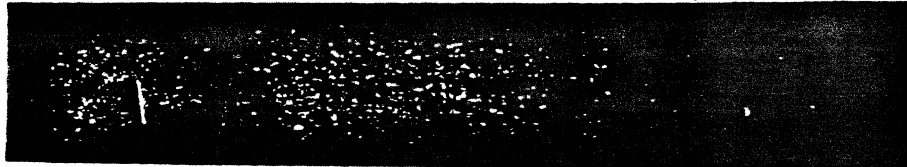
## THIN FILM HEAD



THIN FILM HEAD FOR DISK RECORDING



# DOMAIN STRUCTURE OF MAIN POLE OF A THIN FILM HEAD

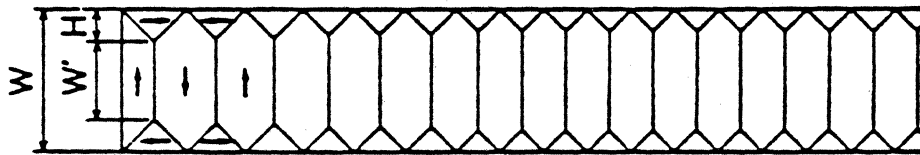


(b)  $H_k = 6.0 \text{ Oe}$

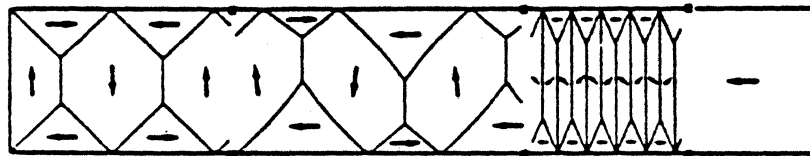


(c)  $H_k = 2.4 \text{ Oe}$

Domain structures of main pole films having track width of  $50 \mu\text{m}$ , thickness of  $0.3 \mu\text{m}$  and length of  $3.5 \text{ mm}$  for various anisotropy fields.



(a)

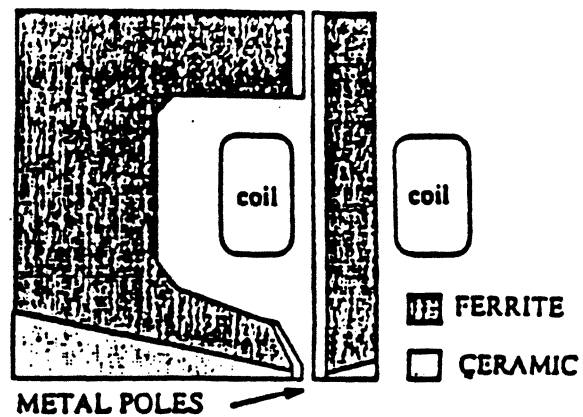
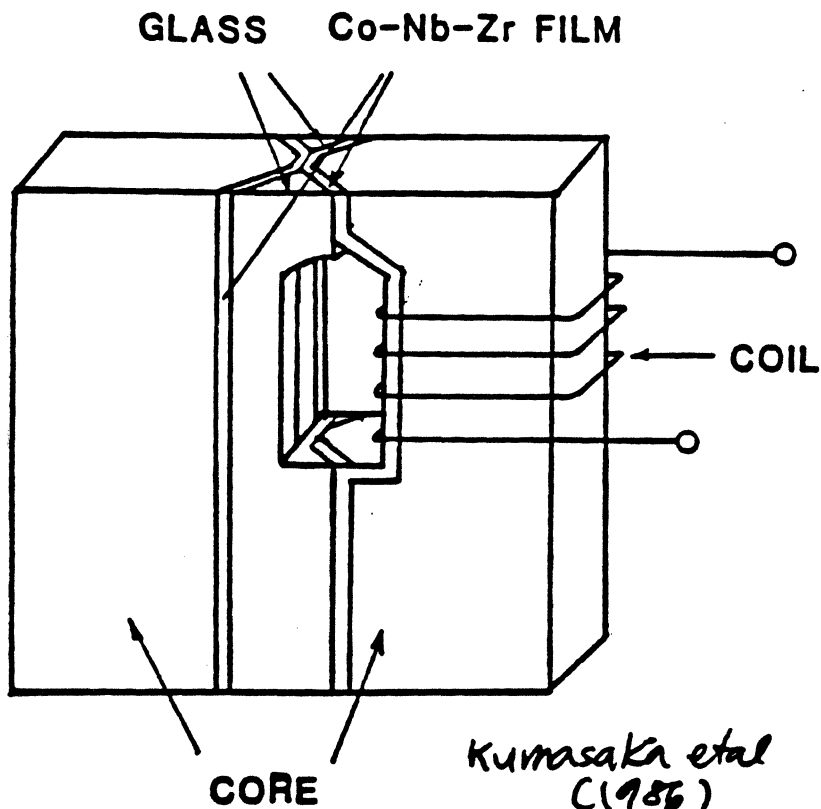


(b)

Schematic models of domain structure for films of (a) wide track or high  $H_k$ , (b) narrow track and low  $H_k$ .

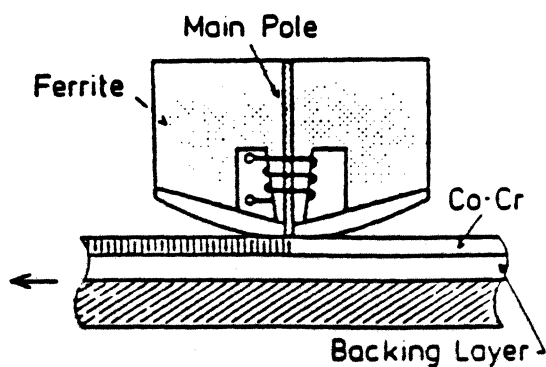
# COMPARISON OF RING AND SINGLE POLE HEADS

## METAL-IN-GAP RINGS HEADS

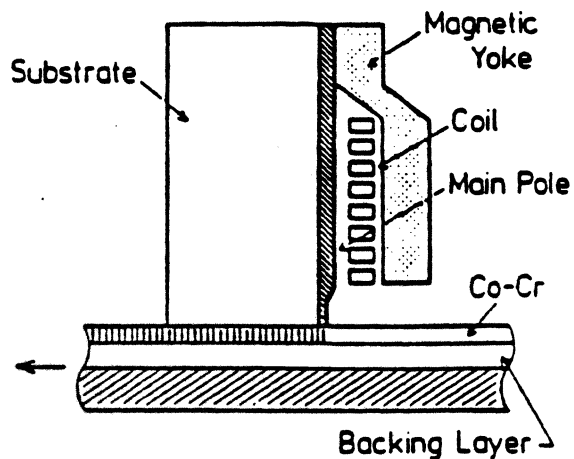


## SINGLE POLE HEADS

### MAIN-POLE DRIVEN



### THIN FILM HEAD



SENDUST METAL-IN-GAP MINI-COMPOSITE FERRITE RING HEAD

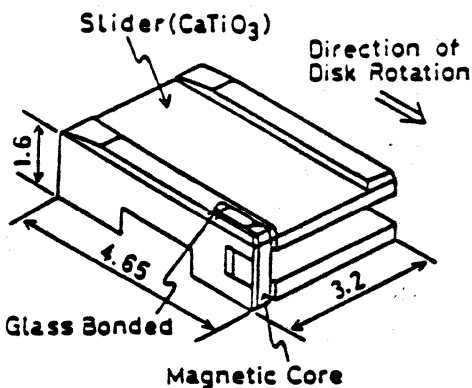
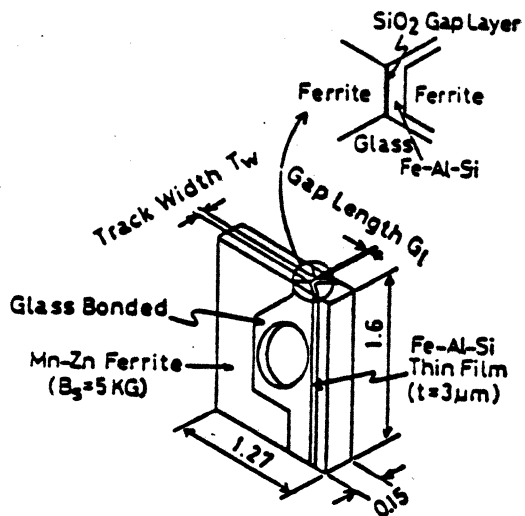
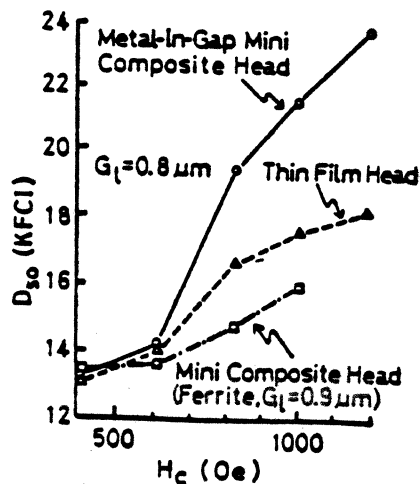
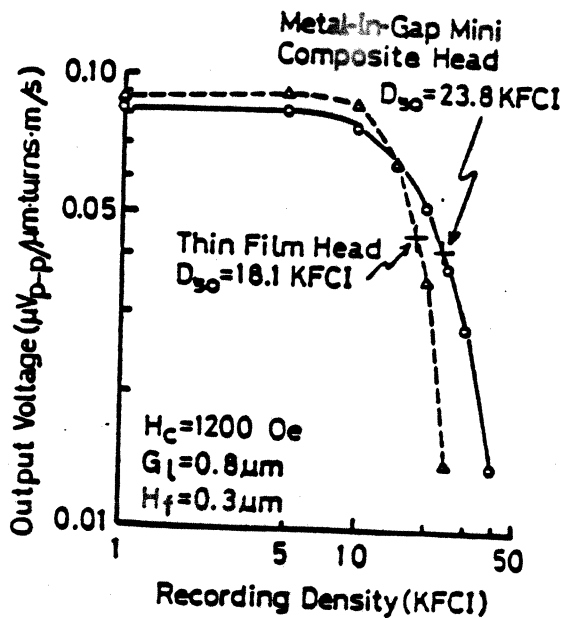
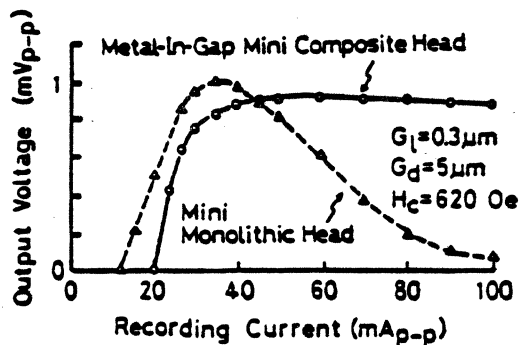


Table I Properties of magnetic materials

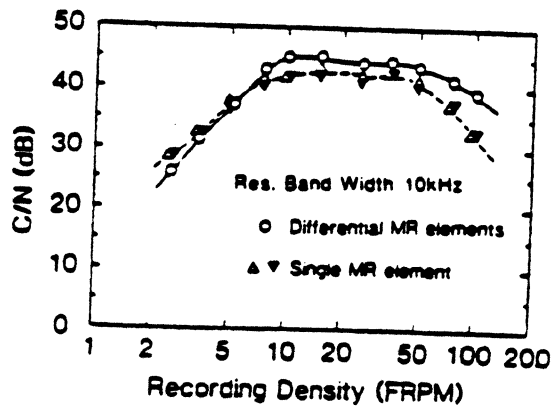
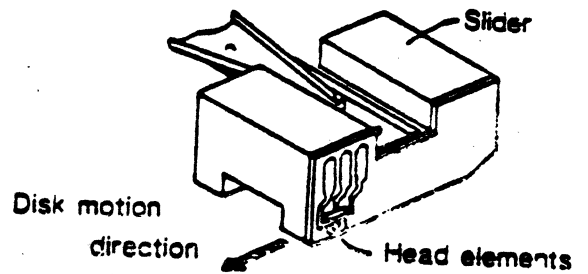
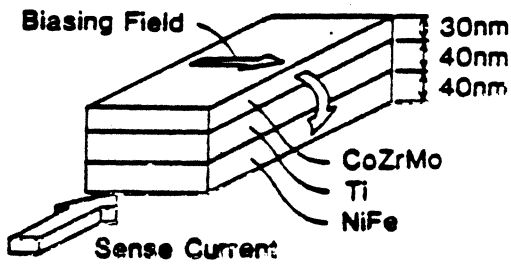
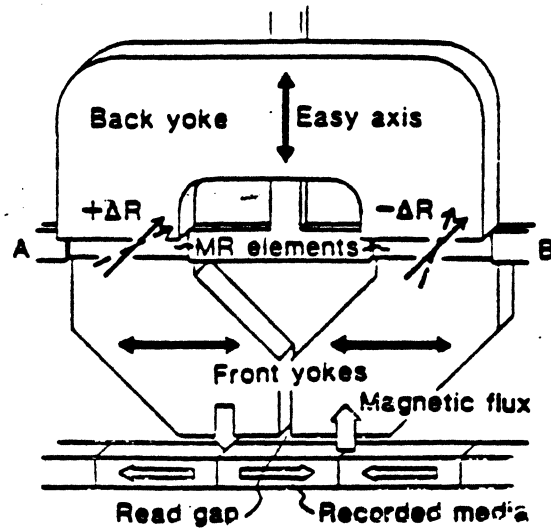
	$B_s$ (KG)	$\mu$ at 5MHZ
Fe-Al-Si	11-12	1000-2000
Mn-Zn Ferrite	5	900-1000



Noguchi et al (Hitachi Metals) (1987)



# A YOKE MAGNETORESISTIVE HEAD FOR HIGH TRACK DENSITIES



Maruyama et al (NEC) (1987)

# Head Comparison

<b>Inductive</b>	<b>MR</b>
Thin film processing	Thin film processing
Velocity dependent	Velocity independent
Same read/write devices	Separate read/write devices
Lower signal levels	High output level
Higher input impedance	Low input impedance
Compromised writer/reader	Optimized writer/reader
Currently at near maximum	Higher track densities
Need to fly low to disk	Can fly higher
Equal read/write widths	Write wide/ read narrow

# FILM VERSUS PARTICLES FOR RECORDING MEDIA

## FILMS

ROUGHNESS MORE CRITICAL

OVERCOAT REQUIRED

HARMONIC DISTORTION AT LOW  
FREQUENCY

OPTICAL READOUT POSSIBLE

HIGHER RESOLUTION

THIN LAYERS EASILY MADE

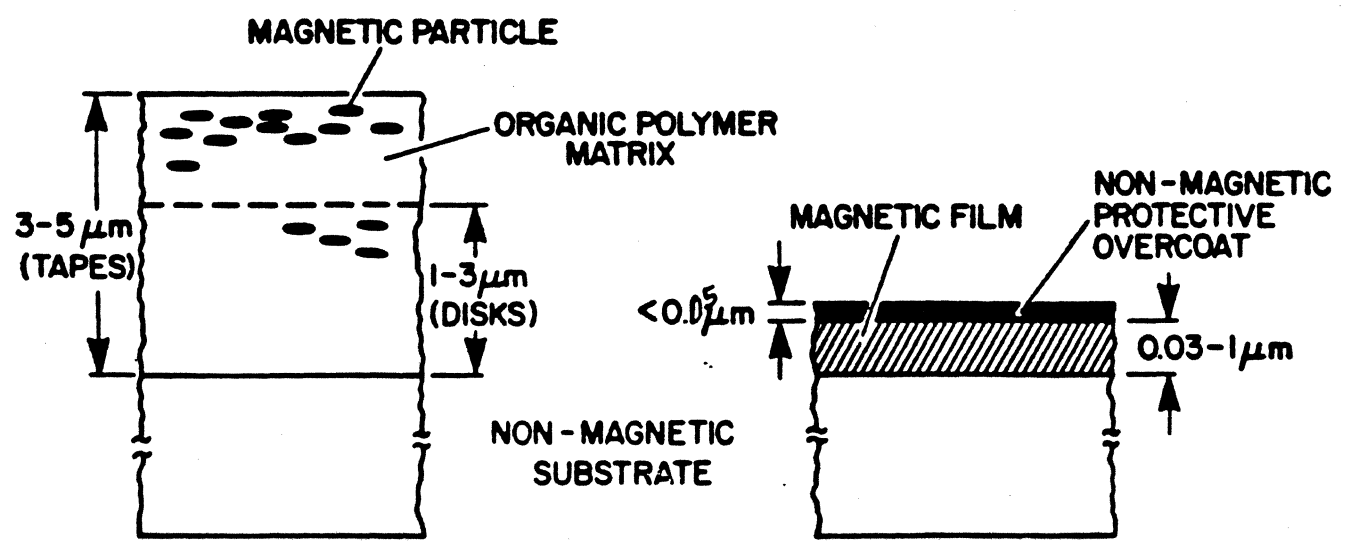
BETTER SATURATION RECORDING

## PARTICLES

CANNOT BE MADE VERY THIN

MECHANICAL RESILIENCE IS  
GOOD

BETTER WIDE BAND RECORDING



## EFFECT OF SQUARENESS OF HYSTERESIS LOOP

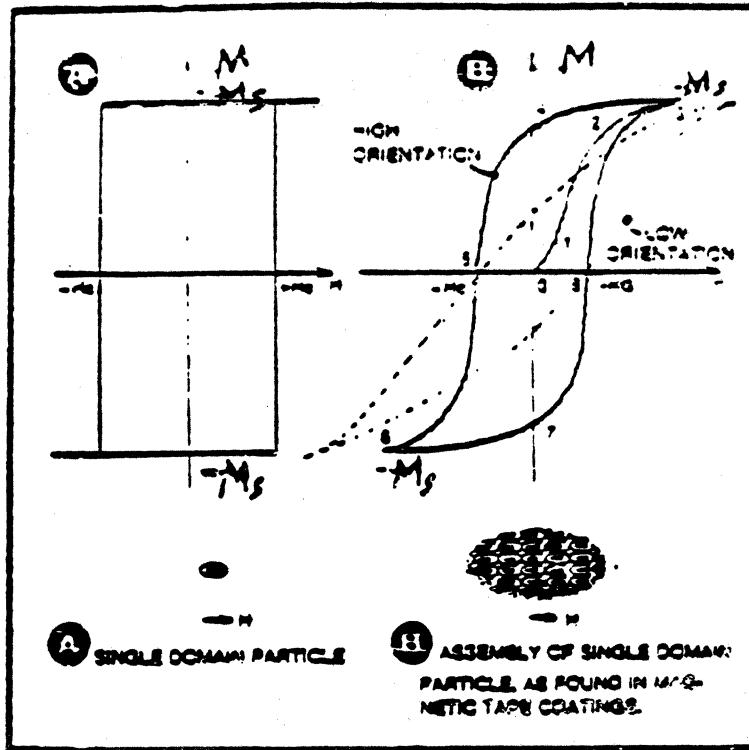


Fig. 3-7. Different hysteresis loops for tape materials. (A), single domain particle (B), assembly of single domain particle, as found in magnetic tape coatings.

## EFFECT OF COERCIVITY AND SQUARENESS

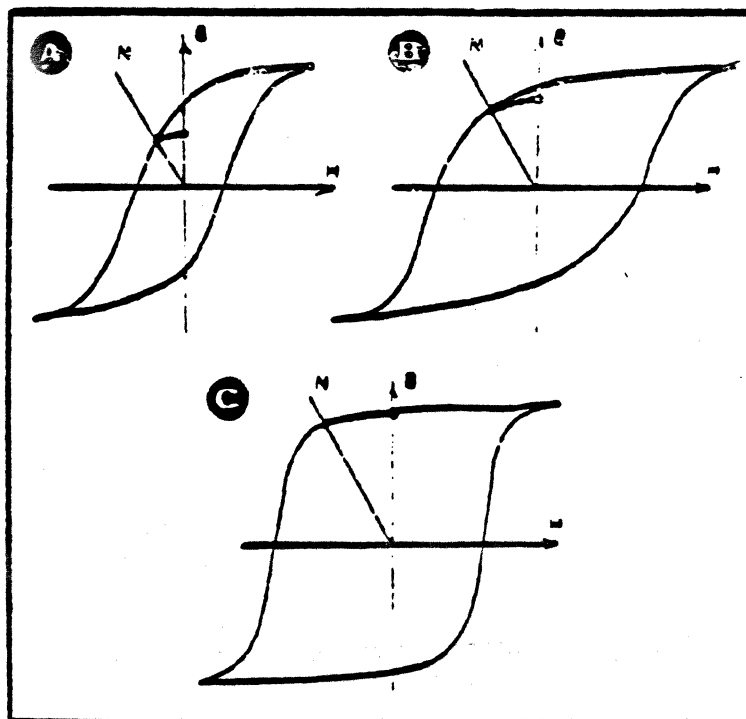
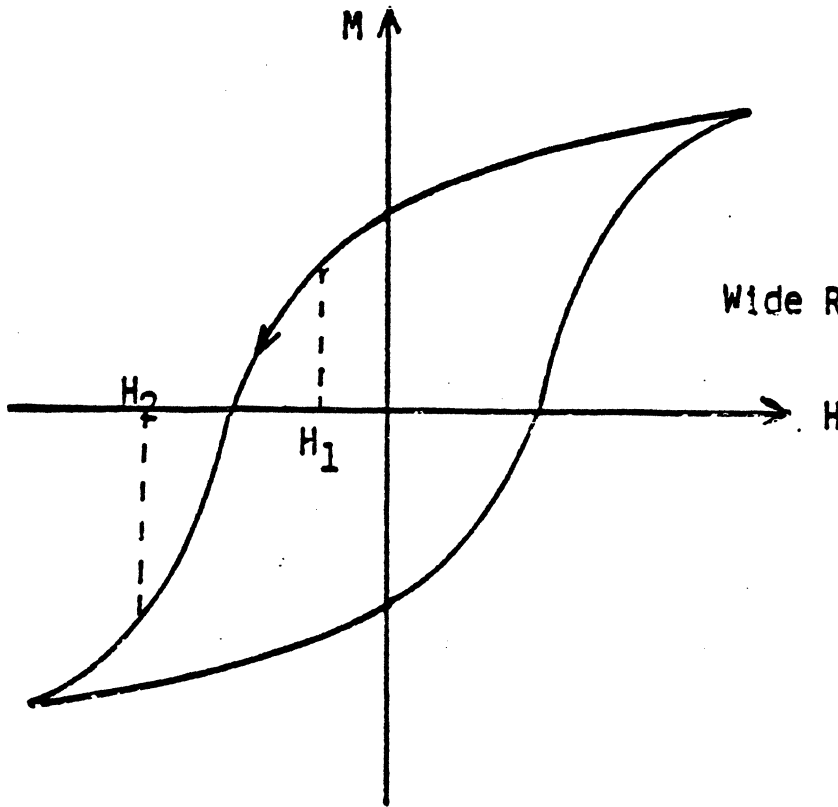


Fig. 6-1. Maximum remanence in magnetic tapes: (A), low coercivity; (B), high coercivity; (C), high coercivity, good orientation.

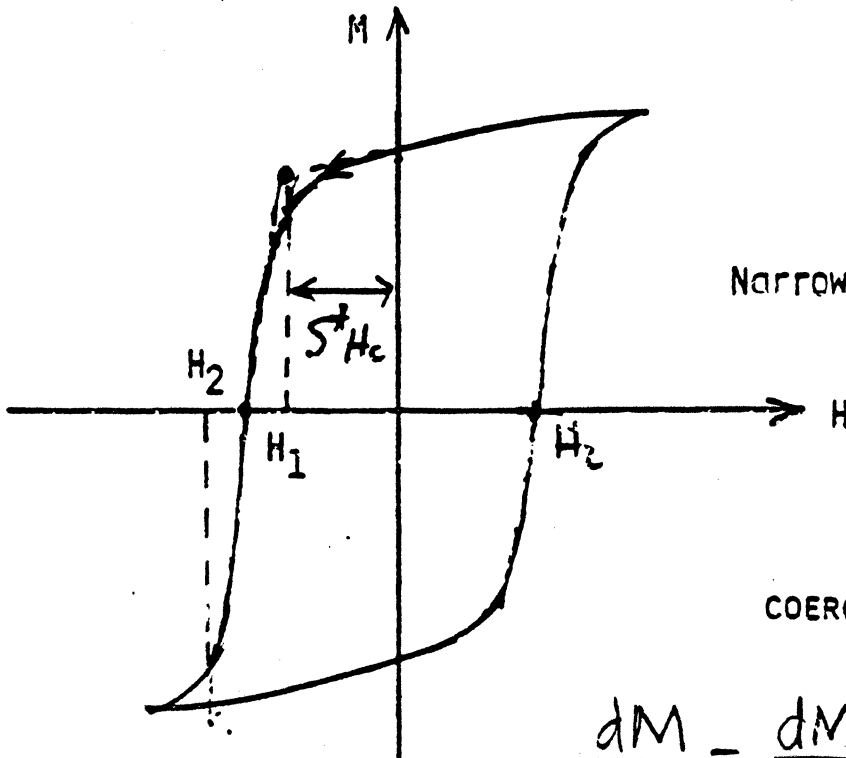
# SWITCHING FIELD DISTRIBUTION



Low Squareness

Wide Range of Switching Fields

$$\Delta H = H_2 - H_1$$



High Squareness

Narrow Range of Switching Fields

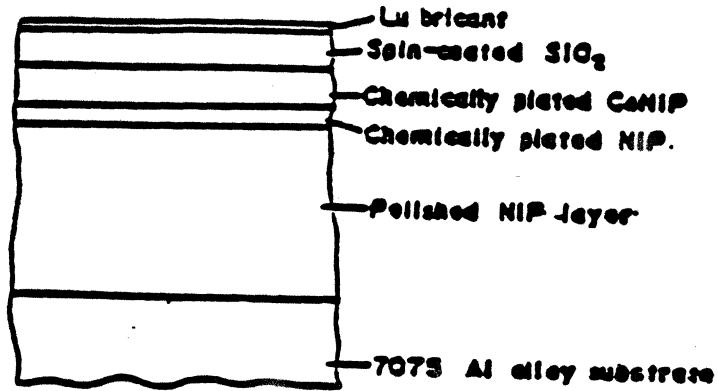
$$\text{COERCIVITY SQUARENESS} = S^* = 1 - \frac{\Delta H}{2 H_c}$$

$$\frac{dM}{dx} = \frac{dM}{dH} \cdot \frac{dH}{dx}$$

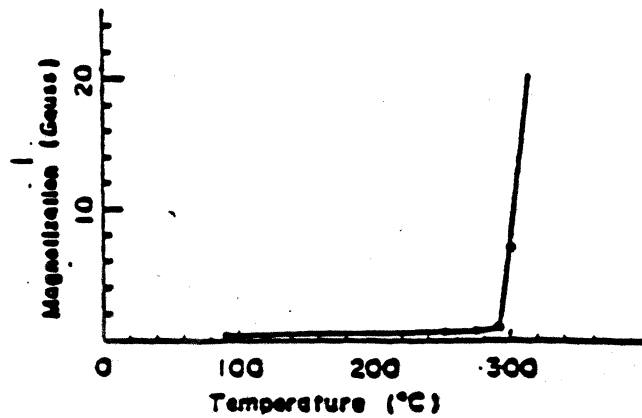
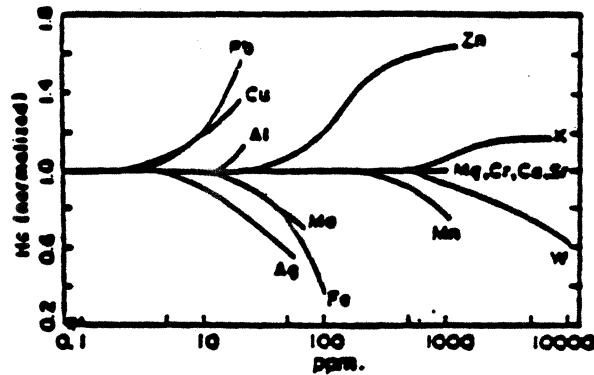
$\uparrow$  slope on side of loop       $\uparrow$  Head field gradient

# THIN FILM LONGITUDINAL MEDIA

## CHEMICALLY PLATED MAGNETIC DISKS



Plated disk cross-section structure.



Y. Suganuma et al, IEEE MAG-18, 1215 (1982)

# MAGNETIC RECORDING MEDIA EVAPORATED AT OBLIQUE INCIDENCE

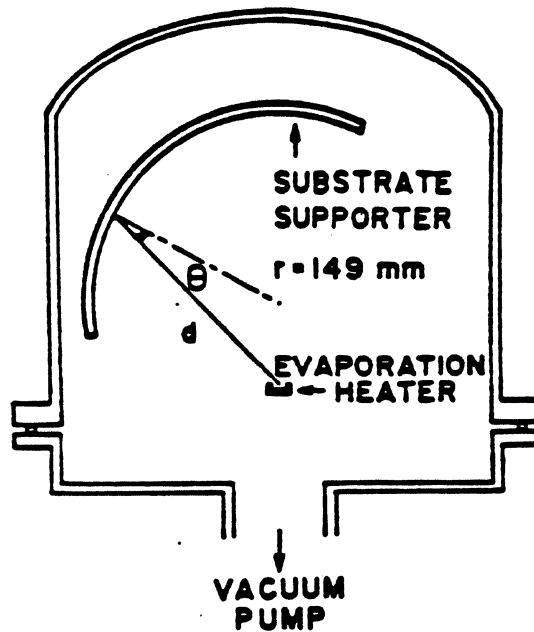


Fig. 1. Illustration of used vacuum system for the oblique incidence. Ferromagnetic alloys were evaporated on a polyimide film which was fixed on a cylindrical shaped substrate supporter.

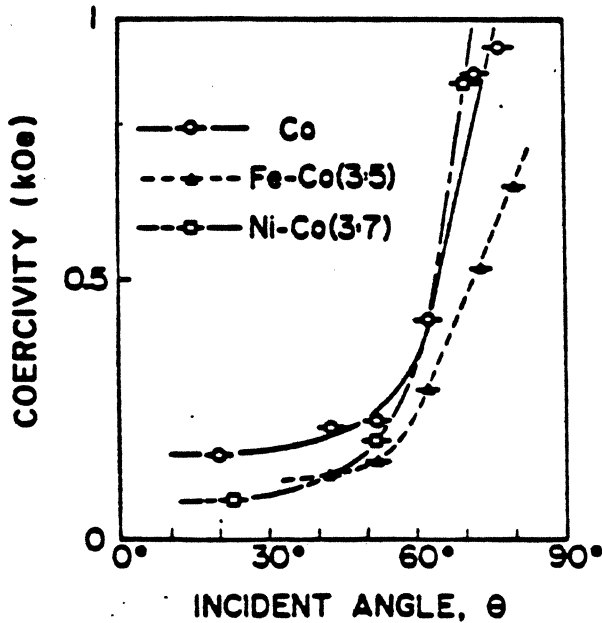


Fig. 2. The coercive force of Co, Fe-Co and Ni-Co thin films were plotted against the angle of incidence.

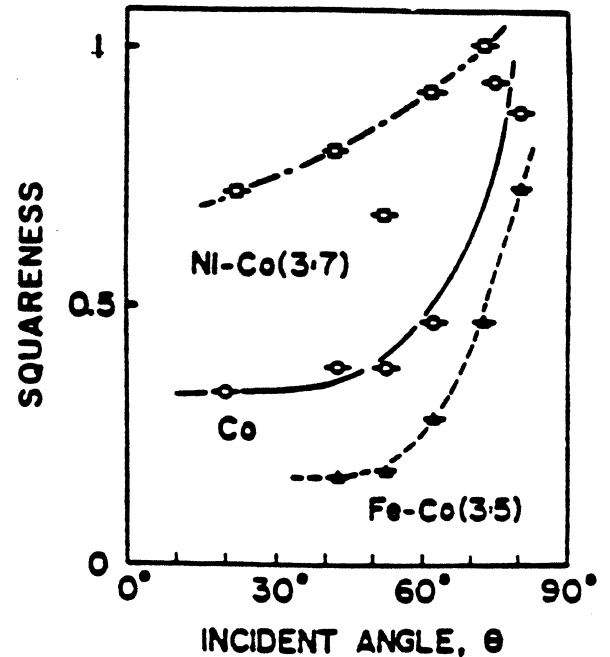


Fig. 3. The squaresness in easy direction of Co, Fe-Co and Ni-Co thin films were plotted against the angle of incidence.

# SPUTTERED CO-Pt FILMS FOR HIGH DENSITY RECORDING

Table 2 Medium properties.

Items	Co <sub>0.80</sub> Ni <sub>0.10</sub> Pt <sub>0.20</sub>	Plated Co-Ni-P
Coercivity (Oe)	893	640
Remanence (Gauss)	10,470	7,200
Squareness Br/Bs	0.90	0.76
Coercive Squareness S <sup>2</sup>	0.97	0.82
Medium thickness (Å)	300	300
Overcoat thickness (Å)	200	200

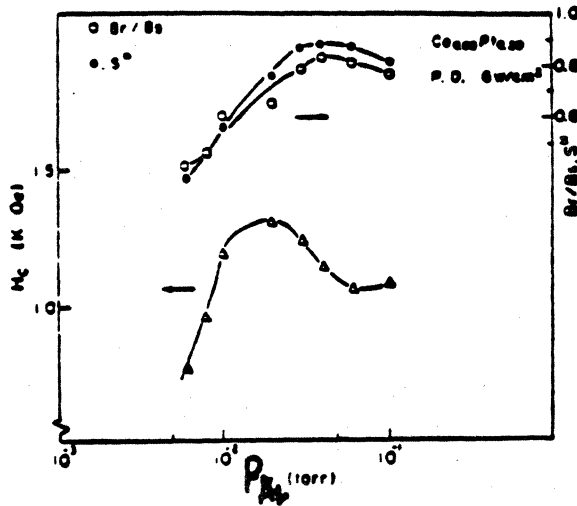


Fig. 6 Coercivity and squareness dependences on argon pressure in the Co<sub>0.80</sub> Pt<sub>0.20</sub> film.

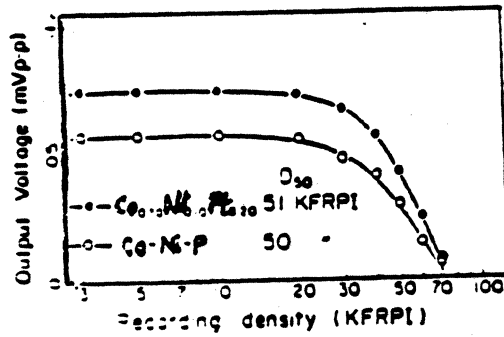


Fig. 7 Output voltage versus recording density.



CONTINUOUS THIN FILM MEDIA  
3.2 GByte Disk System

(PATTY)

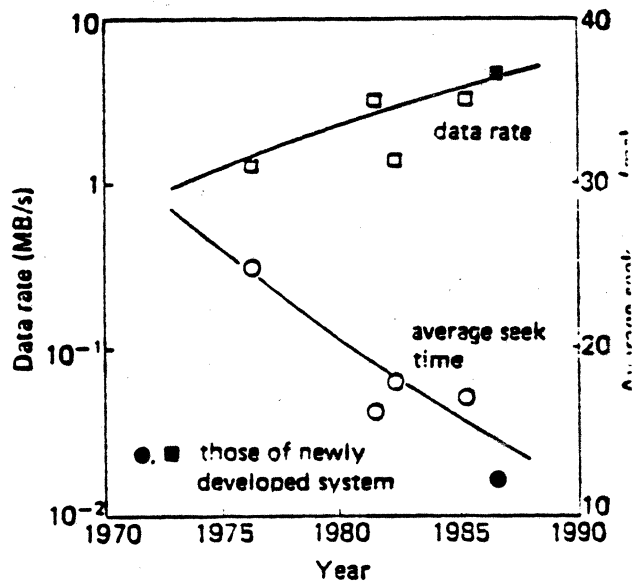
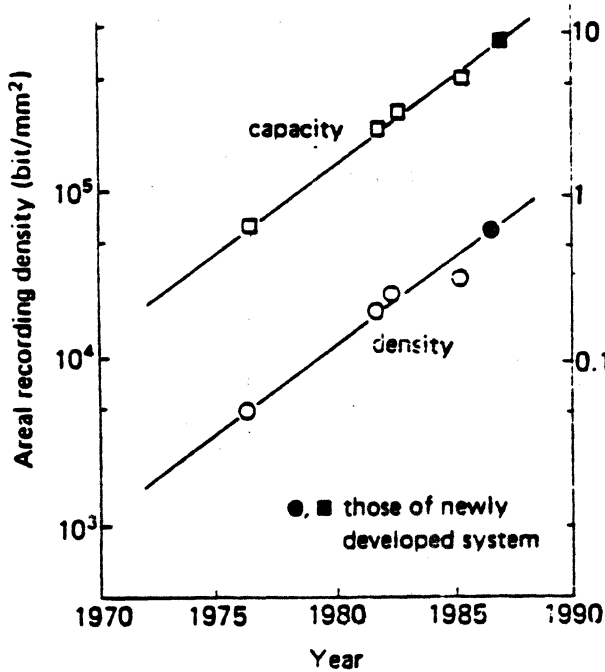
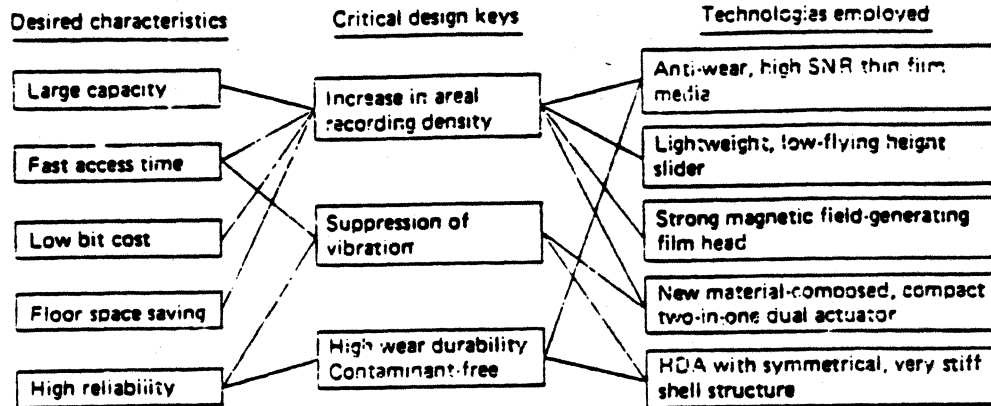
	$\gamma\text{-Fe}_2\text{O}_3$ Thin Film	Co-Ni-P Thin Film
<b>1. Read-write Characteristics</b>		
• Output Signal Voltage	$\geq 0.60 \text{ mV}_{p-p}$	$\geq 0.55 \text{ mV}_{p-p}$
• Resolution	$\geq 75\%$	$\geq 55\%$
• Recording Density	$\geq 550 \text{ FRPM}$	$\geq 620 \text{ FRPM}$
• Over-write Characteristics	$\leq -26 \text{ dB}$	$\leq -26 \text{ dB}$
• SNR	$> 32 \text{ dB}$	$> 28 \text{ dB}$
<b>2. Signal Quality</b>		
• Number of Defects per Surface	$\leq 100$	$\leq 100$
<b>3. Disk Size</b>		
• Inner Diameter	$100 + 0.1 \text{ mm}$ $-0.0 \text{ mm}$	$100 + 0.1 \text{ mm}$ $-0.0 \text{ mm}$
• Outer Diameter	$210 \pm 0.1 \text{ mm}$	$210 \pm 0.1 \text{ mm}$
• Thickness	$1.905 \pm 0.025 \text{ mm}$	$1.905 \pm 0.025 \text{ mm}$
<b>4. Thin Film Media Properties</b>		
• Film Thickness	$0.17 \pm 0.01 \mu\text{m}$	$0.08 + 0.005 \mu\text{m}$ $-0.003 \mu\text{m}$
• Coercivity	$700 \pm 40 \text{ Oe}$	$600 \pm 30 \text{ Oe}$
• Residual Flux Density	$2500 \pm 200 \text{ Gauss}$	$7200 \pm 300 \text{ Gauss}$
• Coercive Squareness	$\geq 0.77$	$\geq 0.77$
<b>5. Mechanical Properties</b>		
<b>5.1 Surface Roughness</b>		
• Arithmetic Average	$\leq 0.01 \mu\text{m}$	$\leq 0.01 \mu\text{m}$
• Axial Runout	$\leq 40 \mu\text{m}$	$\leq 40 \mu\text{m}$
• Acceleration of Axial Runout ( $a$ )	$ a  \leq 40 \text{ m/sec}^2$	$ a  \leq 40 \text{ m/sec}^2$
• Minimum Head Flying Height	$\leq 0.18 \mu\text{m}$	$\leq 0.15 \mu\text{m}$
<b>5.2 Lubricating Properties</b>		
• Maximum Coefficient of Friction	$\leq 0.3$	$\leq 0.3$
• CSS Characteristics	$\geq 20,000 \text{ cycles}$	$\geq 20,000 \text{ cycles}$
<b>6. Protective Film Thickness</b>	$0.000 \mu\text{m}$	$0.08 \pm 0.01 \mu\text{m}$
<b>7. Reliability</b>	<ul style="list-style-type: none"> <li>* No deterioration is caused at <math>40^\circ\text{C}</math> for 7 months under 80% relative humidity</li> <li>* Output signal quality does not deteriorate</li> </ul>	

S. Hattori et al, NEC (1983)

# ADVANCED CONTINUOUS THIN FILM MEDIA

## 8.8 GBYTE DISK SYSTEM

(GEMMY)



### Thin Film Media

	<u>Y-Fe<sub>2</sub>O<sub>3</sub></u>	<u>CoNiP</u>
B <sub>R</sub> (G)	2200	8000
H <sub>c</sub> (G)	700	800
δ(Å)	1600	500

### Thin Film Head

Gap(μm)	0.5
Pole(μm)	3
Slider	Al <sub>2</sub> O <sub>3</sub> -TiC
height(μm)	< 0.2

### GEMMY

Specifications	Newly developed	PATTY
Storage capacity (GByte) per Unit	8.8	3.2
per HDA	2.2	0.4
per Actuator	1.1	0.4
Data rate (MByte/s)	4.4	1.344
Average seek time (ms)	12	18
Latency time (ms)	3.3	10
Recording density		
Areal density (bit/mm <sup>2</sup> )	62k	24k
Linear density (bit/mm)	1240	550
Track density (track/mm)	50	43
F. C. S	1987	1982

IBM  
3380

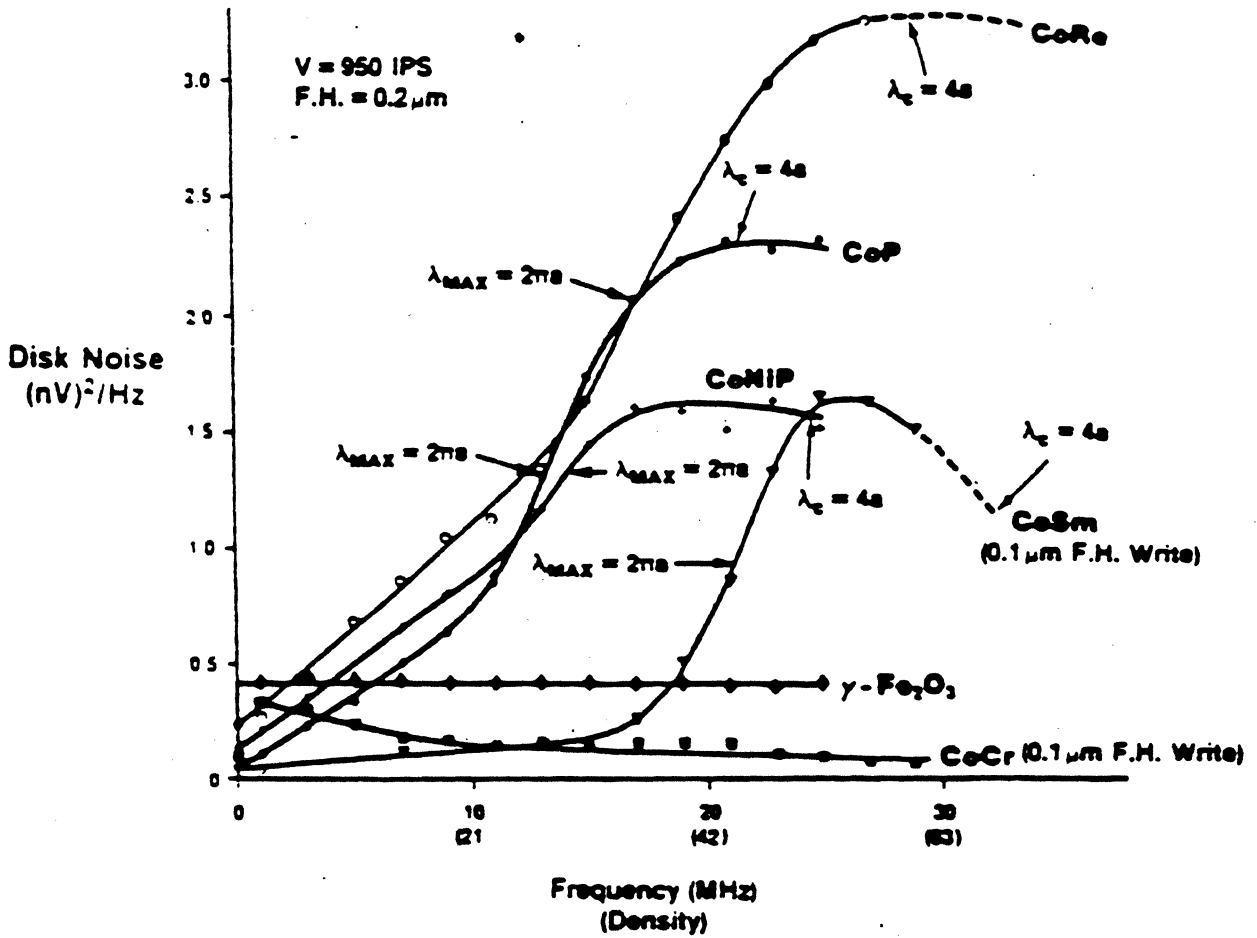
5  
1.26, 2.52  
1.26  
3  
17  
8.3

Mitsuya  
etal

(NTT,  
1987)

SNR = 28 db  
O/W = 32 db

1985



**S/N AND PERFORMANCE SURVEY  
(950 IPS/0.2  $\mu\text{m}$  F.H. READ)**

Media	$\gamma\text{-Fe}_2\text{O}_3$	Co-P	Co-Ni-P	CoSm	CoRe	CoCr	
$D_{70}$ (KFCI)	12.5	19	18	20	21	22	25
$S_{70}$ ( $\mu\text{V}_{0-p}$ )	185	170	154	133	126	59	108
$N_{DC}$ ( $nV/\sqrt{\text{Hz}}$ )	0.67	0.21	0.40	0.20	0.48	.34	.31
$N_{AC}$ ( $nV/\sqrt{\text{Hz}}$ )	0 (120ms)	1.17 (80ms)	1.16 (80ms)	0.52 (150ms)	>1.61 (80ms)	~ 0 (150ms)	.22 (150ms)
$(S/N)_{TOTAL}$ (dB) MEDIA	36	30	29	35	25	32	36
$(S/N)_{OW}$ (dB) ON TRACK	28	39	35	27.5	34	20	23

↑  
0.1  $\mu\text{m}$  F.H.  
Write

↑  
0.1  $\mu\text{m}$  F.H.  
Write

Belk et al (1985)

# REVERSED DC ERASED MAGNETIC RECORDING MEDIA NOISE

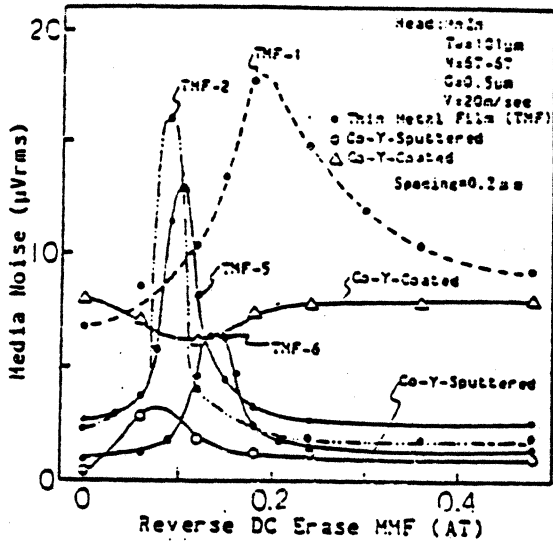


Fig.1 Media Noise vs. Reverse DC Erase MMF

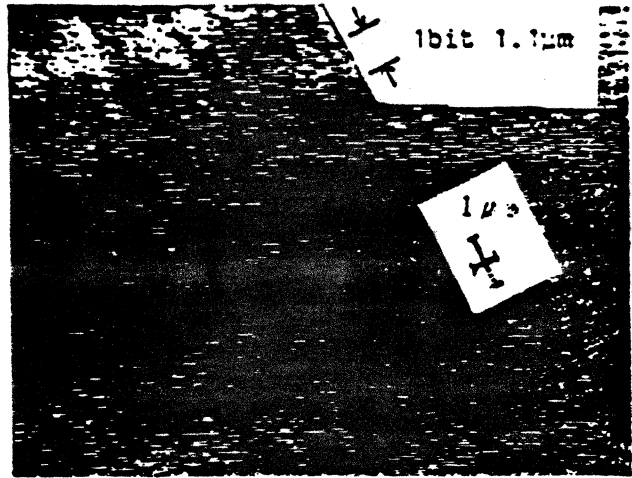


Fig.2 Signal Recorded Magnetic Domain Structure

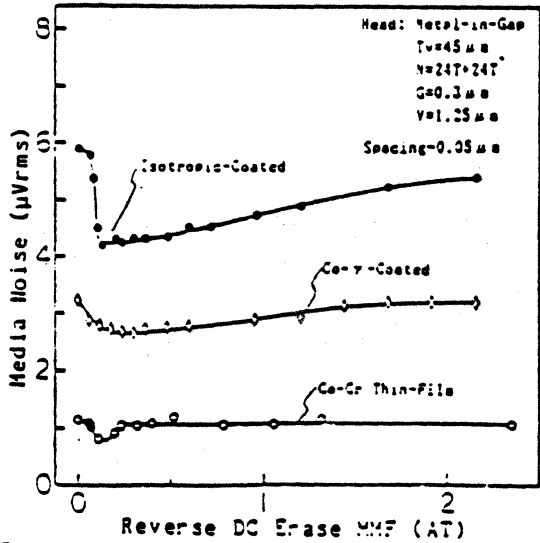


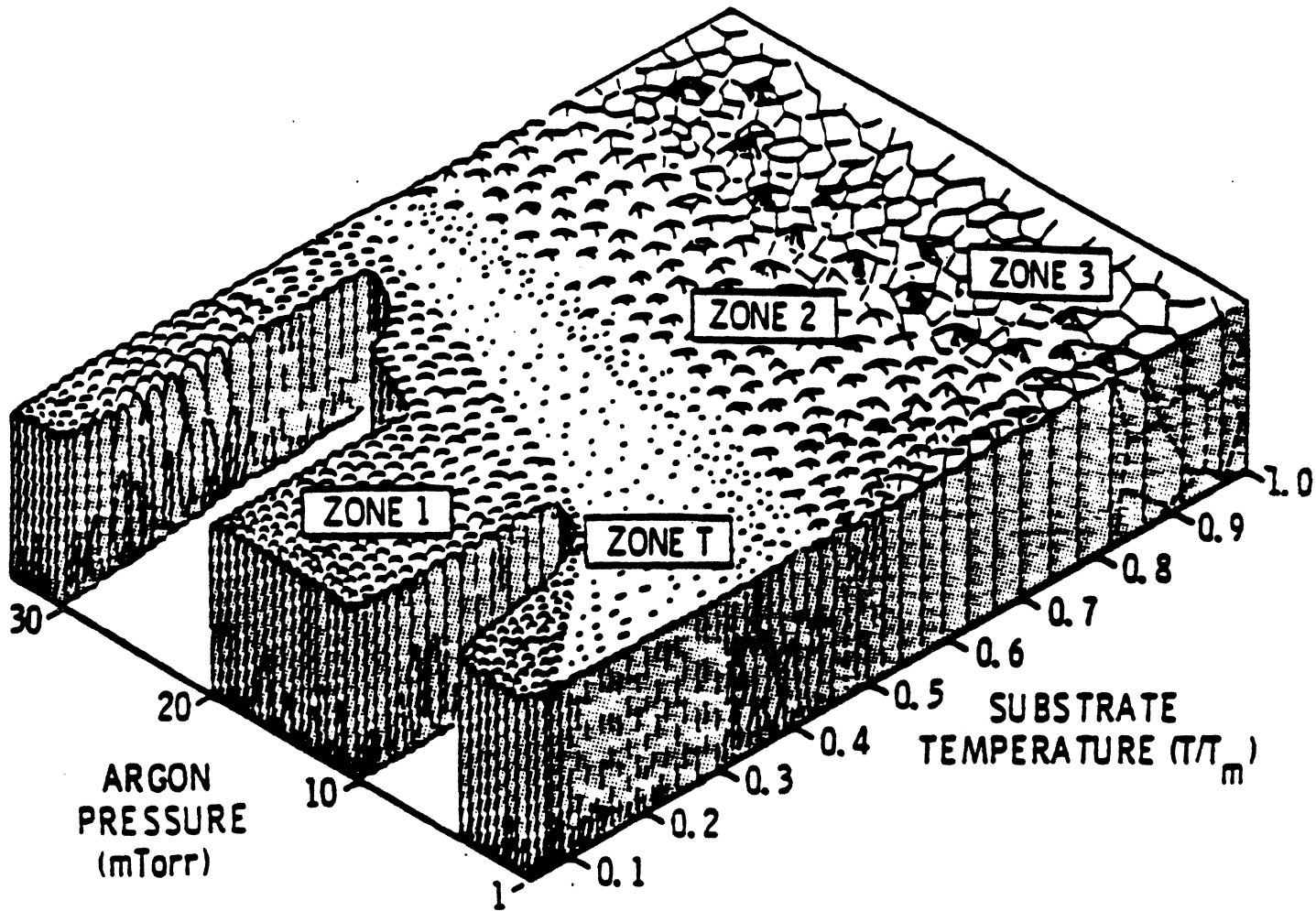
Fig.4 Media Noise vs. Reverse DC Erase MMF



Fig.3 Reversely DC Erased Magnetic Domain Structure

Aoi et al (1987)

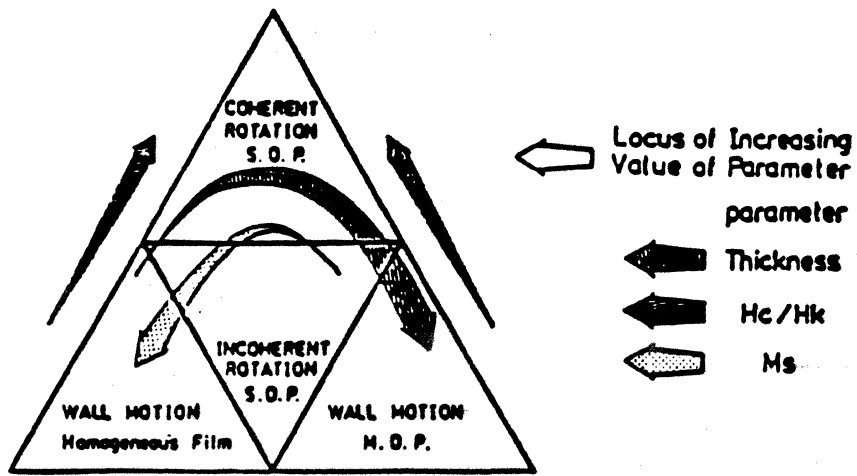
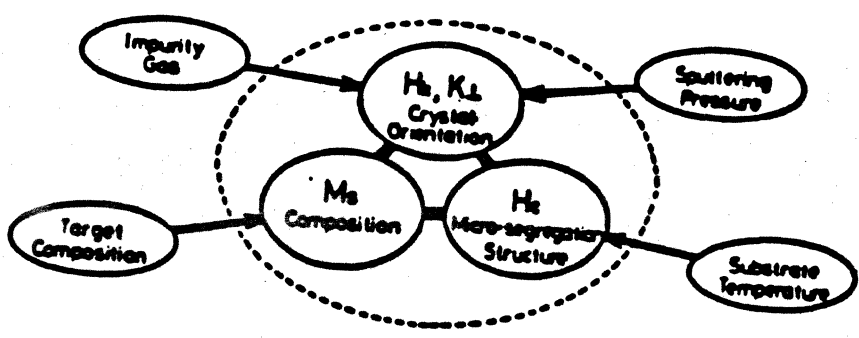
# MICROSTRUCTURE OF SPUTTERED THIN FILMS



Thornton

# FACTORS AFFECTING THE MAGNETIC AND REVERSAL PROPERTIES OF THIN FILMS

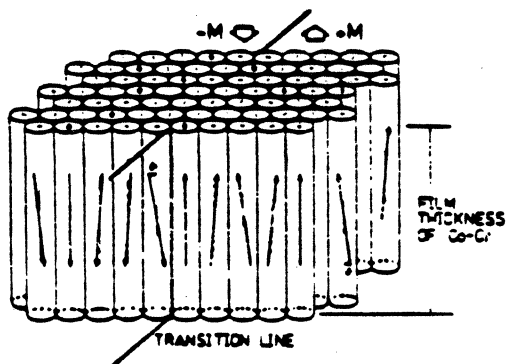
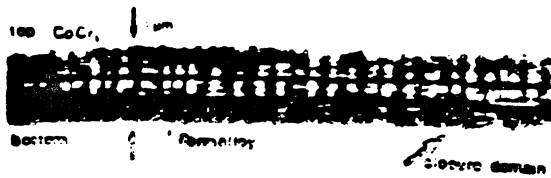
1. COMPOSITION
2. TEMPERATURE
3. STRESS
4. SIZE, SHAPE, ORIENTATION OF GRAINS
5. CONCENTRATION AND DISTRIBUTION OF CRYSTAL IMPERFECTIONS
6. IMPURITIES



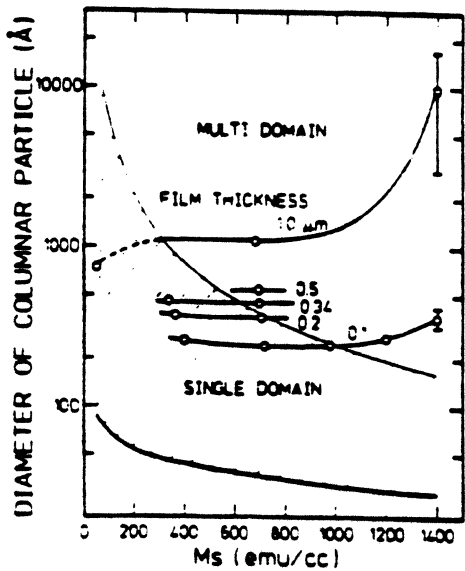
Ouchi (1987)

# MICROMAGNETICS OF SPUTTERED COCR FILMS

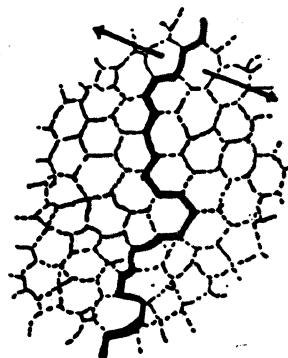
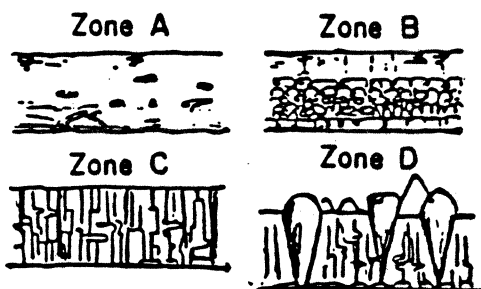
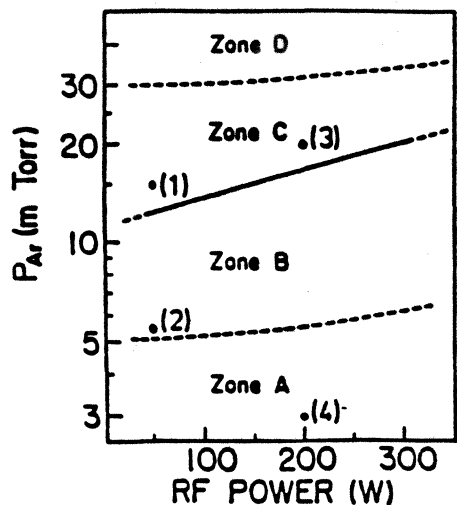
## LORENTZ MICROGRAPH OF CROSS SECTION OF COCR/PERMALLOY FILMS



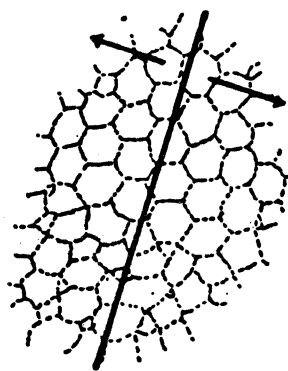
STRUCTURE OF MAGNETIZATION TRANSITION



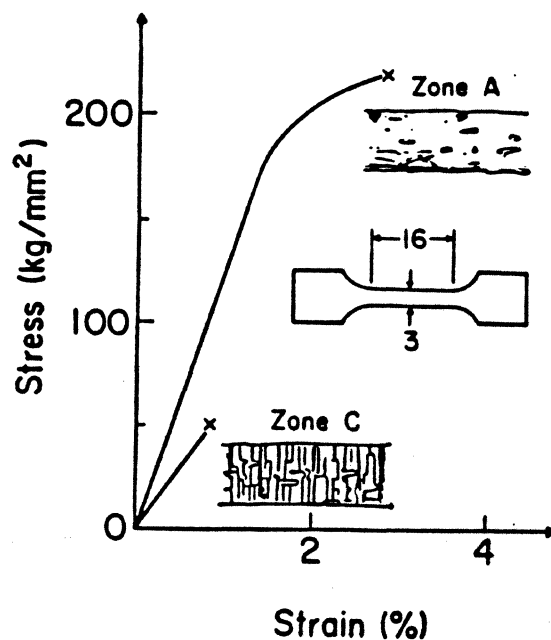
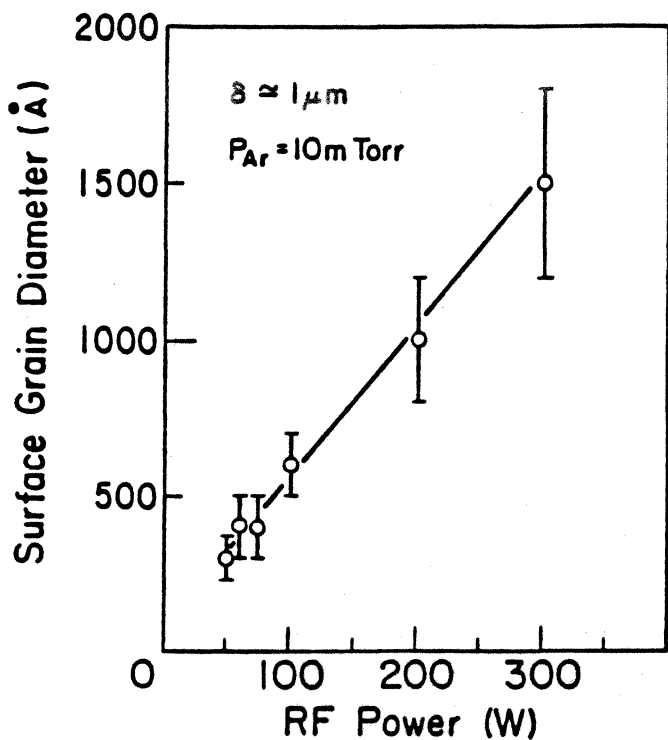
# MICROSTRUCTURES AND MECHANICAL PROPERTIES OF RF SPUTTERED CoCr FILMS



Zones C and D



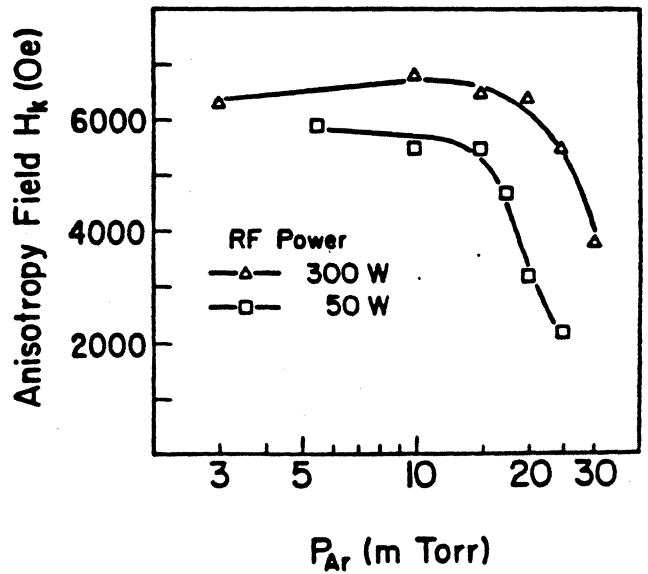
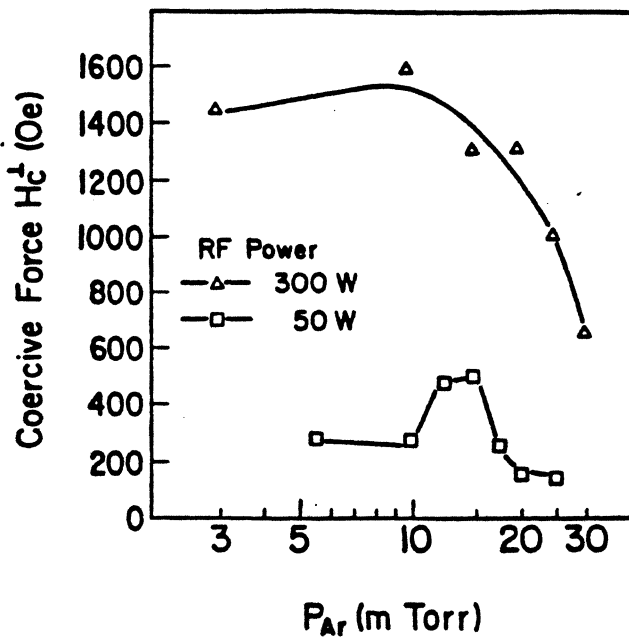
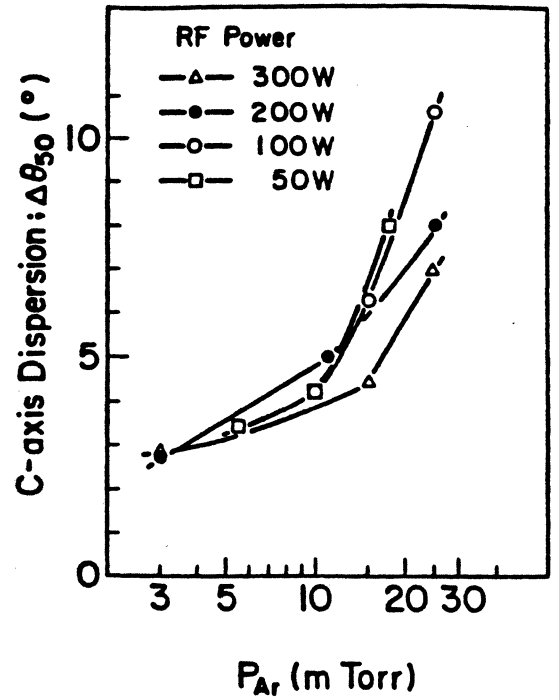
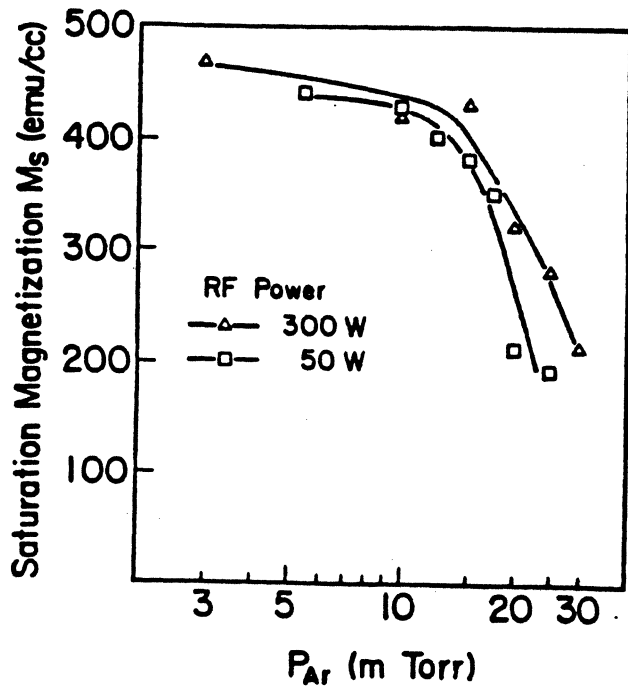
Zones A and B



Sagoi et al (1984)

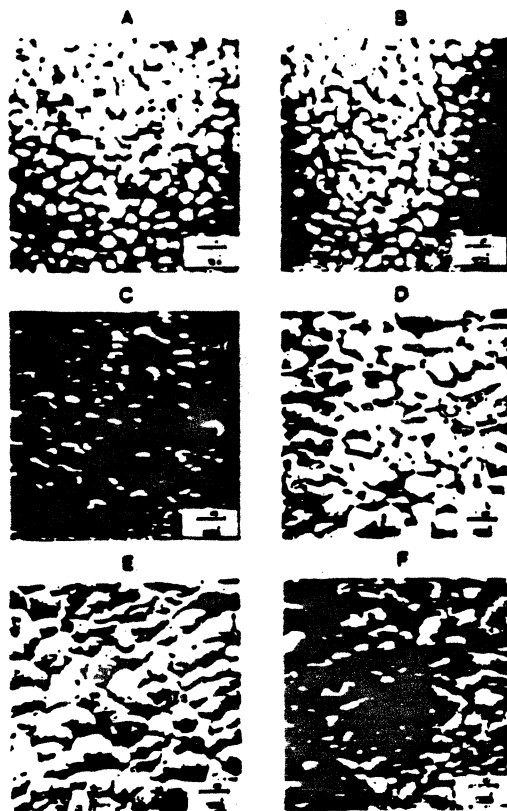


# ARGON PRESSURE DEPENDENCE OF MAGNETIC PROPERTIES OF RF SPUTTERED CoCr



Sagoi et al (1984)

# MICROSTRUCTURE AND COERCIVITY OF COCR FILMS DEPOSITED ON VARIOUS SUBSTRATES BY DC MAGNETRON SPUTTERING



Sem micrographs of 10,000 Å thick Co-Cr thin films sputtered on six different substrates: (A) Al, (B) NiP, (C) Si(111), (D) Si(100), (E) Cover glass, (F) Si water with SiO<sub>2</sub>.

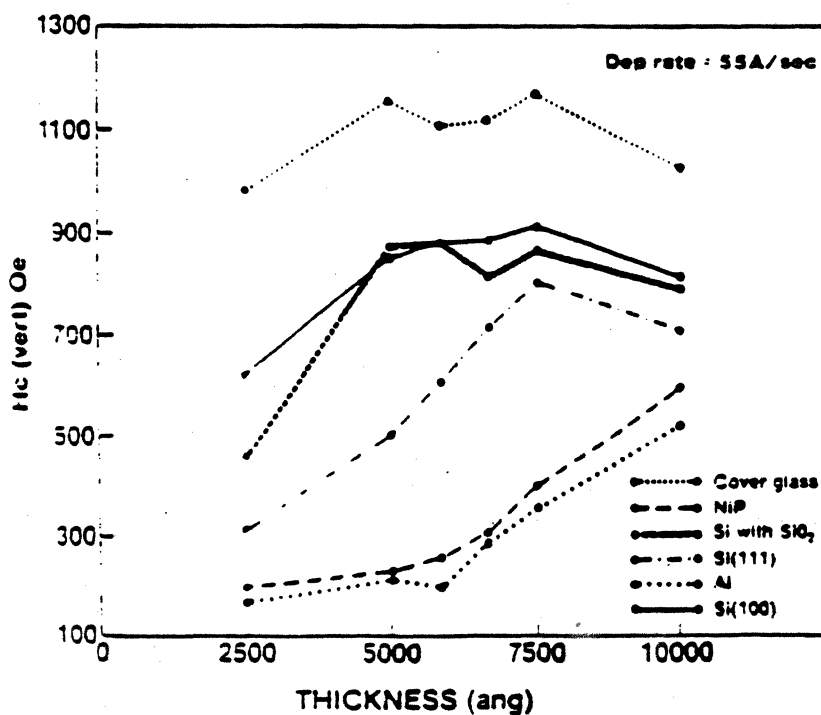
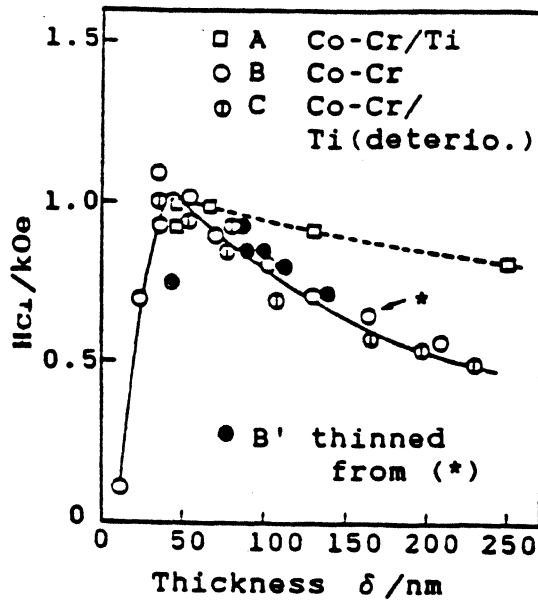


Fig. 3: Relationship between Hc (vert) and thickness for the six substrates sputtered at 55 Å/sec.

Ravipati (19's)

# VACUUM DEPOSITED CoCr PERPENDICULAR MEDIA (TAPE)



PET  
Substrate

Table Head dimensions.

Head	A	B	C
Length ( $\mu\text{m}$ )	0.16	0.28	0.2
Track Width ( $\mu\text{m}$ )	50	22	5
Number of Coil Turns (turn)	20	22	20
Track Depth ( $\mu\text{m}$ )	8	25	14

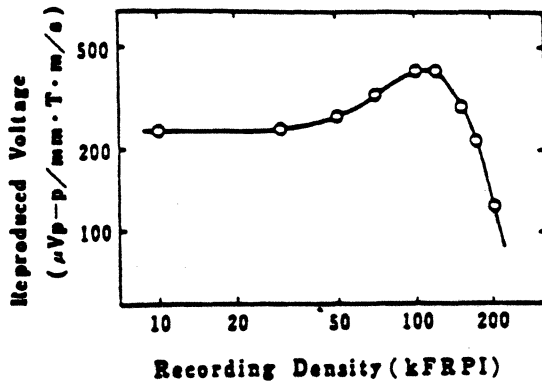


Fig. 2 Recording density characteristics.

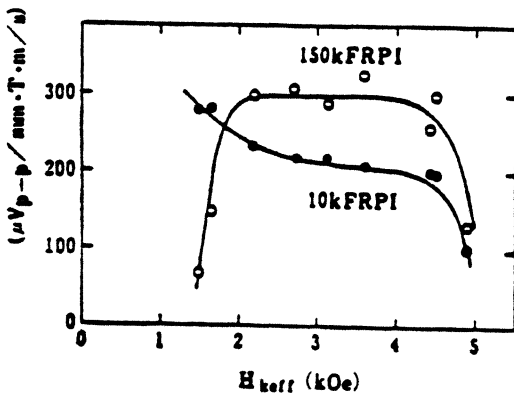


Fig. 3 Dependence of reproduced voltage on  $H_{keff}$ .

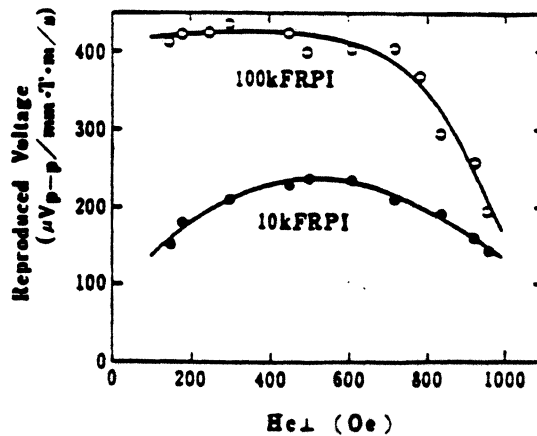
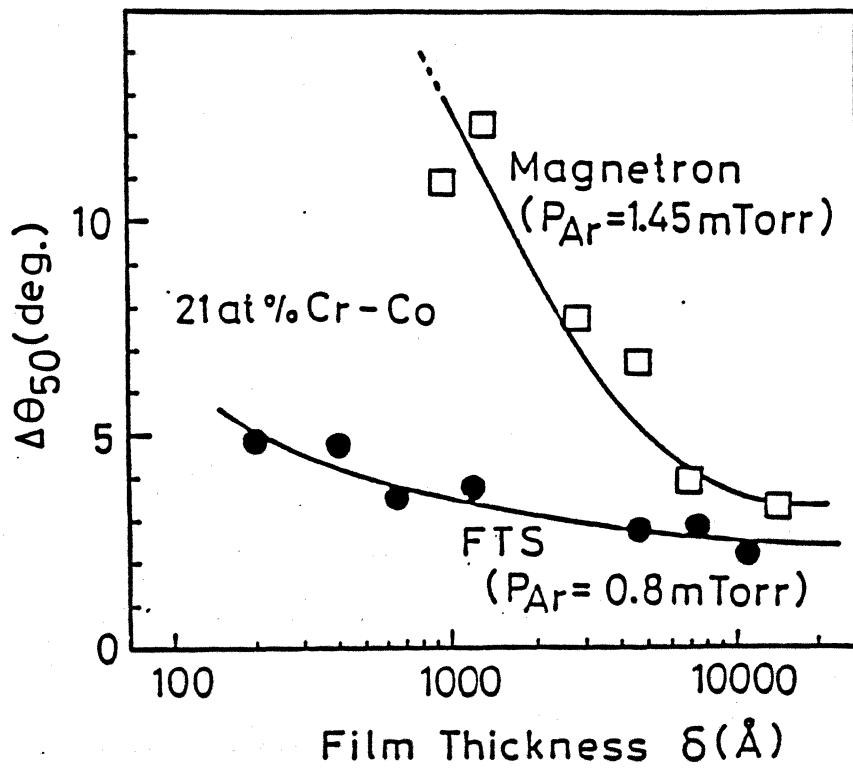
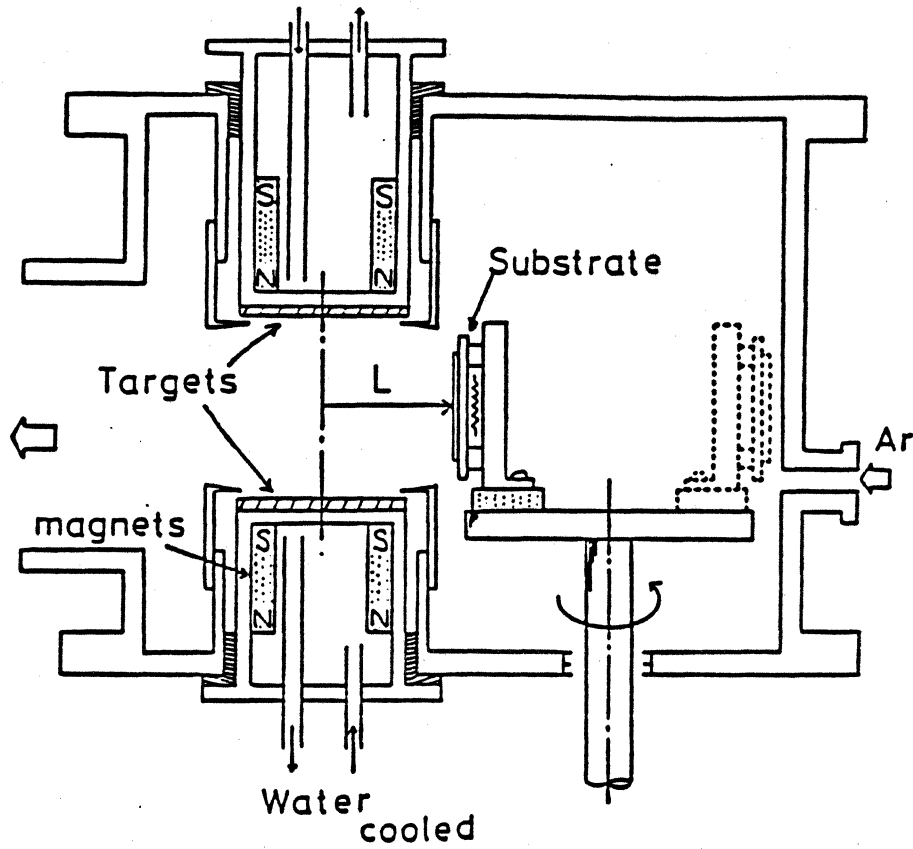


Fig. 4 Dependence of reproduced voltage on  $H_{c1}$ .

# FACING TARGET SPUTTERING OF CoCr FILMS

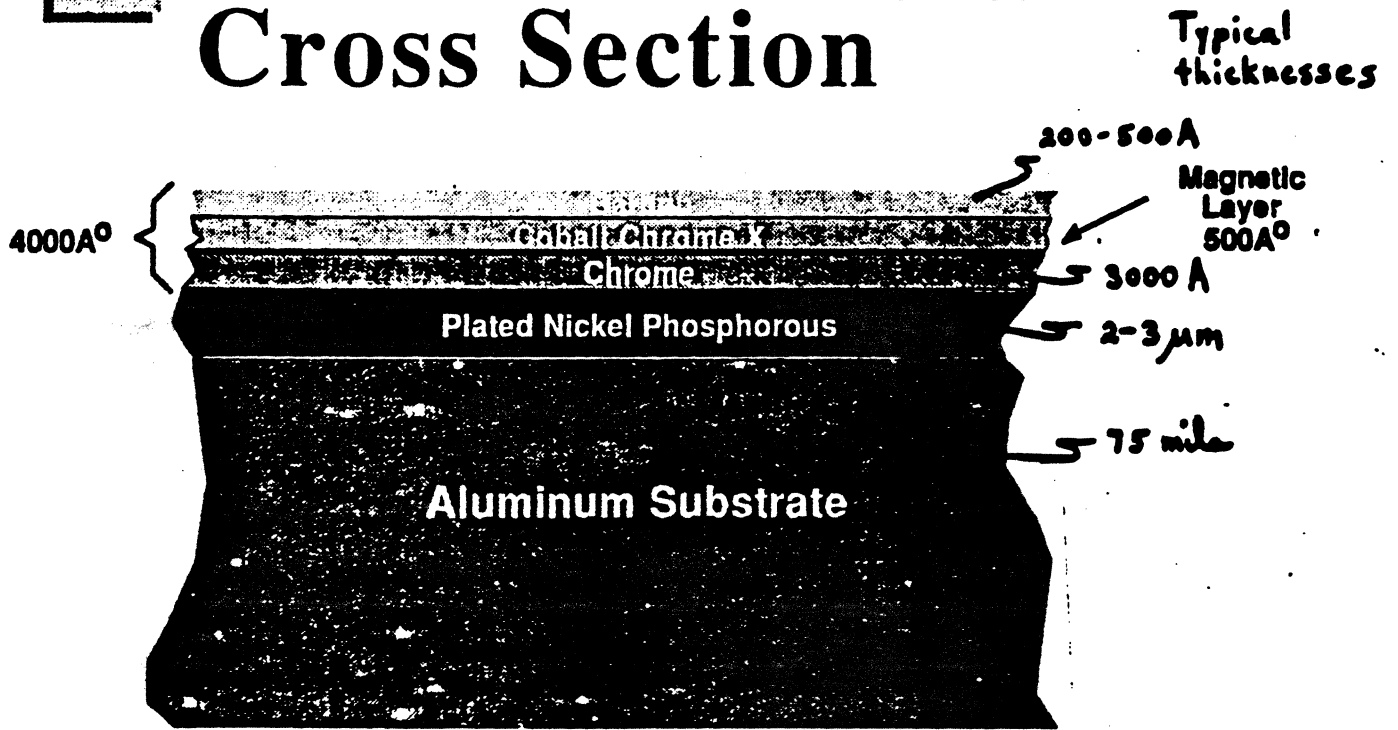
(FTS)



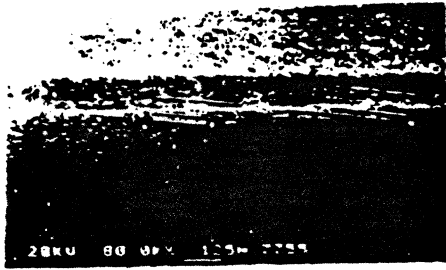
Niimata  
(198-

# SEMIPARTICULATE THIN FILM RIGID DISK MEDIA

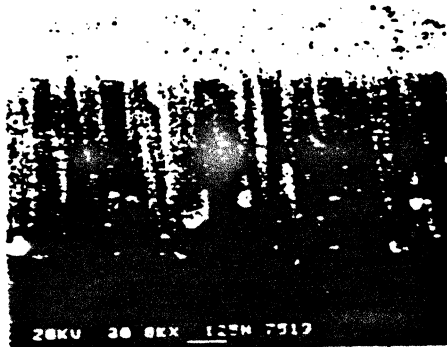
## Thin-Film Media Cross Section



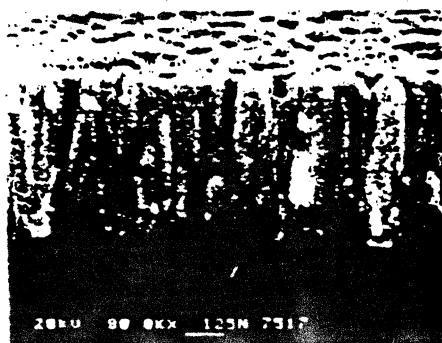
# MICROSTRUCTURE AND COERCIVITY OF CONICR SPUTTERED FILMS



CoNiCr/Glass



Cr/Glass



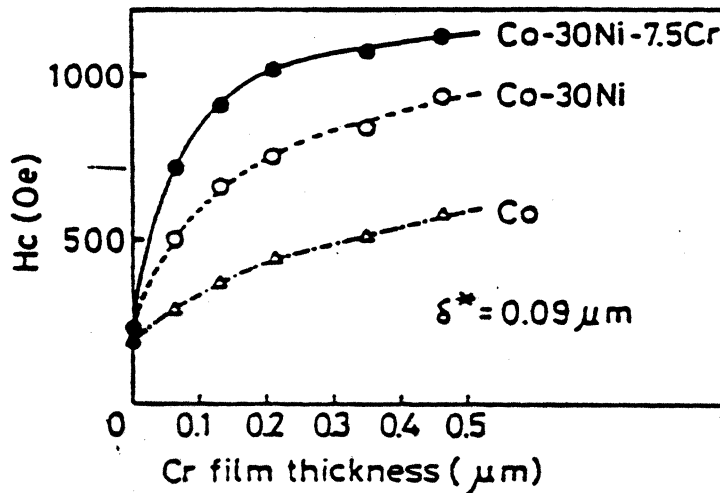
CoNiCr

CoNiCr/Cr/Glass

5000Å

"Semiparticulate"

SEM cross section micrographs of CoNiCr and Cr single layer and CoNiCr/Cr double layer films.



Relationship between Cr underlayer thickness and Hc of Co, Co-30Ni and Co-30Ni-7.5Cr film.

Ishikawa et al (1986)

# SPUTTERED CoCRM AND CoNiM TERNARY ALLOYS ON CR

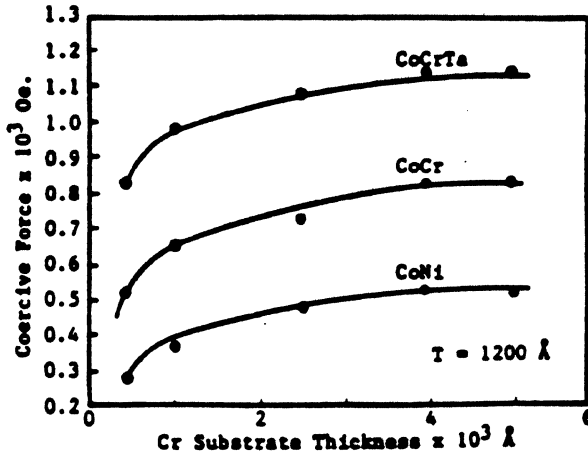


Figure 1: Relationship Between Film Coercivity and Chromium Substrate Thickness

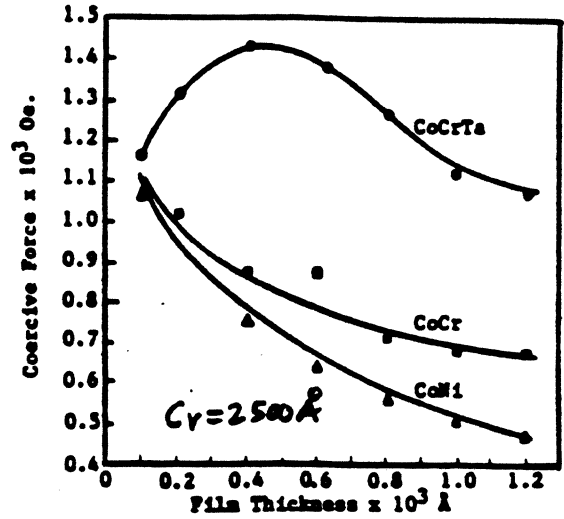


Figure 2: Coercive Force as a Function of Thickness

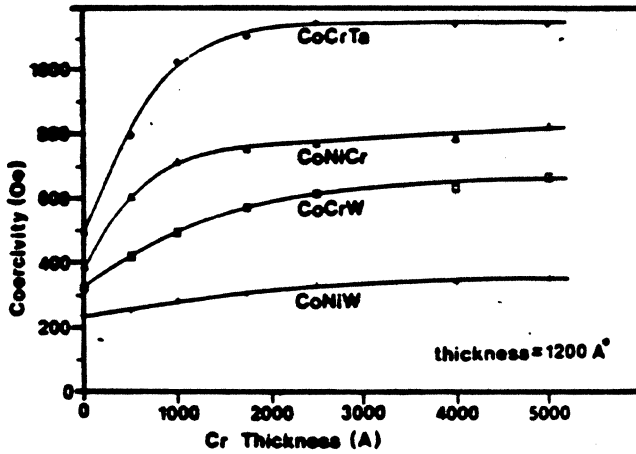


Figure 3: Coercivity Vs. Cr Underlayer Thickness for a Magnetic Thickness of 1200 Å.

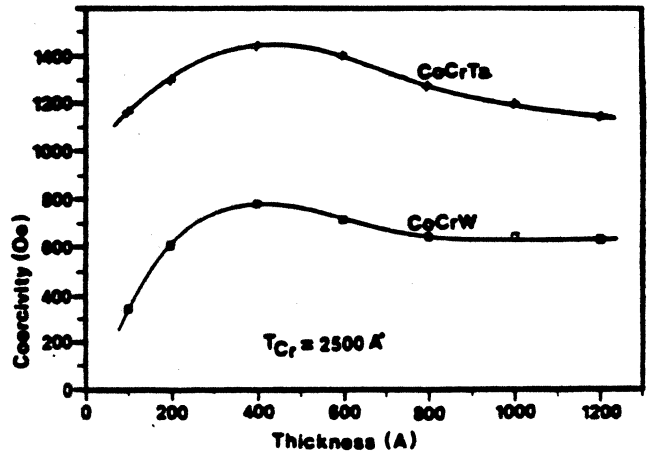


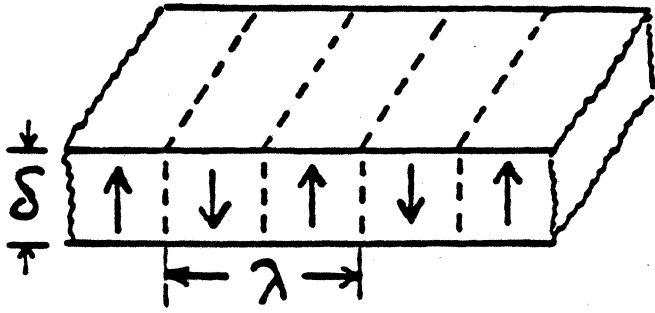
Figure 4: Coercivity of CoCrTa and CoCrW on a Cr Underlayer of 2500 Å.

DISC	A <sub>t</sub> (u <sup>2</sup> )	A <sub>g</sub> (u <sup>2</sup> )	M <sub>r</sub> T (uInT)	H <sub>c</sub> (Oe)	E <sub>70</sub> (uV)	D <sub>70</sub> (KfCl)	D <sub>50</sub> (KfCl)	Res (\$)	OW (dB)
CoCr	9.3	5.0	1.93	774	787	23.3	26.0	84	37.6
CoCr	9.2	5.0	1.78	730	662	23.9	31.0	85	35.0
CoCr	10.5	6.2	2.23	725	773	21.3	27.0	78	33.6
CoCrTa	6.15	2.3	1.41	1253	586	28.1	33.0	85	34.0
CoCrTa	7.3	3.1	1.91	1253	830	25.7	30.0	89	30.8
CoCrTa	8.6	4.2	2.30	1120	929	24.1	28.0	84	32.0

Fisher et al (198)  
Allen et al (198)

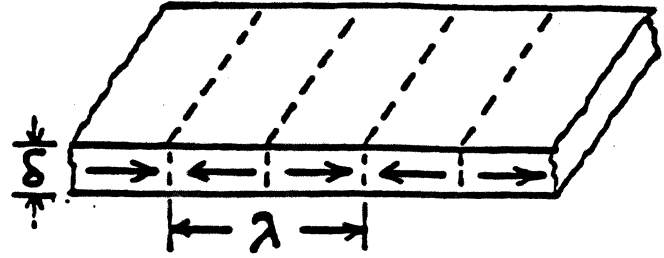
# COMPARISON OF PERPENDICULAR & LONGITUDINAL MODES

(a) Perpendicular Mode

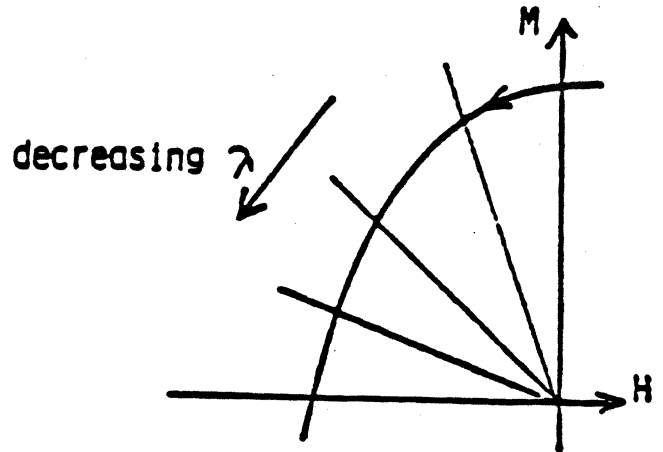
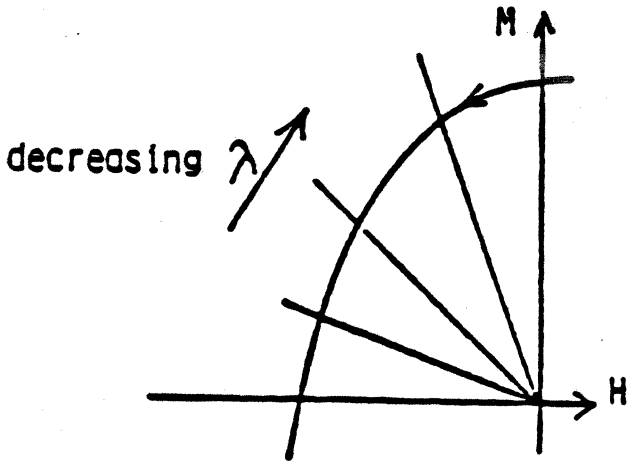


$\lambda \rightarrow 0$       $H_d \rightarrow 0$   
 Thick  $\delta$   
 High  $M_s$   
 High  $H_c$

(b) Longitudinal Mode



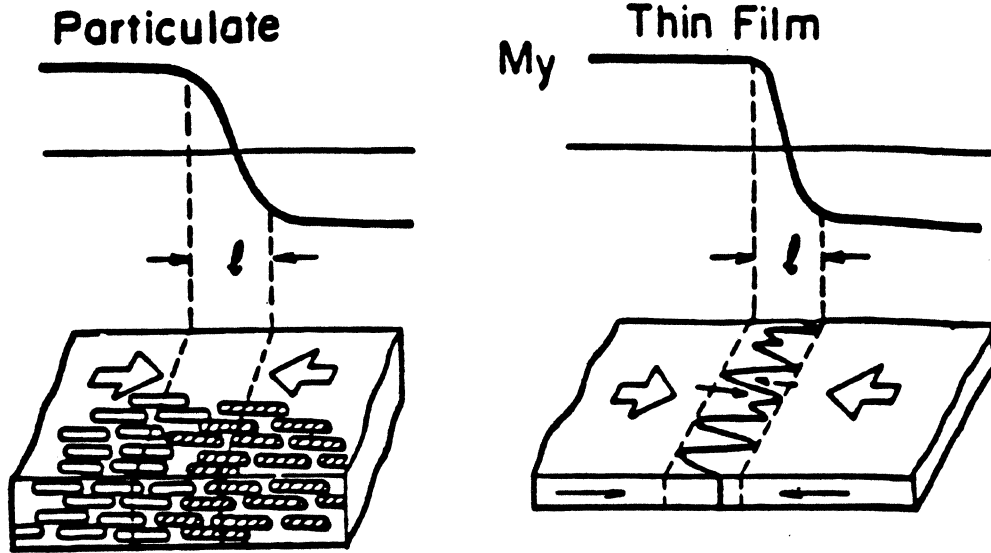
$\lambda \rightarrow 0$       $H_d \rightarrow 4\pi M$   
 Thin  $\delta$   
 Low  $M_s$   
 High  $H_c$





# COMPARISON OF PERPENDICULAR AND LONGITUDINAL RECORDING LIMITS

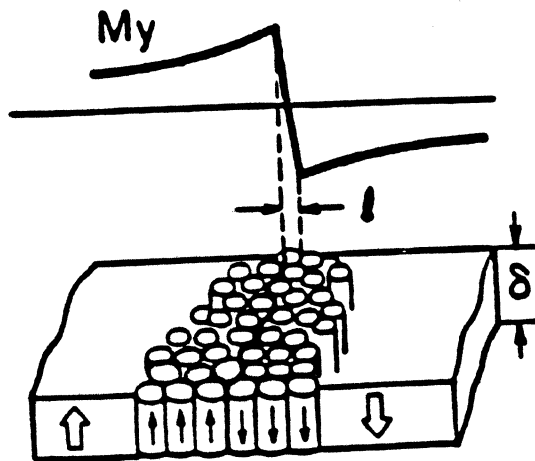
## Longitudinal



$l$ : particle assembly in transition  $\propto \left(\frac{\delta M_r}{H_c}\right)^{\frac{1}{2} \sim 1}$

$l$ : saw-tooth amplitude  $\approx \frac{\delta M_r}{H_c} \left( = \frac{\delta}{2} \sim \frac{\delta}{3} \right)$

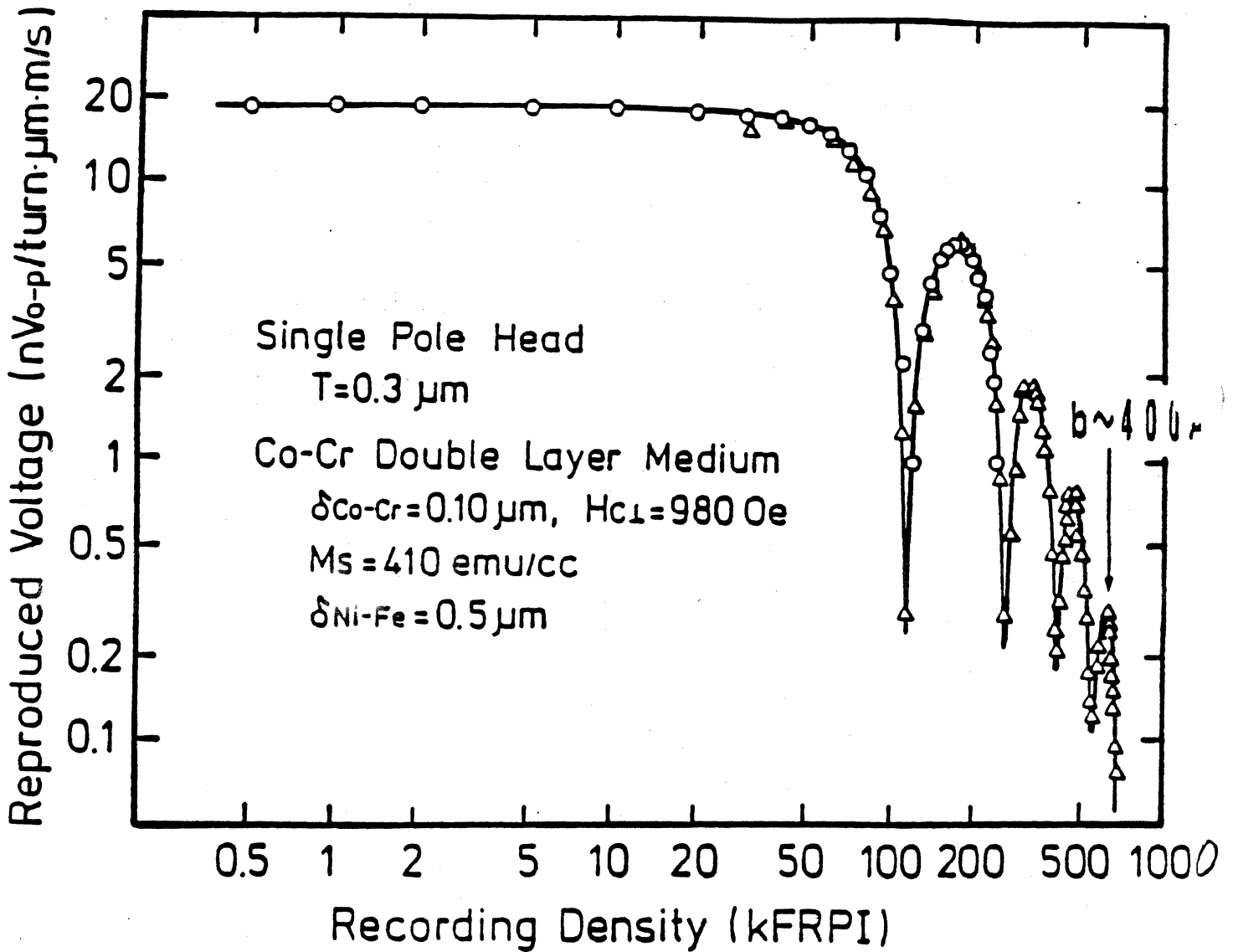
## Perpendicular



$l$ : column diameter (Co-Cr)

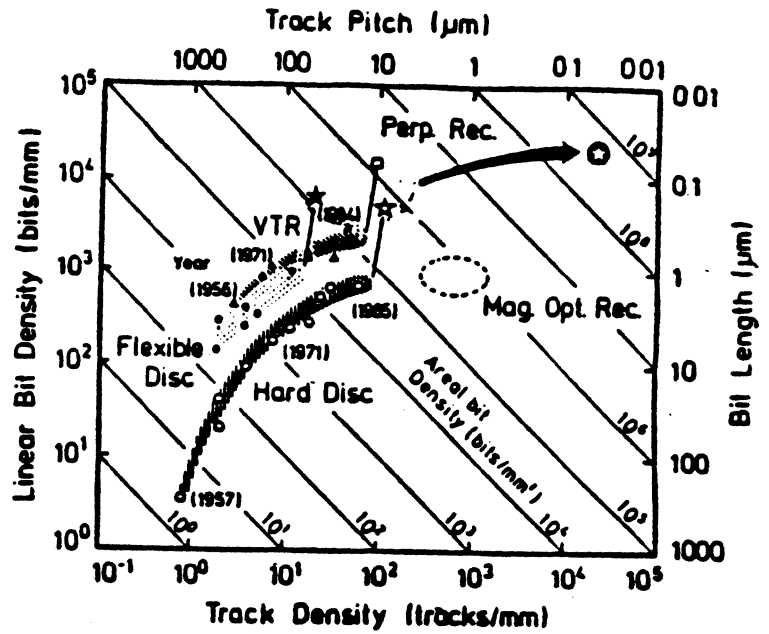
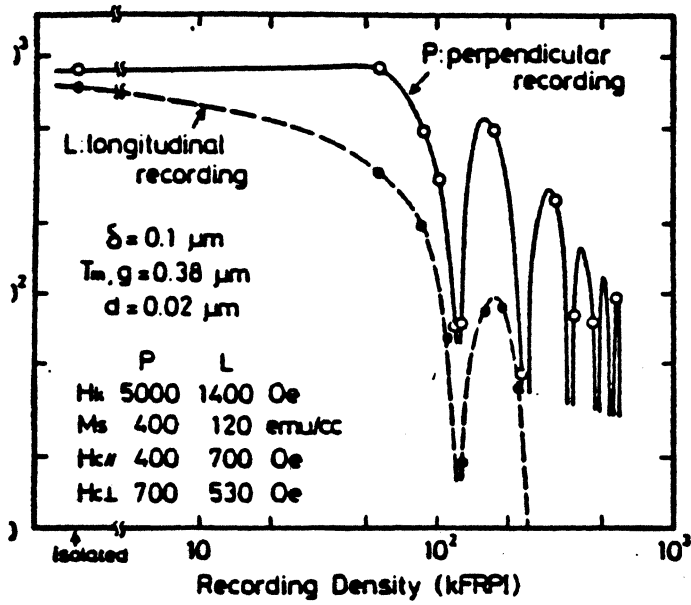
$= \frac{\delta}{10} \sim \frac{\delta}{20}$  (independent of  $H_c, M_s$ )

# PERPENDICULAR RECORDING CHARACTERISTICS <sup>21)</sup>

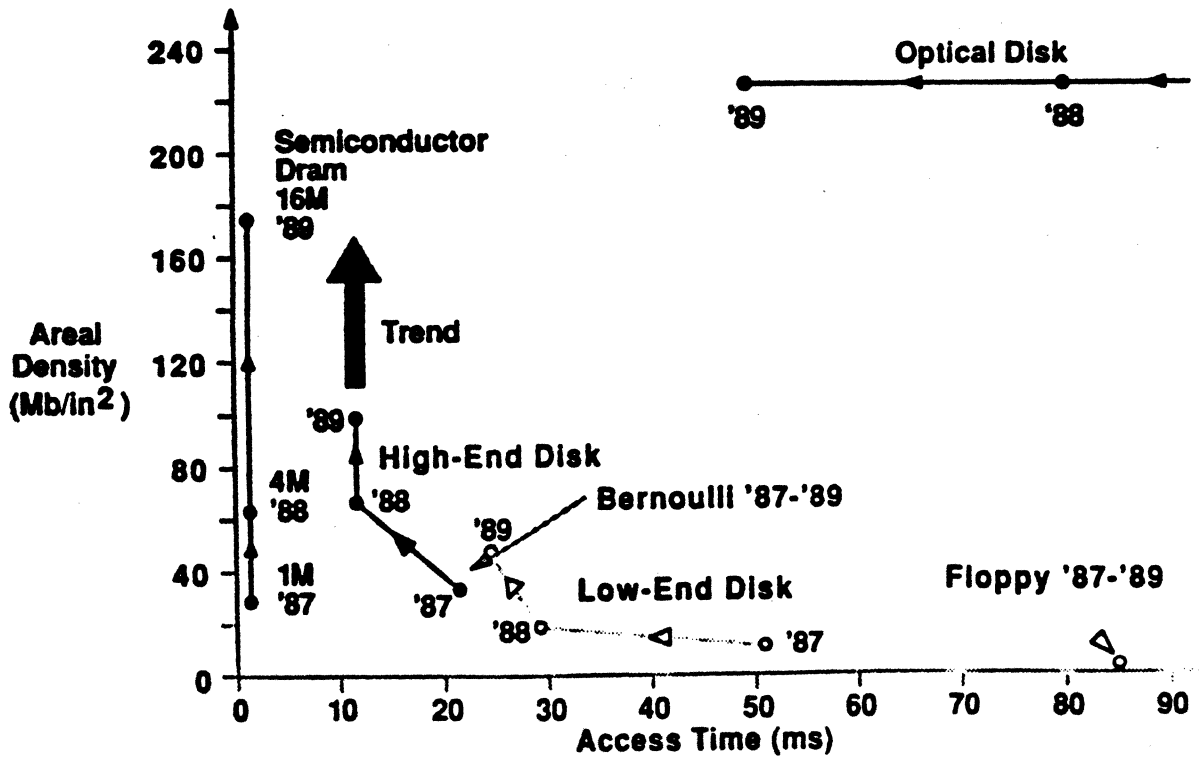


Nakamura et al (198)

# COMPARISONS OF FUTURE OF LONGITUDINAL AND PERPENDICULAR RECORDING



Nakamura (1988)



George (1988)

## CONCLUSIONS

1. METAL-IN-GAP HEADS WILL REPLACE FERRITE HEADS FOR HIGH AREAL DENSITY RECORDING APPLICATIONS OF RIGID DISKS
2. MIG HEADS WILL COMPETE WITH THIN FILM HEADS AS LONG AS THEIR COST IS LOWER THAN THAT OF THIN FILM HEADS
3. THIN FILM MEDIA WILL REPLACE COATED OXIDE MEDIA FOR HIGH AREAL DENSITY RECORDING APPLICATIONS OF RIGID DISKS
4. METAL EVAPORATED THIN FILM MEDIA WILL COMPETE WITH METAL PARTICLE MEDIA WHEN THE WEAR AND CORROSION PROBLEMS ARE SOLVED
5. HIGH DEFINITION VIDEO WILL BE THE DRIVING FORCE FOR USING PERPENDICULAR MAGNETIC RECORDING
6. SEMIPARTICULATE LONGITUDINAL THIN FILM MEDIA EXTEND THE LIFE OF LONGITUDINAL RECORDING FOR ANOTHER DECADE
7. PERPENDICULAR THIN FILM MEDIA WILL REQUIRE MAJOR DEVELOPMENTS IN SMOOTHER SUBSTRATES AND IMPROVED HEAD DESIGNS

## VII. REFERENCES

1. R.M. BOZORTH, "FERROMAGNETISM", VAN NOSTRAND (1951)
2. S. CHIKAZUMI, "PHYSICS OF MAGNETISM", WILEY (1964)
- 3. B.D. CULLITY, "INTRO. TO MAGNETIC MATERIALS", ADDISON-WESLEY (1972)
- 4. F. JORGENSEN, "HANDBOOK OF MAGNETIC RECORDING", TAB BOOKS (1988)
5. A.H. MORRISH, "THE PHYSICAL PRINCIPLES OF MAGNETISM", WILEY (1964)
6. M. PRUTTON, "THIN FERROMAGNETIC FILMS", BUTTERWORTH (1964)
7. J. SMIT, "MAGNETIC PROPERTIES OF MATERIALS", MCGRAW-HILL (1971)
8. R.F. SOOHOO, "MAGNETIC THIN FILMS", HARPER & ROW (1965)
9. R.S. TEBBLE AND D.J. CRAIK, "MAGNETIC MATERIALS", WILEY (1969)